

THE EFFECTS OF CLIMATE ON FLUVIAL DISCHARGE
AND KEY CONTROLS OF FLUVIAL FANS:
A QUANTITATIVE STUDY

by
Mark R. Hansford

© Copyright by Mark R. Hansford, 2020

All Rights Reserved

A thesis submitted to the Faculty and the Board of Trustees of the Colorado School of Mines in partial fulfillment of the requirements for the degree of Doctor of Philosophy (Geology).

Golden, Colorado

Date _____

Signed: _____

Mark R. Hansford

Signed: _____

Dr. Piret Plink-Björklund
Thesis Advisor

Golden, Colorado

Date _____

Signed: _____

Dr. Wendy Bohrson
Professor and Head
Department of Geology and Geological Engineering

ABSTRACT

Rivers have long been characterized by their average discharge and assumed to be sediment bypass conduits carrying sediment to its final depositional sinks. This dissertation combines daily discharge data from river gauging stations with satellite imagery to better understand both river discharge and fluvial fans. We examine fluvial discharge in the context of different hydroclimates. The importance of the role of discharge variability is increasingly being recognized and this work shines a quantitative light on the climatic controls of river discharge and identifies linkages between discharge and fluvial fan formation scaling relationships.

Through these investigations, we 1) develop a new set of dimensionless metrics to quantify discharge variability, 2) identify how river discharge variability falls into four statistically different and predictable groups that are characterized by flood magnitude, hydrograph shape, and inter-annual variability in discharge and are controlled by climate, 3) demonstrate that 75% of modern fluvial fans have fan-forming rivers with high discharge variability, and 4) characterize important geomorphometric scaling relationships in fluvial fans between discharge, channel width, and fan size.

These findings have implications for both terrestrial and extraterrestrial landscape evolution, paleoclimate modeling, and flood prediction and mitigation. Furthermore, the quantitative identification of scaling relationships intrinsic to fluvial fans should provide useful information for hydrocarbon exploration and production.

TABLE OF CONTENTS

| | |
|--|------|
| ABSTRACT | iii |
| LIST OF FIGURES | viii |
| LIST OF TABLES | x |
| ACKNOWLEDGMENTS | xi |
| DEDICATION | xii |
| CHAPTER 1 INTRODUCTION TO THE DISSERTATION | 1 |
| 1.1 Introduction | 1 |
| 1.2 Organization | 1 |
| 1.2.1 Chapter 2 | 2 |
| 1.2.2 Chapter 3 | 2 |
| 1.2.3 Chapter 4 | 3 |
| 1.2.4 Chapter 5 | 4 |
| CHAPTER 2 GLOBAL QUANTITATIVE ANALYSES OF RIVER DISCHARGE VARIABILITY AND HYDROGRAPH SHAPE WITH RESPECT TO CLIMATE TYPES | 5 |
| 2.1 Abstract | 5 |
| 2.2 Introduction | 6 |
| 2.3 Discharge Variability and Climate: Previous Quantitative Approaches | 9 |
| 2.4 Additional Discharge Variability Index | 15 |
| 2.5 Hydroclimate Types | 16 |
| 2.6 Dataset and Methods | 18 |

| | | |
|--|--|----|
| 2.6.1 | Dataset | 18 |
| 2.6.2 | Assignment of Hydroclimate Types | 20 |
| 2.6.3 | Statistical Methods | 20 |
| 2.7 | Quantitative Discharge Analysis | 21 |
| 2.7.1 | Assessment of Discharge Variability Indexes | 21 |
| 2.7.2 | Quantitative Analyses of River Discharge by Hydroclimate Types | 23 |
| 2.7.2.1 | Tropical Rainforest Rivers | 23 |
| 2.7.2.2 | Monsoonal Rivers | 24 |
| 2.7.2.3 | Humid Subtropical Rivers | 25 |
| 2.7.2.4 | Arid Rivers | 25 |
| 2.7.2.5 | Temperate Rivers | 26 |
| 2.7.2.6 | Cold Dfa Rivers | 27 |
| 2.7.2.7 | Cold and Polar Rivers | 28 |
| 2.7.3 | Hydrological River Groups | 28 |
| 2.8 | Discharge Variability and Drainage Area | 30 |
| 2.9 | Discharge Variability within Individual Rivers | 31 |
| 2.10 | Conclusions | 32 |
| CHAPTER 3 RIVER DISCHARGE VARIABILITY AS THE LINK BETWEEN CLIMATE AND FLUVIAL FAN FORMATION | | 55 |
| 3.1 | Abstract | 55 |
| 3.2 | Introduction | 56 |
| 3.3 | Data and Methods | 57 |
| 3.3.1 | Data | 57 |

| | | |
|--|--|----|
| 3.3.2 | Methods | 58 |
| 3.4 | Results | 59 |
| 3.4.1 | Quantitative Assessment of Discharge Variability | 59 |
| 3.4.2 | Down-Fan Changes in Discharge Variability | 59 |
| 3.4.3 | Discharge Variability and Hydroclimates | 60 |
| 3.5 | Discussion | 60 |
| 3.5.1 | Link Between River Discharge Variability and Fluvial Fan Formation | 60 |
| 3.5.2 | Low Discharge Variability Fans | 61 |
| 3.6 | Conclusions | 62 |
| 3.7 | Acknowledgements | 63 |
| CHAPTER 4 GEOMORPHOMETRIC SCALING RELATIONSHIPS IN FLUVIAL FANS | | 69 |
| 4.1 | Abstract | 69 |
| 4.2 | Introduction | 70 |
| 4.3 | Data and Methods | 72 |
| 4.3.1 | Satellite Imagery Data | 72 |
| 4.3.2 | Discharge Data | 73 |
| 4.4 | Results | 75 |
| 4.4.1 | Channel Width and Discharge | 75 |
| 4.4.2 | Fan Size | 76 |
| 4.4.3 | Drainage Area | 77 |
| 4.4.4 | Down-Fan Channel Width Change | 77 |
| 4.4.5 | Fan Adjacency to Mountainous Topography | 78 |

| | | |
|---------------------------------|---|-----|
| 4.5 | Discussion | 78 |
| 4.5.1 | Channel Forming Discharge | 78 |
| 4.5.2 | Large Rivers Do Not Build Large Fans | 80 |
| 4.5.3 | Comparison of Modern and Ancient Channel Widths | 81 |
| 4.5.4 | Adjacency to Mountainous Hinterland | 82 |
| 4.6 | Conclusions | 82 |
| 4.7 | Acknowledgments | 83 |
| CHAPTER 5 CONCLUSIONS | | 104 |
| 5.1 | Summary Conclusions and Contributions | 104 |
| 5.1.1 | Chapter 2 Conclusions and Contributions | 104 |
| 5.1.2 | Chapter 3 Conclusions and Contributions | 105 |
| 5.1.3 | Chapter 4 Conclusions and Contributions | 105 |
| 5.2 | Future Work | 105 |
| REFERENCES CITED | | 107 |

LIST OF FIGURES

| | | |
|-------------|--|----|
| Figure 2.1 | A comparison of the cumulative frequency discharge of three rivers | 34 |
| Figure 2.2 | Link between precipitation and discharge variability | 35 |
| Figure 2.3 | Map distribution of the 575 discharge stations | 36 |
| Figure 2.4 | Colorado River Hydrographs | 37 |
| Figure 2.5 | Comparison of inter-annual variability | 38 |
| Figure 2.6 | Discharge variability values of the 7 hydroclimate groups | 39 |
| Figure 2.7 | Multiple comparison tests on the Kruskal-Wallis test results. | 40 |
| Figure 2.8 | Discharge variability indexes grouping. | 41 |
| Figure 2.9 | Normalized monthly average discharge graphs | 42 |
| Figure 2.10 | Largest flood examples for the representative rivers for each hydroclimate zone. | 43 |
| Figure 2.11 | Multiple-year hydrographs (7 years) | 44 |
| Figure 2.12 | Hydrographs of the representative rivers for each hydroclimate zone. . . . | 45 |
| Figure 2.13 | Relationship between drainage area and discharge variability (DVI_y) | 46 |
| Figure 2.14 | Change in DVI_a along a river from the updip station to the downdip station. | 47 |
| Figure 2.15 | Columbia River hydrograph | 48 |
| Figure 3.1 | Examples of fluvial fans. | 64 |
| Figure 3.2 | Streamflow hydrographs | 65 |
| Figure 3.3 | Map of fluvial fan locations | 66 |
| Figure 3.4 | Discharge variability in fan forming rivers | 67 |

| | | |
|-------------|--|-----|
| Figure 4.1 | Examples of fluvial fans. | 84 |
| Figure 4.2 | Map of fluvial fan locations | 85 |
| Figure 4.3 | Channel width measurements examples for single-thread and multi-thread rivers. | 86 |
| Figure 4.4 | Apex channel width and discharge correlations. | 87 |
| Figure 4.5 | Toe channel width and discharge correlations. | 88 |
| Figure 4.6 | Channel width and discharge variability metrics. | 89 |
| Figure 4.7 | Binned frequency histogram of fan area. | 90 |
| Figure 4.8 | Fan area vs apex-to-toe distance. | 91 |
| Figure 4.9 | Fluvial fan size and discharge. | 92 |
| Figure 4.10 | Fluvial fan size and channel width. | 93 |
| Figure 4.11 | Tectonic regime controls on fluvial fan size. | 94 |
| Figure 4.12 | Climatic controls on fluvial fan size. | 95 |
| Figure 4.13 | Climatic controls on Q_{99} discharge | 96 |
| Figure 4.14 | Drainage area and discharge correlations. | 97 |
| Figure 4.15 | Changes in channel width from apex to toe. | 98 |
| Figure 4.16 | Fluvial fan size and apex adjacency. | 100 |
| Figure 4.17 | Fluvial fan maximum discharge and apex adjacency. | 101 |
| Figure 4.18 | Channel width comparison between modern and ancient. | 102 |

LIST OF TABLES

| | | |
|-----------|--|-----|
| Table 2.1 | Hydroclimate types defined by general precipitation patterns. | 49 |
| Table 2.2 | Discharge variability metrics and equations | 50 |
| Table 2.3 | Discharge variability metrics for the 7 hydroclimate types | 51 |
| Table 2.4 | Discharge variability metrics for representative rivers of the seven hydroclimate zones | 53 |
| Table 2.5 | Median discharge variability metrics for small (<25,000km ²) and large (>25,000km ²) rivers. | 54 |
| Table 2.6 | Downriver increase and decrease in discharge variability. | 54 |
| Table 3.1 | Discharge variability metrics | 68 |
| Table 4.1 | Discharge variability metrics | 99 |
| Table 4.2 | Channel width change from apex to toe | 103 |

ACKNOWLEDGMENTS

I would first like to thank my advisor, Dr. Piret Plink-Björklund, for supporting and encouraging me through the research process. I have learned so much from Piret about sedimentary processes, critical thinking, and perseverance in grant writing. I am eternally grateful for her willingness to the many hours she spent investing in my growth and improving the manuscripts included in this dissertation.

I would also like to thank my committee members: Dr. Kamini Singha for forcing me to learn MATLAB and pushing me to become more quantitative as well as providing an extra round of review on my first paper; Dr. Zane Jobe for making me question how to link sediment transport to the sedimentary record, and Dr. Adrienne Kroepsch for encouraging me to consider how I communicate.

Next, I would like to thank the rest of my research group at Colorado School of Mines for helping with the research process, refining my thoughts through winding discussions, and commiserating together. This project was supported by the RioMAR consortium as well as additional support from AAPG, SEPM, NSF, GSA, the Bartshe Endowment Fund, the Geological Society of Nevada, QEP Resources, and Andarko Petroleum Company (now Occidental Petroleum Corporation).

Finally, I would like to thank my family, friends, and fiancée for supporting me throughout this process. In particular, I would like to thank Dr. David Fairchild Wheatley for taking me on as a research assistant all those years ago and all the great times we spent in the desert discussing rocks as well as his continued mentorship and advice throughout the PhD. And lastly, the mountains, for without skiing this would have been finished a year sooner, but without my sanity.

This dissertation is dedicated to my family:

My loving fiancée Dante Huff. As well as our fluffy cat Kodiak.

My parents, Brendon and Christine, for their ongoing support.

My siblings, Elizabeth and Douglas, who continue to inspire me.

CHAPTER 1

INTRODUCTION TO THE DISSERTATION

1.1 Introduction

This dissertation critically examines the climatic controls on fluvial discharge around the world and the resulting controls on fluvial fans. This dissertation is the combination of two linked projects, the first of which provides a quantitative analysis of modern fluvial discharge around the world (paper 1) and the second which examines the intrinsic properties and processes of fluvial fans (papers 2 and 3). The importance of the role of discharge variability is increasingly being recognized and this work shines a quantitative light on the climatic controls of river discharge and identifies linkages between discharge and fluvial fan formation scaling relationships. This work is intended to reach a broad audience and be beneficial for sedimentologists, geomorphologists, hydrogeologists, data scientists, and even civil engineers in light of a changing climate and growing urbanization.

1.2 Organization

This dissertation is composed of three papers: the first (chapter 2) is published in Elsevier's *Earth-Science Reviews*, the second (chapter 3) is currently in the submission/re-submission stage with the journal of *Geology*, and the third (chapter 4) will be submitted to the journal of *Sedimentology*. Each chapter is formatted according to the journal to which it was submitted and therefore, each chapter contains a separate abstract, introduction, data and methods, and conclusion. This dissertation serves as a unifying document tying together the three separate papers into a collective whole to impart the findings to the broader scientific community. A brief summary of the three manuscripts and their key contributions is provided below. Finally, chapter 5 is the conclusion of this dissertation and summarizes the conclusions and contributions of each preceding chapter.

1.2.1 Chapter 2

Chapter 2 (1st paper) reviews quantitative methods in river discharge variability analyses and utilizes a global daily discharge database of 575 gauging stations to analyze discharge variability patterns. Discharge variability, such as the frequency, magnitude, and duration of floods is a key control on hydrological behavior in rivers. We develop new quantitative criteria and use a combination of multiple discharge variability criteria to compare hydrograph shapes to hydroclimate types. These analyses show that river discharge patterns fall into four statistically different and predictable groups as characterized by flood magnitude, hydrograph shape, and inter-annual variability in discharge. These four hydrological groups are: (1) persistent hydrology rivers, (2) single storm controlled variable discharge rivers, (3) rivers with seasonal hydrology, and (4) extreme and erratic hydrology rivers.

While we hope this paper reaches a broad range of geomorphologists, hydrologists, and engineers, we wrote it with the sedimentologist in mind. Before this paper there were woefully few, well described, modern analogues to link sedimentary processes to. This paper provides a wide range of example river systems based on discharge, discharge variability, drainage area, and climate. We hope this paper is part of a collective push by a new generation sedimentologists to quantify our science and better capture the range of uncertainty inherent to interpretation.

1.2.2 Chapter 3

There are two contrasting, published hypotheses debating whether fluvial fans need specific climate conditions to form or whether they can form regardless of climatic conditions. Chapter 3 (2nd paper) tests these hypotheses by quantitatively analyzing the discharge patterns of 68 fan forming rivers. Using an ensemble of dimensionless metrics, we show that 75% of the fan-forming rivers in our dataset have a high discharge variability. Additionally, we analyze down-fan changes in discharge variability and discuss the nature of discharge variability in different hydroclimates as a function of intra- and inter-annual precipitation

fluctuations. We examine the fan-forming rivers with moderate to low discharge variability and conclude that although river discharge variability strongly promotes fluvial fan formation, fluvial fans may also be formed by rivers with a moderate or low discharge variability if other favorable conditions that promote avulsions occur.

Fluvial fans are still a relative newly accepted concept and there are still many open questions that sedimentologists are attempting to answer. Facies models are still being developed and key controls are actively being debated. Our goal with this paper is to start to answer the questions of climate and discharge. By better understanding the underlying conditions needed for fluvial fan formation, sedimentologists can more effectively interpret the rock record.

1.2.3 Chapter 4

Chapter 4 (3rd paper) examines important geomorphometric scaling relationships in fluvial fans. We build upon our first two studies and present an analysis of discharge variability, channel width, drainage area, and areal fan size for 415 fluvial fans. Our measurements for channel width and fan size were made in Google Earth and discharge data comes from the 85 gauging stations on 68 fan forming rivers of chapter three (2nd paper). We found inverse relationships between discharge and channel width at the apex and toes of the fan where channel width at the apex best correlations to extremely high discharge values such as $Q_{99.863}$ while channel width at the toe best correlates Q_{50} discharge values. We found that in approximately three-quarters (72.5%) of fluvial fans the channel width decreases from the apex to the toe. Additionally, we found that fan area is not correlated with channel width or drainage area, but tectonic and climatic settings exert control on the size of the fan.

As previously mentioned, fluvial fans are a relative newly accepted sedimentological concept. Recognition criteria are not yet firmly established and this paper aims to lend quantitative aid to sedimentologists who are creating new facies and depositional models as well as those are working in the field making interpretations of the rock record. The range of possible fan sizes, channel widths, and known correlating discharge values can be used as

independent tests to check, guide, and give weight to interpretations.

1.2.4 Chapter 5

Chapter 5 is the conclusion to this dissertation and summarizes the conclusions and contributions of each preceding chapter. It also contains recommendations for future work for all those who follow afterwards.

CHAPTER 2

GLOBAL QUANTITATIVE ANALYSES OF RIVER DISCHARGE VARIABILITY AND HYDROGRAPH SHAPE WITH RESPECT TO CLIMATE TYPES

Mark R. Hansford¹, Piret Plink-Björklund², and Evan R. Jones³

Originally published in Elsevier's *Earth-Science Reviews*⁴

2.1 Abstract

Discharge variability is a key control on hydrological behavior in rivers, such as the frequency and magnitude of floods. A better understanding of discharge variability and how that variability is linked to global climate has implications for flood prediction, risk analyses, and mitigation strategies. Furthermore, river discharge variability is a key control on river morphodynamics, and thus on river facies and architecture. Here we present a review of quantitative methods in river discharge variability analyses and utilize a global daily discharge database of 575 gauging stations from the Global Runoff Data to analyze global discharge variability patterns and compare those patterns to hydroclimate conditions. Our approach differs from previous attempts to link river discharge patterns to climate in that we define hydroclimate types that combine the Köppen-Geiger climate types with precipitation variability. We develop new quantitative criteria and use a combination of multiple discharge variability criteria to compare hydrograph shapes to hydroclimate types. These analyses show that river discharge patterns fall into four statistically different and predictable groups as characterized by flood magnitude, hydrograph shape, and inter-annual variability in discharge. These four hydrological groups are: (1) persistent hydrology rivers, (2) single storm controlled variable discharge rivers, (3) rivers with seasonal hydrology, and

¹Primary author, graduate student, Colorado School of Mines

²Associate Professor, Colorado School of Mines

³Co-author, Geologist, Occidental Petroleum Company

⁴Reprinted with permission of Earth-Science Reviews, 2020, 200, 1-20.

(4) extreme and erratic hydrology rivers.

2.2 Introduction

The variations in discharge of a river constitute its hydrological regime that is influenced by climate and the nature of the Earth's surface and subsurface (Haines et al., 1988). Studies of river hydrological regimes have implications for understanding the interactions between hydrology and the ecosystem, and determining to what extent hydrologic predictions such as of floods may be transferred from one area to another (Haines et al., 1988; Hayden, 1988). Variations in discharge of a river further constitute a first-order control on landscape evolution and on the specific nature of the consequent sedimentary record of rivers (e.g. McKee et al., 1967; Williams, 1971; Picard and High, 1973; Frostick and Reid, 1977; Jones, 1977; Foley, 1978; Tunbridge, 1981; Sneh, 1983; Stear, 1985; Langford and Bracken, 1987; Graf, 1988; Abdullatif, 1989; Bromley, 1991; Kale et al., 1994; Kale, 2003, 2007; Gupta and Dawdy, 1995; North and Taylor, 1996; Fielding and Alexander, 1996; Knighton and Nanson, 1997; Reid and Frostick, 1997; Alexander et al., 1999; Tooth, 2000; Amos et al., 2004; Latrubesse et al., 2005; Leier et al., 2005; Fielding, 2006; Billi, 2007; Fielding et al., 2009, 2011; 2018; Powell, 2009; Fiorillo et al., 2010; Allen et al., 2013; Plink-Bjorklund, 2015; 2018; Nicholas et al., 2016; Gall et al., 2017; Plink-Björklund, 2017; Ghinassi et al., 2018; Dingle et al., 2019). Some studies also suggest that sediment yield is strongly linked to river hydrology and that rivers with variable discharge have relatively higher sediment yields (e.g. Wilson, 1973; Cecil and Dulong, 2003; Cecil et al., 2003; Clift et al., 2008; Sinha et al., 2012; Jones, 2017; Milliken et al., 2017). Thus hydrological regimes should also constitute a key component in sediment transport, mass balance, source to sink sediment dispersal, and provenance analyses (Latrubesse et al., 2005; Blum and Pecha, 2014; Holbrook and Wanas, 2014; Eide et al., 2017; Froude et al., 2017; Jones, 2017).

The link between global climate and river hydrology has received considerable attention in the context of predicting floods, expanding flood predictions to data poor areas, and considering the future changes in the light of the changing climate and growing urbanization

(e.g. Hayden, 1988; Smith et al., 2015; Alfieri et al., 2017; Blöschl et al., 2019; François et al., 2019). However, with a few exceptions (McMahon et al., 1987, 1992; Haines et al., 1988; Hayden, 1988) river hydrology is commonly represented by average discharge. The same method is common in the community’s approaches for calculating sediment discharges and linking sediment yields to drainage basin size (e.g. BQART, Syvitski et al., 2003; Syvitski and Milliman, 2007), despite the significant dependence between river hydrology and the scaling relationship to drainage basin size (Meybeck et al., 2003; Eide et al., 2017; Jones, 2017)(Fig. 2.1). Some approaches add a measure of extreme discharges (e.g. Asadih et al., 2016; Pechlivanidis et al., 2017), but while annual means and extreme values are important general characteristics, the distribution of hydrological extremes and moderate events, together with seasonal behavior of variables are even more important in hydrology and water resources management. This lack in understanding of river hydrological regimes has been deemed “the greatest impediment to the mitigation of flood hazards” (Baker, 1994), and the link between climate and floods remains one of the most significant questions in hydrology (Blöschl et al., 2019).

The scientific community that has highlighted the significance of river hydrological regimes concerns studies of dryland, subtropical and tropical rivers and their corresponding sediments (e.g. McKee et al., 1967; Williams, 1971; Picard and High, 1973; Jones, 1977; Foley, 1978; Tunbridge, 1981; Sneh, 1983; Stear, 1985; Langford and Bracken 1987; Graf, 1988; Abdulatif, 1989; Bromley, 1991; North and Taylor, 1996; Kale, 1994; 2003; 2007; Gupta, 1995; Fielding and Alexander, 1996; Knighton and Nanson, 1997; Reid and Frostick, 1997; Alexander et al., 1999; Tooth, 2000; Amos et al., 2004; Latrubesse et al., 2005; Leier et al., 2005; Fielding, 2006; Billi, 2007; Fielding et al., 2009; 2011; 2018; Powell, 2009; Fiorillo et al., 2010; Allen et al., 2013; Flaig et al., 2014; Plink-Björklund, 2015; 2018; Nicholas et al., 2016; Gall et al., 2017; Dingle et al., 2019; Ghinassi et al., 2019). This community has established that river hydrology is closely linked to rainfall patterns, such that high rainfall variability and the occurrence of extreme rainfall events is considered to cause high river runoff variability

and higher magnitude floods (Fig. 2.2). However, even this community lacks consensus on how to define and quantify river discharge variability (compare Latrubesse, 2005; Leier et al., 2005; Plink-Bjorklund, 2015; Jones, 2017; Fielding et al., 2018). While it is broadly recognized that variable discharge rivers have a large discharge range as compared to mean discharge, whereas in persistent discharge rivers both low and high magnitude discharge events are rare occurrences, and the differences between discharge minima and maxima are small relative to annual mean discharge (Fig. 2.2), it is unclear how this variability manifests itself in different climate zones (e.g. Syvitski et al., 2014; Dingle et al., 2019).

In this paper, we take a holistic approach and explore river hydrology by using an ensemble of dimensionless metrics that reflect different aspects of discharge variability. We evaluate statistically the existing quantitative criteria for river discharge variability and develop a new criterion in an attempt to capture the different aspects of river hydrology. Using global discharge data of 575 gauging stations of 490 rivers from the Global Runoff Data Centre (GRDC) (<https://www.bafg.de/GRDC/EN/Home/homepage-node.html>) (Fig. 2.3), we combine the quantitative analyses of dimensionless metrics with hydrograph shape analyses and attempt to cluster rivers globally according to their hydrology. The potential mechanistic relation between the discharge variability and precipitation regime is the key focus of this paper. In order to test whether river hydrology differs as a function of precipitation pattern, we group rivers empirically. Rather than following previous groupings by continent (McMahon et al., 1987) or flood season and magnitude (Haines et al., 1988), we group rivers by hydroclimate types as defined by general precipitation patterns (Table 2.1). This analysis is meant as a test-of-concept to be followed by a more rigorous, algorithm-based clustering of rivers.

We show that incorporating hydrograph shape analyses significantly improves the understanding of river hydrology, whereas the metrics provide important quantitative boundaries. Our analyses differentiate between 4 global river clusters with distinct hydrology. We go beyond just differentiating persistent and variable discharge rivers and distinguish variable

discharge river behavior based on erratic, single storm controlled and seasonal flood patterns. We further test the link between drainage basin size and discharge variability, and analyze multiple gauging stations on the same rivers to test downstream changes in discharge variability.

2.3 Discharge Variability and Climate: Previous Quantitative Approaches

This section provides an overview of previous quantitative approaches of global river discharge analyses and the link to climate. We further introduce the metrics that will be used in quantitative analyses in section 6.

Early attempts of flow regime classifications at the global scale were limited by the lack of adequate global coverage of runoff data (e.g. Parde', 1933a; Lvovich, 1945; Keller, 1968; Beckinsale, 1969). The first dataset that allowed global runoff to be analyzed on the basis of streamflow data alone without the necessity for extrapolation from water balance models or climatic regions was assembled by Finlayson et al. (1986). This dataset was used in multiple studies that mark the start of comparative hydrology and global river discharge analyses. McMahon et al. (1987) analyzed annual streamflow data from 938 gauging stations and annual peak flow data from 921 stations globally. They grouped rivers by continents to study discharge variability patterns and their continental-scale differences, using the coefficient of variation of annual flows (C_{vr}) calculated as the standard deviation divided by the mean annual discharge, and the coefficient of variation of the annual peak flow (I_v). They conclude that there are significant differences in both C_{vr} and I_v values and trends on different continents when compared to mean annual precipitation, drainage basin area and to the Köppen-Geiger climate types, and Australia and Southern Africa show levels of annual and peak flow variability nearly twice that of the other continents. By analyzing rainfall data from 421 stations the authors show that this difference is not linked to mean annual precipitation, but rather to the variability of effective precipitation that is a function of high evaporative demand in the atmosphere.

A follow-up global study on river hydrological regimes and their link to climate by Haines et al. (1988) examined monthly streamflow data of 969 rivers worldwide and classified flow regimes based on cluster analysis of monthly mean flows as percentages of mean annual flow. An average flow regime was determined by averaging the streamflow in each month over all years of record. These average monthly flows were then recalculated as a percentage of the average annual flow. Haines et al. (1988) first separated non-seasonal or uniform flows, defined as those with all monthly means within 5-12% of the average discharge. Building on Gentili (1952) classification for Australian rivers, they separated rivers into 15 groups based on the time of the year of flood occurrence and the monthly averaged flood magnitude (as a percentage of mean annual flow). They analyzed each of the groups in the context of river water supply, such as snowmelt or cyclones or seasonal monsoon rain. A comparison to Köppen-Geiger climate types showed a poor relationship between the hydrological regime groups and climate types. The authors noted that since the Köppen-Geiger climate classification has a strong thermal emphasis it is not ideal classification for that purpose.

McMahon et al. (1992) examined 974 rivers, grouping them by continental region and by climate type, using annual flow volumes (Q_{mean}) and annual peak discharges (Q_{max}). This study looked at how the annual flow and annual peak flow varies according to the five groups (A, B, C, D, and E) of the Köppen-Geiger climate types, and identified regional hydrological differences and similarities in order to ascertain the transferability of hydrological theory and practice between different continents and climate types. The work of McMahon et al. (1987, 1992) and Haines et al. (1988) was instrumental in highlighting the need for comparative hydrology as hydrological textbooks at the time focused on perennial streams and did not consider discharge variability.

A set of global studies that focused on long-term sediment flux of rivers, however, abandoned the consideration of discharge variability (the BQART model; Milliman and Syvitski, 1992; Syvitski et al., 2003; Syvitski and Milliman, 2007). These studies examined 280, 340 and 488 rivers, respectively, but only considered mean annual discharge and incorporated

climate through basin temperature. This seminal work has strongly influenced research in hydrology, geomorphology, and geology towards focus on drainage basin size and topography as the key defining factor of river behavior.

Consequently, there are relatively few global quantitative studies that have explored the role of river hydrology in sediment transport, landscape evolution or flood magnitude-frequency relationships, or attempted to establish the link between river hydrology and climate. Leier et al. (2005) studied 202 rivers globally and establish a strong link between precipitation and discharge variability, and suggest no correlation between annual mean, maximum or minimum precipitation and discharge (Fig. 2.2). In order to compare rivers globally, they use discharge peakedness (Table 2.2), defined as the average discharge during the month with the greatest discharge divided by the mean annual discharge. This comparison links the formation and construction of fluvial megafans to rivers with variable discharge and quantitatively differentiates the low peakedness rainforest and temperate climate rivers from the high peakedness monsoonal and subtropical rivers. They further suggest that seasonal discharge variability is related to high sediment yields, which promotes channel aggradation and avulsions.

Latrubesse et al. (2005) considered 34 rivers with catchments larger than 10,000 km². They show in their review of tropical river systems that hydrology of tropical rivers varies considerably when comparing highest daily and mean annual discharges (Q_{max}/Q_{mean}) and maximum and minimum daily discharges (Q_{max}/Q_{min}) of rainforest and monsoon zone rivers. They further conclude that rivers with high discharge variability (Q_{max}/Q_{min}) also correspond to high magnitude flood regimes characterized by high Q_{max}/Q_{mean} ratios. The authors conclude that since their dataset considers large drainages, the drainage area is not a primary factor controlling extreme floods and flood variability. They rather link the flood behavior to Q_{max}/Q_{min} and Q_{max}/Q_{mean} ratios and show that rainforest zone rivers are distinct from the variable discharge rivers in humid and arid subtropics and the monsoon zone.

A different review of tropical rivers (Syvitski et al., 2014) conducted a semi-quantitative analyses where 60 rivers were examined qualitatively with quantitative monthly stream-flow data from <http://www.sage.wisc.edu/riverdata/> presented for a subset of 12 rivers. The quantitative analysis includes mean discharge, standard deviation, minimum discharge, maximum discharge, record discharge, and discharge coefficient of variation. Their analyses show that tropical river basins are among the highest runoff basins regardless of basin area, but rivers draining tropical savanna have much lower runoff values due to the seasonality of rainfall. They analyze the 12 rivers in context of drainage basin size and conclude that in general, the coefficient of variation for discharge is very small for large rivers and increases for smaller ones, with some exceptions. This smaller dataset thus contradicts the Latrubesse et al. (2005) conclusions on relative independence of discharge variability and drainage basin size. The authors do acknowledge that strong seasonality is a dominant feature of most tropical rivers. For example, rivers draining the Indian subcontinent can have maximum discharges in the tens of thousands of m^3/s , yet run dry that same year. Yet, because both seasonally variable (monsoonal) and persistent (rainforest) discharge rivers are considered as a group, this work concludes that although strong seasonality is a dominant feature of tropical climate, temperate and sub-polar regions are equally seasonal, even if the forces at play are different (e.g. pattern and intensity of cold fronts, freshet snow-melt release in the spring). Furthermore, there are important rivers in the tropics that are not seasonal in areas not influenced by either tropical cyclones or tropical monsoons, and thus do not appear to experience significant or unusual flooding. This conclusion is perhaps not surprising, as Köppen-Geiger tropical climate type (type A; see Peel et al., 2007) combines the tropical rainforest characterized by extremely persistent precipitation with the monsoon and savanna climates with highly seasonal precipitation (Haines et al., 1988; Latrubesse et al., 2005).

Based on monthly discharge data, and following precipitation variability analyses (Wang and Ding, 2008), Plink-Björklund (2015) uses the Leier et al. (2005) dataset of 202 rivers and 16 additional rivers from <http://www.sage.wisc.edu/riverdata/> and introduces a seasonal

variability index that quantitatively separates rivers with persistent hydrology from those with variable hydrological regimes. This discharge variability index is calculated as the average discharge of the wettest minus the driest month divided by the annual mean discharge (Table 2.2) and was later renamed (Jones, 2017) as the average discharge variability index (DVI_a). Rivers with a DVI_a value < 2 are considered persistent discharge rivers, and rivers with a DVI_a value > 2 as variable discharge rivers, but with a reservation that there is a continuum and that some rivers may have a relatively high discharge variability even with DVI_a values below 2 (see also Nicholas et al., 2016). Based on the comparison of deposits from modern rivers with known DVI_a values to ancient river deposits this work suggests specific sedimentary styles for rivers with different styles of discharge variability.

Critical differences in the hydrology of variable discharge rivers were also suggested by studies of scaling relationships between river discharge and drainage basin size (Eide et al., 2017; Jones, 2017). Using daily discharge data from 415 rivers from the Global Runoff Data Centre (GRDC), Jones (2017) showed that DVI_a does not work well for highly erratic river systems with large inter-annual variability, where floods are more sporadic and may occur during different month in different years, and thus showed that just comparing persistent and variable discharge styles does not efficiently explain hydrological differences in rivers (Fig. 2.1). In order to quantify these differences, Jones (2017) introduced the cumulative discharge variability index (DVI_c), which compares the driest and the wettest months on the record with the mean discharge (Table 2.2), capturing the total range in discharge variability. DVI_c efficiently differentiates between seasonal rivers, which have low inter-annual variability and a pronounced wet season, and erratic rivers with a high inter-annual variability and single-storm controlled peak floods (Fig. 2.1). Jones (2017) further shows that river hydrological regime significantly affects discharge yields and the scaling relationships between river discharge and drainage basin area, and that peak discharge values, such as Q_{max} , Q_{99} or $Q_{99.87}$ (calculated 2-year return frequency flood) provide better correlations with drainage basin size than the mean annual discharge.

Smith et al., 2015 regional flood frequency analyses on a global scale, utilizing 703 data-points from the Global Runoff Data Centre and 242 from the United States Geologic Survey stream gauge network (<http://nwis.waterdata.usgs.gov/nwis>). They used catchment area, mean annual precipitation, and catchment slope to determine index floods, and also analyzed 1- and 7-day maximum flows. They conclude that this method improves characterization of flood behavior in data-poor regions and identifies patterns in flood behaviors between climate zones. However, although the partitioned catchment groups can provide plausible discharge estimates on a global scale, the performance of the flood-index method varies between climate regions and was found to have poor skill in replicating observed data in some cases.

The link between climate and flooding was studied by Hodgkins et al. (2017), who analyzed 1204 rivers with minimal anthropogenic influence from North America and Europe with the focus on providing historical data for the potential impact of anthropogenic climate change. This study took the approach of the 25, 50, and 100-year return period inundation level scaling of floods and grouped the rivers by continent, catchment area (small <100 km², medium 100–1000 km², large >1000 km²), and the Köppen-Geiger climate types to compensate for the relatively short historical records that individually only capture very few major floods. This study found no compelling evidence for consistent changes in major flood occurrence over time and suggested that the documented flood variability was strongly linked to wetting and drying trends caused by large-scale multidecadal ocean/atmospheric variability, such as the Atlantic Multidecadal Oscillation rather than different climate types.

The significance of inter-annual variability was emphasized by Fielding et al. (2018), who use daily discharge data from 16 rivers. They characterize rivers according to variance in peak discharge or the coefficient of variation, CVQ_p , which is equal to the standard deviation of the annual peak flood discharge over the mean annual peak flood discharge. The rivers in the study are divided into 5 groups with very low ($CVQ_p < 0.20$), low CVQ_p 0.20–0.40), moderate (CVQ_p 0.40–0.60), high (CVQ_p 0.60–0.90), and very high ($CVQ_p > 0.90$)

discharge variability. Each of the discharge variability classes is further linked to specific river depositional styles.

In summary, the Köppen-Geiger climate type (A, B, C, D and E) and mean annual discharge approach has led to a conclusion that there is at best a weak link between river hydrology and climate (e.g. Syvitski et al., 2014; Hodgkins et al., 2017), and that the key influence of climate on rivers is temperature as it affects sediment yields (Syvitski and Milliman, 1992; Syvitski et al., 2003; Syvitski and Milliman, 2007). River discharge is considered primarily a function of drainage basin size (Syvitski and Milliman, 1992; Syvitski et al., 2003; Syvitski and Milliman, 2007), although tropical rivers have been suggested to have unusually large discharges (Syvitski et al., 2014). The studies that focused on comparison of precipitation and discharge patterns (Haines, 1988; Latrubesse et al., 2005; Leier et al., 2005; Plink-Björklund, 2015; Jones, 2017; Fielding et al., 2018) establish the link between precipitation and discharge variability, and show that precipitation pattern, rather than mean annual temperature or mean annual precipitation, has a significant control on river hydrology and morphodynamics (Fig. 2.2). These efforts further provide useful dimensionless metrics (Latrubesse et al., 2005; Leier et al., 2005; Plink-Björklund, 2015; Jones, 2017; Fielding et al., 2018) that we will assess below quantitatively using a global daily discharge dataset. These studies also show the need for a more holistic river discharge analyses, as they indicate considerable variability in the hydrological behavior, morphodynamics, and the corresponding deposits of the variable discharge rivers.

2.4 Additional Discharge Variability Index

In order to examine river hydrology on the individual year scale as well as to better capture inter-annual variability with a metric calculated in a similar way to DVI_a and DVI_c , we propose the yearly discharge variability index (DVI_y , Table 2.2). DVI_y measures the difference between the highest discharge day in a year compared with the lowest discharge day in the same year divided by the average discharge. Examining the daily discharge allows for a more in detail investigation of the discharge variability as compared with discharge

averaged over a month. This new metric allows for examination of discharge variability at different temporal resolutions, from the annual to inter-annual scale, capturing variability of a single year as well as how this variability changes over time. For example, the Colorado River is an arid river that experiences major floods most years, yet the magnitude of the floods is very different year to year. Examining the hydrograph of a single year shows that the Colorado river has a bimodal flow regime, fluctuating between very low baseflow and large floods that flash through the system (Fig. 2.4a). Figure 2.4b highlights the variability of the Colorado River over 70 years of discharge records. Large decadal scale storms start to stand out as well as longer term trends such as the influence of dams and irrigation, reducing the variability through time. This variability through time gets averaged into the high DVI_y value of 43.47, with a minimum value of 1.81 and maximum value of 186.21. The mean DVI_y value is important for statistical comparison with the rest of the database and graphs of the inter-annual variability are important for comparing the nature of flooding and variability of individual rivers with each other. Figure 2.5a shows how the Colorado River ($DVI_y=43.47$) is more variable than compared with the Little River ($DVI_y= 9.11$) and the Little Beaver River ($DVI_y= 6.79$). Figure 2.5b compares the Little River and the Little Beaver River with each other, revealing how the temperate Little River is more variable year to year, while the cold and polar Little Beaver River has less variability on the interannual scale. A dam was installed approximately 50 km upstream of the Little River in 1969 which led to a marked decreased in interannual variability.

2.5 Hydroclimate Types

Based on the above presented previous quantitative approaches, we conclude that grouping rivers by the Köppen-Geiger climate types A, B, C, D, and E is not ideal due to the strong thermal emphases of this classification. Grouping by flood season and magnitude (Haines et al., 1988) is a better approach but does not allow to analyze differences in flood seasonality vs erratic occurrence of floods, or differences in intra- and inter-annual discharge variability as a function of precipitation pattern. However, the Köppen-Geiger climate classification

is widely accepted by researchers across a range of disciplines and has the highest precision as it is based on measurements from 12396 precipitation and 4844 temperature stations (Peel et al., 2007). It is also similar to the classification used in another pioneering work on flood climate by Hayden et al. (1988), in which "barotropic and baroclinic conditions of the atmosphere are an "unintended" proxy of temperature". In order to compensate for the temperature bias, we combine the Köppen-Geiger climate sub-types that are defined using precipitation patterns in addition to temperature (Peel et al., 2007), with the precipitation variability analyses of Wang and Ding (2008) (see their Figure 10 and Figure 6, respectively). The Wang and Ding (2008) precipitation analysis distinguishes perennial persistent precipitation patterns in rainforest and temperate precipitation zones from variable precipitation patterns where the precipitation range between wet and dry seasons is large as compared with the annual mean. Variable precipitation zones include the seasonally variable monsoon zone, the surrounding subtropics that receive monsoon precipitation but have a larger inter-annual variability, and the winter-wet variable discharge zones (Wang and Ding, 2008).

We define seven hydroclimate types that group some of the Köppen-Geiger climate types A, B, C, D, and E, but split others into sub-types depending on precipitation patterns as defined in Peel et al. (2007) and Wang and Ding (2008) (Fig. 3). The tropical rainforest hydroclimate type is the Af climate sub-type in the Köppen-Geiger climate classification and is defined based on the perennial precipitation style with little seasonal variability and ever-wet conditions (see Wang and Ding, 2008). The monsoon hydroclimate type is the Am sub-type in the Köppen-Geiger climate classification, and is defined based on variable and highly seasonal precipitation (Wang and Ding, 2008), linked to global monsoon circulation and related cyclones, as a function of the seasonal migration of the Inter-Tropical Convergence Zone (ITCZ; e.g. Wang and Ding, 2008). More than 80-90% of annual precipitation in monsoon regions falls during the summer monsoon (Wang and Ding, 2008). Another hydroclimate type defined by seasonally variable precipitation is the humid subtropics that corresponds to savannah sub-type Aw in the Köppen-Geiger climate classification. Mean annual precip-

itation, as well as the annual precipitation range in humid subtropics, may be similar to the monsoon zone, but the dry season precipitation tends to be lower and inter-annual variability considerably higher (Peel et al., 2007; Wang and Ding, 2008). Humid subtropical and especially arid climate types (see below) receive monsoon rain only during extreme monsoon trough migration or abnormal or strengthened monsoon seasons and associated cyclonic flow and thus experience extreme inter-annual precipitation variability. The arid hydroclimate climate type corresponds to BWh, BWk, BSh, BSk climates in the Köppen-Geiger climate classification, and is defined as having highly variable precipitation and sustained aridity (Peel et al., 2007; Wang and Ding, 2008). Temperate hydroclimates correspond to Cs, Cw, Cfa, Cfb, Cfc in the Köppen-Geiger climate classification, based on their relatively low seasonal precipitation variability (Wang and Ding, 2008). Although all temperate climate types do experience some types of seasons, the annual precipitation range as compared with the annual mean is characteristically low (Wang and Ding, 2008). Precipitation in temperate climates may be linked to tropical cyclones and thus monsoon circulation, as well as to extratropical atmospheric circulation and related low-pressure cells. Cold and polar hydroclimate types are defined by high seasonal variability in temperature and surface water availability and combine the cold and polar climate types of the Köppen-Geiger climate classification (Ds, Dw, Dfb, Dfc, Dfd, ET, EF). Separated from this group is the cold Dfa of the Köppen-Geiger climate classification, based on the low seasonal precipitation variability. Flooding in the cold and polar climate type is characteristically generated by snowmelt whereas flooding in the cold Dfa climate type comes from a combination of snowmelt and precipitation (Merz and Blöschl, 2003).

2.6 Dataset and Methods

2.6.1 Dataset

This study examines daily discharge of 499 gauging stations on pristine rivers and 76 gauging stations on non-pristine rivers from the GRDC’s river database (Fig. 2.3, Supplementary Table 2.1). Pristine rivers are defined by the GRDC as having minimal basin

development (less than 10% of the surface area modified) and planning regulations in place to restrict substantial development (to accommodate the GRDC goal of monitoring the impacts of climate change). However, this designation is up to the reporting country and there is no official standard. Non-pristine rivers were included due to their importance as major river systems and for better global coverage. The dataset was screened to include only rivers with a minimum of 20 years of daily discharge data and a minimum of less than 25% of missing data. The 20-year minimum cutoff is necessary for longer scale (decadal and inter-decadal) analysis of discharge variability. The average length of record in the database is 60 years. The drainage basin size in the dataset ranges from 20 to 4680000km² with a median of 4869km². We selected the gauging station furthest downstream for each river, although for some rivers we analyzed multiple gauging stations to examine how discharge variability changes throughout a single river system. There are a few exceptions to our screening process, where the stations are missing more than 25% of their data. Some such cases were allowed to compare two stations with each other on the same river, where only the downstream station meets the screening criteria. In polar river gauging stations winter data are missing because these rivers freeze in the winter. These exceptions were allowed as long as the record still has over 20 years of continuously collected data.

The discharge data are collected unevenly from around the world (Fig. 2.3). Rivers in the United States and Canada are overrepresented in the database with 294 rivers due to the long history of collecting discharge data by the United States Geological Survey and the Canadian National Hydrological Service. Unfortunately, we are lacking data from some critical rivers/areas such as the classic monsoonal rivers in India where we only have monthly data. We also lack data from large swaths of Asia, especially Malaysia, the Middle East, as well as most of Africa. This situation is due to a lack of accessible records or inconsistent records that do not meet the screening requirements. This study necessarily emphasizes the quality and completeness of the record of a river gauging station, as it is needed to understand patterns in discharge variability that have periodicities ranging from years to

multiple decades. There is a tradeoff between coverage and accuracy in discharge data, and the specific aims of this review limit the global coverage when compared with other studies that only examine monthly discharge data or stations with less than 20 years of data (Haines et al., 1988; Latrubesse et al., 2005; Leier et al., 2005; Plink-Björklund, 2015).

2.6.2 Assignment of Hydroclimate Types

Hydroclimate types were assigned to each river depending on the location of the gauging station based on the Peel et al. (2007) and Wang and Ding (2008) maps (Fig. 2.3). For many of the rivers this is an appropriate method. However, some river hydroclimate types needed to be reassigned because the gauging stations are located near the border between two hydroclimate types and the majority of the river length was in a different hydroclimate than the gauging station. Accordingly, we modified climate type assignments for 61 rivers (Supplementary Table 1, rivers with “†” symbol) in two geographical areas. A subset of rivers in Texas were reclassified from temperate to arid as the majority of the river length is within the arid climate zone, but the gauging stations are located across the climate boundary in a temperate climate. A subset of rivers in France were reclassified from cold and polar to temperate because their gauging stations and majority of their length was sufficiently far from the Alps.

2.6.3 Statistical Methods

The dataset is not normally distributed, as confirmed by Lilliefors testing. Therefore, to test for statistical significance of differences in discharge variability according to the defined hydroclimate types, we used a Kruskal-Wallis test paired with a multiple comparison test in MATLAB. The Kruskal-Wallis test, or one-way ANOVA on ranks, is a non-parametric method for testing whether samples originate from the same distribution, and tests the null hypothesis that $H_0 : \mu_1 = \mu_2 = \mu_3 = \dots = \mu_k$ where μ = group median and k = number of groups. Rejection of the null hypothesis H_0 leads to the conclusion that not all group medians are equal. A Kruskal-Wallis test does not determine which group medians are statistically

different from each other, only that they are different. Therefore, the *post-hoc* multiple comparison test is used to confirm where the difference occurred between the groups.

Discharge values for every river were normalized by their median discharge (Q_{50}) values (Benson, 1952) in order to compare discharge ratios across drainage basins of different sizes. For each hydroclimate type an example river was selected in order to graphically illustrate hydrograph patterns. These example rivers were chosen as close to the median value of the discharge variability indexes for each hydroclimate type as possible, considering they have drainage basins larger than 1,000km².

We include the previously published dimensionless indexes (Table 2.2). Many of the arid rivers and some polar rivers do not transmit discharge during the dry or cold seasons, respectively. Thus, in order to test the Q_{max}/Q_{min} metric all zero discharge values were replaced by value of one.

2.7 Quantitative Discharge Analysis

2.7.1 Assessment of Discharge Variability Indexes

Here we assess statistically the previously used metrics for quantitative discharge analyses. A Kruskal-Wallis and *post-hoc* comparison of means tests demonstrate that DVI_a (Plink-Björklund, 2015) splits the seven hydroclimate types into two groups (DVI_a values in Supplementary Table 2.1). The tests statistically separate the medians of persistent (rain-forest and temperate) and variable (monsoonal, humid subtropics, arid, and cold and polar) rivers with cold Dfa rivers spanning the two groups due to the range of variability (Figs. 2.6a and 2.7a, Table 2.1). Kruskal-Wallis tests further show that the discharge peakedness metric (Q_{max}/Q_{mean} of Leier et al., 2005) reveals quite similar results (Fig. 2.8a), although DVI_a measures the range of discharge divided by mean discharge, whereas discharge peakedness measures the discharge of the wettest month divided by mean discharge (Table 2).

Testing DVI_c (Jones, 2017) shows that this metric splits the highly erratic arid rivers from other river types and groups the other river types into four groups (Fig. 2.7a). The arid rivers stand out as highly variable with a median DVI_c value of nearly 20 while the

rainforest rivers have low variability with a median of ca two. Monsoon, humid subtropical, temperate, and cold and polar rivers group tightly together with cold Dfa rivers having slightly higher values (Fig. 2.7a, Table 2.3). Because DVI_c compares the wettest and driest month on record it captures longer recurrence interval extremely high and low magnitude flows that occurred within the dataset and highlights the extremes across the whole dataset. Using DVI_a and DVI_c together suggests three groups of rivers: persistent rivers (rainforest, temperate, cold Dfa) with $DVI_a < 2$ and $DVI_c < 10$, seasonal rivers (monsoonal, humid subtropical, cold and polar) with $DVI_a \geq 2$ and $DVI_c < 10$, and highly variable or erratic rivers (arid) with $DVI_c \geq 10$ (see also Jones, 2017) (Fig. 2.8b).

Testing DVI_y using a Kruskal-Wallis test and a *post-hoc* multiple comparison test shows that this metric splits the seven climate types into four groups: rainforest; monsoonal, humid subtropical, and cold and polar; temperate and cold Dfa; and arid (Figs. 2.6a and 2.7a). Using DVI_a and DVI_y together suggests the following quantitative boundaries: rainforest $DVI_a < 2$ and $DVI_y < 3$; monsoonal, humid subtropical, and cold and polar with $DVI_a > 1.5$ and $3 < DVI_y < 10$; temperate and cold Dfa with $DVI_a < 2.2$ and $5 < DVI_y < 15$; and arid with $DVI_y > 15$.

Testing CVQ_p (Fielding et al., 2018) using a Kruskal-Wallis test and a *post-hoc* multiple comparison test reveals similar results to DVI_a and DVI_c with three groups and two subgroups. Arid rivers and rainforest rivers are statistically different with group medians of 0.11 and 1.11, respectively. The five remaining hydroclimate types can be divided into two subgroups, but with overlap. The first subgroup is monsoonal, cold and polar, and humid subtropical rivers, and the second subgroup is temperate, cold Dfa, and humid subtropical rivers (Figs. 2.6b and 2.7b).

Testing Q_{max}/Q_{mean} (Latrubesse et al., 2005) splits the highly erratic arid rivers with a group median of 706. The second well-defined group is temperate and Cold Dfa. Further two somewhat overlapping groups emerge: rainforest and monsoonal; monsoonal, humid subtropical and cold and polar (Figs. 2.6b and 2.7b). Lower values for monsoonal rivers

are likely due to the multiple month duration of the monsoonal season, leading to higher Q_{mean} values and lower overall Q_{max}/Q_{mean} values. Q_{max}/Q_{min} testing does not separate statistically significant groups (Figs. 2.6b and 2.7b).

Testing $Q_{99.863}/Q_{50}$ (Jones, 2017) using a Kruskal-Wallis test and a *post-hoc* multiple comparison test reveals a split of four groups similar to DVI_y . The groups are: rainforest; monsoonal, humid subtropical, temperate, and cold and polar; cold Dfa; and arid (Figs. 2.6b and 2.7b). This is the only metric that does not group cold Dfa with another hydroclimate type. Cold Dfa rivers do not group together with temperate river as with the DVI_y , possibly because they experience more frequent flooding due to snowmelt influence. Inversely, the humid subtropical rivers have lower than expected values, with median $Q_{99.863}/Q_{50}$ of 11.49, possibly due to large inter-annual variability.

2.7.2 Quantitative Analyses of River Discharge by Hydroclimate Types

Although the dimensionless metrics presented above help to group rivers statistically, there is a large overlap between some groups. To further explore the nature of river discharge variability, below we combine the dimensionless metrics with hydrograph shape analyses.

2.7.2.1 Tropical Rainforest Rivers

Rivers in tropical rainforests (Köppen-Geiger climate type Af) have the most persistent discharge with a median DVI_a of 1.27, discharge peakedness of 1.68, DVI_c of 2.03, and DVI_y of 1.72 (Table 2.3). Due to ample and perennial precipitation, the rainforest rivers can have enormous discharges, with a median discharge of 2760m³/s and an average discharge of 23890m³/s (heavily influenced by the Amazon). Flood magnitude (median $Q_{99.863}/Q_{50}$ flow) is only 2.53 times the 50th percentile flow (Q_{50}) and the variance in peak discharge or the coefficient of variation (CVQ_p) is very low at 0.11 (Table 2.3). An example of rivers in this climate type that emerges as the median in our dataset, is the Paraná River in Brazil. The Paraná has a DVI_a of 1.27, discharge peakedness of 1.69, DVI_c of 2.14, DVI_y of 1.42, and CVQ_p of 0.14 (Table 2.4, Figure 2.9). The hydrograph of its largest flood year (Fig.

2.10a) illustrates the common nature of flooding in the tropical rainforest river; discharge slowly builds and slowly falls over the course of several months as near daily rain swells the river. Part of the drainage basin of the Paraná is in the monsoon zone and thus this rainfall pattern creates a predictable sinusoidal shape in the yearly hydrograph (Fig. 2.11), where individual flood peaks are low and there is extremely little inter-annual variation (Fig. 2.12a). For example, the peak discharge of the largest flood on record for the Paraná river, which occurred in 2009, is 17518 m³/s greater than Q₅₀, which is only 2.55 times Q₅₀ discharge.

2.7.2.2 Monsoonal Rivers

Monsoon climate (Köppen-Geiger climate type Am) rivers have the second highest median DVI_a of 2.43, discharge peakedness of 2.68, DVI_c of 5.37, and DVI_y of 4.81 (Table 2.3). Flood magnitude (median Q_{99.863}/Q₅₀ flow) is 14.04 and CVQ_p is low at 0.33 (Table 2.3). Flood regime in monsoonal rivers is defined by wet seasons that consist of multiple months of storms which occur every year. The peaks of the larger storms can be discerned on the hydrographs whereas smaller storms are difficult to discern due to the high frequency of storms and the dramatic increase in base flow during the wet season. This behavior is captured by the high DVI_a values, whereas DVI_c and DVI_y values are relatively low because the duration of the wet season raises the annual average discharge of the river. Our dataset does not include some of the classic monsoonal rivers such as the Indus or Ganges drainages due to restricted public data availability of daily discharge records. Thus the DVI and flood magnitude values may be lower than expected, as the Ganges drainage floods are known to produce flood discharges 40-50 times higher than Q₅₀ (Sinha and Friend, 1994), but the dataset does an adequate job capturing the nature and characteristics of flooding in monsoonal rivers. An example is the Chao Phraya river in Thailand. It has a DVI_a of 2.36, discharge peakedness of 2.70, DVI_c of 6.21, DVI_y of 3.25, and CVQ_p of 0.46 (Table 2.4). The hydrograph of the largest flood year (Fig. 2.10a) illustrates the nature of flooding in the monsoonal climate as storms occur one after another in the monsoon season, result-

ing in a hydrograph where individual storm peaks are barely discernable as base flow rises. Monsoonal rivers generally experience similar levels of flooding each year, as demonstrated in Figures 2.11 and 2.12a where the Chao Phraya river discharge is elevated every year on a consistent scale of five to ten times Q_{50} during the monsoon season. The DVI_y range of the Chao Phraya is very small, reflecting the consistent nature of the monsoonal climate, with a minimum of 1.23 and a maximum of 6.69.

2.7.2.3 Humid Subtropical Rivers

Rivers in humid subtropics (Köppen-Geiger climate type Aw) are characterized by a median DVI_a of 2.00, discharge peakedness of 2.21, DVI_c of 5.18, and DVI_y of 4.73 (Table 2.3). The flood magnitude (median $Q_{99.863}/Q_{50}$ flow) is 11.49 and CVQ_p is moderate at 0.43 (Table 2.3). There is a possible bias in the dataset as it is overrepresented by rivers in South America and by larger rivers. In the humid subtropics precipitation is variable on the inter-annual scale as only extreme monsoon years, or related tropical cyclones, produce intense precipitation. This inter-annual variability is indicated by higher DVI_c and DVI_y values relative to monsoonal rivers. An example of this hydroclimate type river is the Caiapo river in Brazil. It has a DVI_a of 2.17, discharge peakedness of 2.34, DVI_c of 11.38, DVI_y of 7.52, and CVQ_p of 0.44 (Table 2.4). The hydrograph of the largest flood year (Fig. 2.10a) illustrates the stark difference between the wet and dry seasons and the multiple-year hydrograph (Fig. 2.11) demonstrates the large inter-annual variability that can range from multiple years to decades. Figure 2.12a further illustrates the large inter-annual variability by demonstrating how some years consistently flood at similar levels while there are a few years that have significantly higher discharges.

2.7.2.4 Arid Rivers

Rivers in arid hydroclimates (Köppen-Geiger climate types BWh, BWk, BSh, BSk) are characterized by a median DVI_a of 2.04, discharge peakedness of 2.08, and extremely high median DVI_c and DVI_y values of 19.67 and 32.67 respectively (Table 2.3). Flood magnitude

(median $Q_{99.863}/Q_{50}$ flow) is 176.22 and CVQ_p is very high at 1.15 (Table 2.3). The extreme DVI_c and DVI_y values are related to an extreme discharge range, with low or no baseflow and large storms that can quickly cause Hortonian overland flow (Bracken and Croke, 2007). These rivers have the most variable and erratic hydrology, as indicated by the low DVI_a values. Arid climates are dominated by irregular, large-intensity storm events that last from just hours to days. The intense rainfall events trigger large-magnitude flash floods. These irregular storms and the related floods are hard to predict, due to large inter-annual variability (Figs. 2.4 and 2.11). Arid rivers may remain dry for years or decades and transmit flood discharges that exceed their average discharge 100-1500 times in response to storms. An example of this climate type river is the Smoky Hill river in the USA. It has a DVI_a of 2.10, discharge peakedness of 2.34, DVI_c of 27.20, DVI_y of 29.69, and CVQ_p of 0.95 (Table 2.4). The largest flood year on record (Fig. 10a) had three large flood events and several smaller flood events that elevated baseflow from the normal near-zero or zero-flow levels. The multiple-year hydrograph in Figure 2.11 demonstrates the large inter-annual variability where half of the years have extreme floods that are 150 times Q_{50} . Figure 2.12b demonstrates how over 96 years of record, the Smoky Hill River is dominated by individual, extremely large floods.

2.7.2.5 Temperate Rivers

Rivers in temperate hydroclimates (Köppen-Geiger climate types Cs, Cw, Cfa, Cfb, Cfc) are characterized by a median DVI_a of 1.45, discharge peakedness of 1.80, DVI_c of 5.41, and DVI_y of 8.21 (Table 2.3). Flood magnitude (median $Q_{99.863}/Q_{50}$ flow) is 17.60 and CVQ_p is moderate at 0.48 (Table 2.3). Flood events in temperate rivers are characterized by distinct events that are five to 30 times median Q_{50} discharge (Fig. 2.10b). Thus, these individual storms have a large influence on river hydrology, but not of the same order of magnitude as in arid rivers. An example of rivers in this climate type is the Nottoway River in the USA. It has a DVI_a of 1.47, discharge peakedness of 1.94, DVI_c of 10.42, DVI_y of 7.27, and CVQ_p of 0.60 (Table 2.4). The hydrograph of the largest flood year (Fig. 2.10b) demonstrates the

impact of single storms throughout the year that are not connected to seasonal factors as in monsoonal systems. The multiple-year hydrographs in Figures 2.11 and 2.12a show both inter-annual variation in frequency and range, as well as a lack of seasonal controls.

2.7.2.6 Cold Dfa Rivers

Rivers in cold Dfa hydroclimates (Köppen-Geiger climate type Dfa) are characterized by a median DVI_a of 1.68, discharge peakedness of 2.03, DVI_c of 8.51, and DVI_y of 10.01 (Table 2.3). Flood magnitude (median $Q_{99.863}/Q_{50}$ flow) is 31.99 and CVQ_p is moderate at 0.57 (Table 2.3). The relatively low DVI_a and relatively high DVI_c and DVI_y values indicate the relatively low seasonality and the significance of individual storm events exhibited as peaks on hydrographs. These systems are characterized by a mix of winter wet precipitation and snow melt runoff later in the year that can be ten to 40 times the median Q_{50} discharge as is demonstrated in the largest flood hydrograph of the example river in Figure 2.10b. The cold Dfa climate type as defined by Peel et al. (2007) has an average temperature of the hottest month $> 22^\circ\text{C}$ and the average temperature of the coldest month $\leq 0^\circ\text{C}$, with no dry or wet season. The large range in temperature of these systems contributes to the high DVI_y variability due to the influence of both single event storms and snowmelt. The period for snowfall in these systems has a shorter duration than in cold-and-polar systems, leading to less delay in water being released from snowmelt. Due to the larger swings in temperature, the snowmelt may occur over a shorter time period, leading to lower DVI_a and higher DVI_y values. A representative example of rivers in this climate type is the Iowa river in the USA. It has a DVI_a of 1.79, discharge peakedness of 1.70, DVI_c of 10.43, DVI_y of 9.30, and CVQ_p of 0.70 (Table 2.4). The largest flood year hydrograph (Fig. 2.10b) shows a series of single event storms occurring in the spring, a large snowmelt peak in June, and low baseflow for the rest of the year. The multiple-year hydrographs in Figures 2.11 and 2.12b demonstrate a higher inter-annual consistency than in temperate climates, while the lack of more seasonal controls still leads to some inter-annual variation.

2.7.2.7 Cold and Polar Rivers

Rivers in cold and polar hydroclimates (Köppen-Geiger climate types Ds, Dw, Dfb, Dfc, Dfd, ET, EF) are characterized by a median DVI_a of 2.55, discharge peakedness of 2.68, DVI_c of 5.69, and DVI_y of 6.70 (Table 2.3). Flood magnitude (median $Q_{99.863}/Q_{50}$ flow) is 18.93 and CVQ_p is 0.39 (low) (Table 2.3). The higher DVI_a and discharge peakedness values and lower DVI_c and DVI_y values, as compared with the cold Dfa rivers indicate a larger seasonality. The control on these systems is the amount of precipitation stored as snowpack during the winter months and the rate and duration of subsequent snowpack melt. The several months of restrained discharge is released when the temperature rises above 0°C the snow and ice start to melt. This control gives the annual hydrograph in cold and polar systems a characteristic strongly right-skewed distribution curve, where there is very little discharge during the winter months followed an abrupt increase in discharge that decays exponentially. The magnitude of floods in cold and polar rivers is three to 15 times the median Q_{50} discharge. A representative example of rivers in this climate type is the Little Beaver river in the USA. It has a DVI_a of 2.60, discharge peakedness of 2.67, DVI_c of 7.96, DVI_y of 6.80, and CVQ_p of 0.44 (Table 2.4). The right-skewed distribution discharge curve with an immediate peak followed by an exponential decrease is clearly shown in the largest flood hydrograph (Fig. 2.10b). The multiple-year hydrographs in Figures 2.11 and 2.12b show consistent inter-annual discharge patterns due to the strong seasonal snowmelt control.

2.7.3 Hydrological River Groups

Our analysis shows that each of the different temporal resolutions has strengths and weaknesses, which is why it is useful to consider the metrics in ensemble. Annual variability showcases the nature of flooding in a river by examining the hydrograph and considers the magnitude and character of floods. It is useful for event based assessment, such as major flood analysis. However, it is difficult to contrast rivers against each other when only looking at one year's worth of data. Inter-annual variability best demonstrates the range of variability

within a river and statistics can be run on the variability of each river to find the rate of variability. The above discharge analyses of indexes and hydrograph shapes further shows that the indexes alone do not capture the nature of river hydrology and flood behavior, and that a more holistic analysis of hydrograph shape is essential. The above combined analyses suggest that river hydrology falls into four groups:

- Rivers with persistent hydrology: rainforest rivers
- Rivers with single storm controlled hydrological variability: cold Dfa and temperate rivers
- Rivers with seasonal hydrology: monsoonal, cold and polar, humid subtropical rivers
- Rivers with extreme and erratic hydrology: arid rivers

The differences in groups are defined by the character and magnitude of flooding (Figs. 2.10, 2.11, and 2.12). Persistent rivers receive nearly continuous rainfall throughout the year and the largest floods are one and a half to three times the median discharge and build over the course of several months. Single storm controlled rivers are characterized by largest floods that are ten to 40 times the median discharge controlled by single precipitation events that last from hours to days. Seasonal systems are characterized by largest floods that are four to 20 times the median discharge and are caused by the seasonal influence of either monsoons or snowmelt. Extreme systems are characterized by large floods that are 100-1500 times the median discharge and single precipitation events that sweep through the system. We thus show significant differences in flood magnitude and occurrence patterns between the four groups of rivers. These analyses further suggest that the morphodynamics and deposits of these river groups are likely to differ due to large differences in flood magnitude, duration, and variability.

It is interesting that the river groups defined here by hydrograph analyses and the ensemble of dimensionless discharge metrics are quite similar to the results of flood climate

analyses by Hayden et al. (1988), despite that their analyses was based on precipitation not river discharge. Hayden et al. (1988) organized flood regions (see their Figure 9) on the basin of perennial vs seasonal precipitation patterns, and further subdivided perennial precipitation into intertropical convergence zone, organized convective activity at the synoptic scale, and unorganized convective activity as in the case of individual thunderstorms. Thus, their precipitation criteria and our outcomes based on discharge patterns are comparative. Comparison to the results of Haines et al. (1988) discharge analyses is more difficult due to their focus on specific timing of the floods.

2.8 Discharge Variability and Drainage Area

A common assumption is that large river systems will have less variability in discharge (see Syvitski et al., 2003). Using the Syvitski et al. (2003) definition for large rivers as having drainage basins $>25,000\text{km}^2$, 122 rivers in our database are large rivers and 453 are small rivers. Small rivers have a median DVI_a of 1.81, discharge peakedness of 2.11, DVI_c of 6.70, DVI_y of 8.65, CVQ_p of 0.50, and $Q_{99.863}/Q_{50}$ of 24.51. Large rivers have a median DVI_a of 1.88, discharge peakedness of 2.15, DVI_c of 4.41, DVI_y of 3.24, CVQ_p of 0.30, and $Q_{99.863}/Q_{50}$ of 8.22 (see Table 2.5). DVI_a and discharge peakedness values are marginally higher, but nearly equal. This outcome implies that drainage basin size does not affect discharge variability on the average monthly scale (DVI_a and discharge peakedness). The drainage basin size does exhibit minor control on discharge variability when accounting for the range of discharge events (captured by DVI_c). DVI_y and $Q_{99.863}/Q_{50}$ values are significantly lower in large rivers. This is likely influenced by a multitude of factors: storms and other single precipitation events exhibit a stronger influence on smaller systems where a single storm covers a larger proportion of the drainage basin area. Also, rivers in rainforest climate types, which have very persistent discharge and overall low DVI_y values, tend to be larger systems. CVQ_p is also lower in larger rivers than in smaller rivers indicating that smaller rivers are more variable on the interannual scale.

There is no correlation between DVI_a , discharge peakedness, and DVI_c and drainage area. There is a weak negative linear correlation ($r^2=0.22$) between DVI_y and drainage area (Fig. 2.13). Extremely large rivers ($>1,000,000\text{km}^2$, $n=17$) are the main drivers of this correlation. Climate exhibits some control when examining the relationship between drainage area and discharge variability: cold Dfa $r^2=0.47$, humid subtropical $r^2=0.43$, rainforest $r^2=0.39$, monsoonal $r^2=0.21$, temperate $r^2=0.21$, cold and polar $r^2=0.18$, and arid $r^2=0.15$ (Fig. 2.13). Rivers of some hydroclimate types such as humid subtropical, cold, and rainforest are more sensitive to the drainage basin size. Given the different hydrology of these three climate types, it is not clear why there is the stronger link in these climate types. When considering the four different hydrological groups, there is a stronger connection between discharge variability and drainage area in rivers that have a persistent ($r^2=0.39$) or seasonal ($r^2=0.27$) hydrology compared to rivers that have single storm controlled ($r^2=0.19$) or extreme and erratic ($r^2=0.15$) hydrology (Fig. 2.13). Overall the connection between drainage basin size and discharge variability is weak across the global dataset, and this relationship is strongest in rivers with persistent discharge.

2.9 Discharge Variability within Individual Rivers

It is commonly assumed that discharge variability decreases downriver (Syvitski et al., 2003). To determine how discharge variability changes downstream we used multiple gauging stations within 65 rivers. These analyses show that there is a slight decreasing trend in discharge variability as the size of a river system increases. Of the 65 rivers, in 28 ($\sim 46\%$) DVI_a increases downriver and in 37 ($\sim 54\%$) DVI_a decreases downriver (Table 2.6, Fig. 2.14). In 15 rivers ($\sim 23\%$) DVI_a shifted above or below the value of two. Interestingly 12 of the 15 rivers where DVI_a value shifted from above or below the value of two were either cold Dfa or cold and polar rivers. Geographical observations of these rivers indicate that the majority of the polar stations that decrease in DVI_a downriver are further away from topographic highs, suggesting a decreasing snowmelt impact the further away from the snowpack location. CVQ_p has a similar trend with 30 (out of 64, $\sim 47\%$) increasing in discharge variability and

34 (out of 64, $\sim 53\%$) decreasing in discharge variability. Similar to DVI_a , 14 rivers ($\sim 22\%$) have changes in CVQ_p greater than 0.2. What concerns DVI_c , then 28 ($\sim 43\%$) of the rivers increase and 37 ($\sim 57\%$) of the rivers decrease in DVI_c downstream. The decreasing trend gets stronger when examining discharge peakedness where 26 ($\sim 40\%$) of the rivers increase and 39 ($\sim 60\%$) decrease downriver. The strongest decrease trend is measured with the DVI_y metric, as 23 rivers ($\sim 36\%$) increase and 41 ($\sim 64\%$) decrease in DVI_y downriver. These differences may be because DVI_y is driven by the largest yearly precipitation event in the system, which gets buffered as the discharge slug heads downstream whereas DVI_a looks at the averaged discharge for each month and therefore is less influenced by single storm events.

We conclude that there is no simple relationship between downstream decrease or increase in discharge variability. A majority of rivers analyzed have similar levels of discharge variability for the majority of their reach. Furthermore, discharge variability is ultimately influenced by a number of different variables such as hydrological connectivity and whether a river passes through multiple hydroclimate zones. Some rivers pass through multiple hydroclimate zones with distinct precipitation patterns and their hydrology can correspondingly be affected. For example, the Columbia River with its headwaters and gauging station number 4215660 (north of Golden, British Columbia) in a cold and polar climate, correspondingly has a DVI_a value of 2.90 (seasonal) and the characteristic right-skewed snowmelt discharge pattern with a sudden initial peak that slowly tails off through the summer months. As the Columbia River turns south and crosses the border into the United States, the river reaches a temperate climate region. The DVI_a drops to 1.57 (persistent) and the flooding pattern has the characteristic more normal distribution of temperate rivers (Figs. 2.15a and 2.15b).

2.10 Conclusions

Assessment of quantitative methods (metrics) of river discharge variability analyses identifies different strengths in these methods and shows that a combination of multiple dimensionless numbers captures river discharge variability patterns better than any single metric. However, the hydrograph shape analysis is critical for understanding the differences in in-

dexes. The ensemble of dimensionless numbers and hydrograph shape analyses presented in this paper provides better understanding of discharge variability and how that variability is linked to global climate, with implications for flood prediction, risk analyses, and mitigation strategies, as well as for better understanding of river morphodynamics. Some metrics, such as average discharge variability index (DVI_a) and peakedness (Q_{max}/Q_{avg}), distinguish variable and persistent discharge regimes, whereas other metrics, such as cumulative discharge variability index (DVI_c) and yearly discharge variability index (DVI_y) are able to distinguish erratic and single storm controlled hydrology from seasonal regimes. The yearly discharge variability index (DVI_y) and the coefficient of variation, CVQ_p are measures of inter-annual variability. Application of a combination of these metrics to the global daily discharge analyses of 575 gauging stations shows that river discharge patterns fall into four statistically different and predictable groups as characterized by flood magnitude, hydrograph shape, and inter-annual variability. These hydrological groups occur in different hydroclimate types. Rivers with persistent hydrology occur in tropical rainforest zone. Rivers with single storm controlled hydrological variability occur in cold Dfa and temperate climates. Rivers with seasonal hydrology occur in monsoon zone, humid subtropics, and in cold and polar climates. Arid climate rivers have extreme and erratic hydrology. We thus show a strong link between river hydrograph shapes and discharge variability patterns to hydroclimate and precipitation regimes. We also show that there is only a weak correlation between discharge variability and drainage basin size and that there is no simple relationship of downstream decrease in discharge variability.

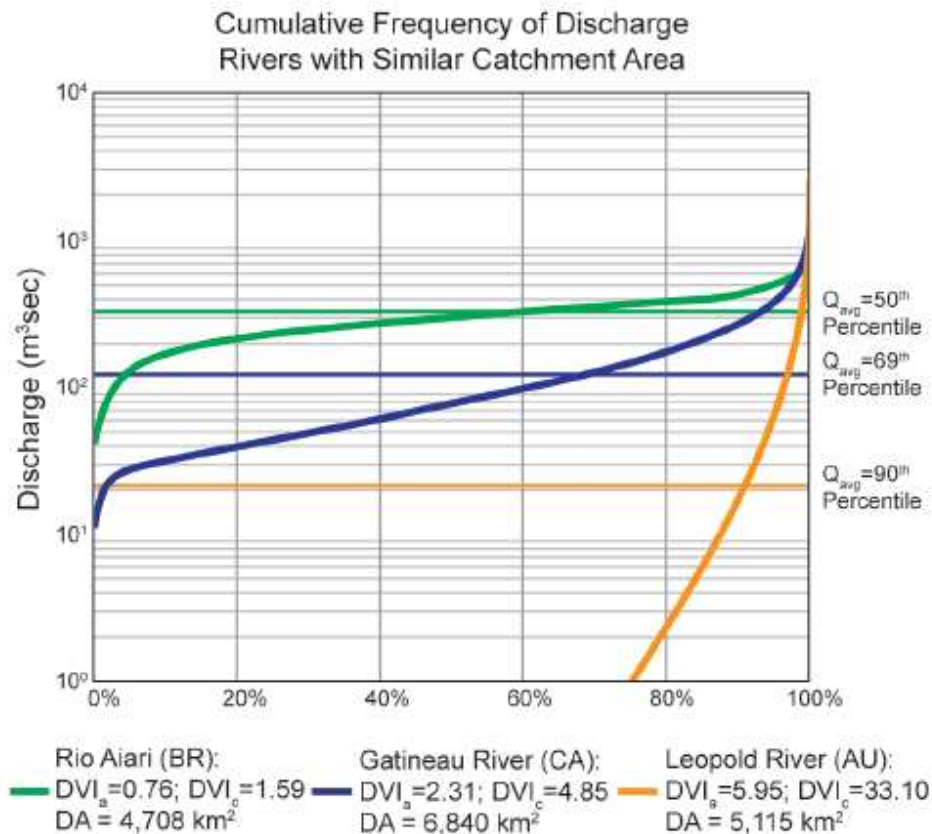


Figure 2.1: A comparison of the cumulative frequency discharge of three rivers with similar drainage basin size (approximately 5000 km^2), but different hydrological regimes (From Jones, 2017). The average discharge of the persistent Rio Aiari is more than one hundred times larger than that of the erratic Leopold River. The hydrograph distributions are clearly different with only the Rio Aiari approaching normal distribution. Data from the Global Runoff Data Base. Drainage Area is represented by “DA”. The definition for the metrics DVI_a and DVI_c can be found in the text or Table 2.2.

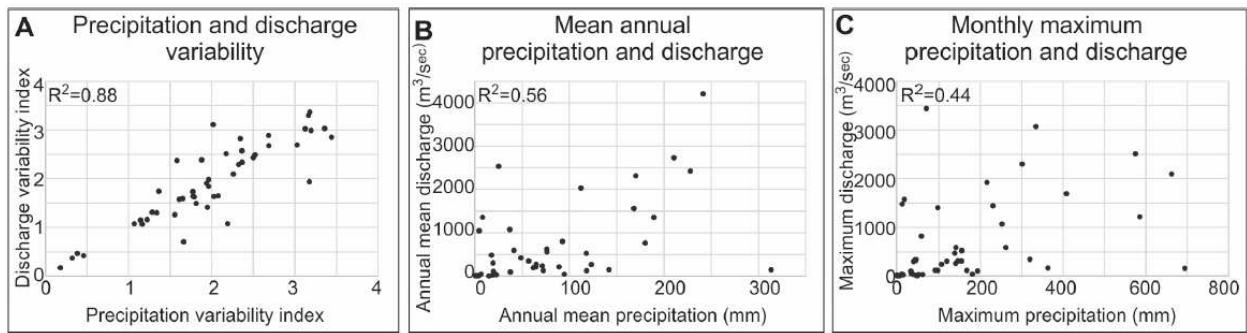


Figure 2.2: Link between precipitation and discharge variability (A), annual mean (B) and monthly maximum (C). Monthly discharge and precipitation data from Leier et al. (2005). Discharge and precipitation variability indexes are calculated as monthly maximum minus monthly minimum divided by annual mean (from Plink-Björklund, 2015).

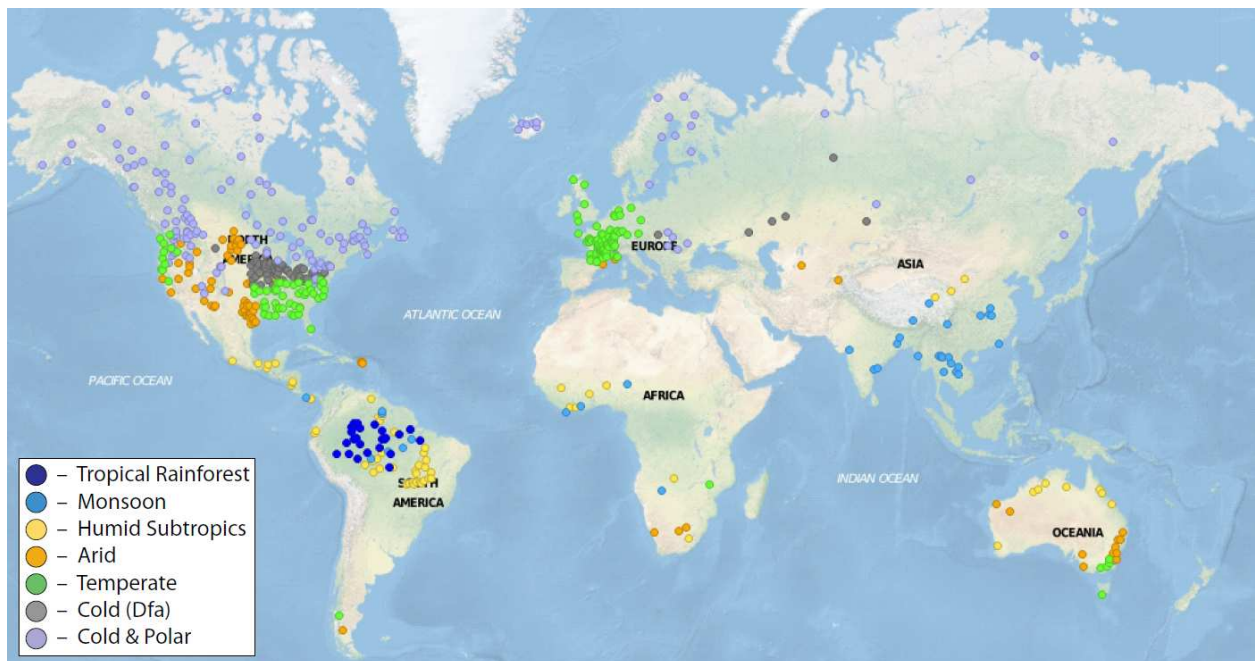


Figure 2.3: Map distribution of the 575 discharge stations from the Global Runoff Data Base, shown as dots that indicate hydroclimate types by color.

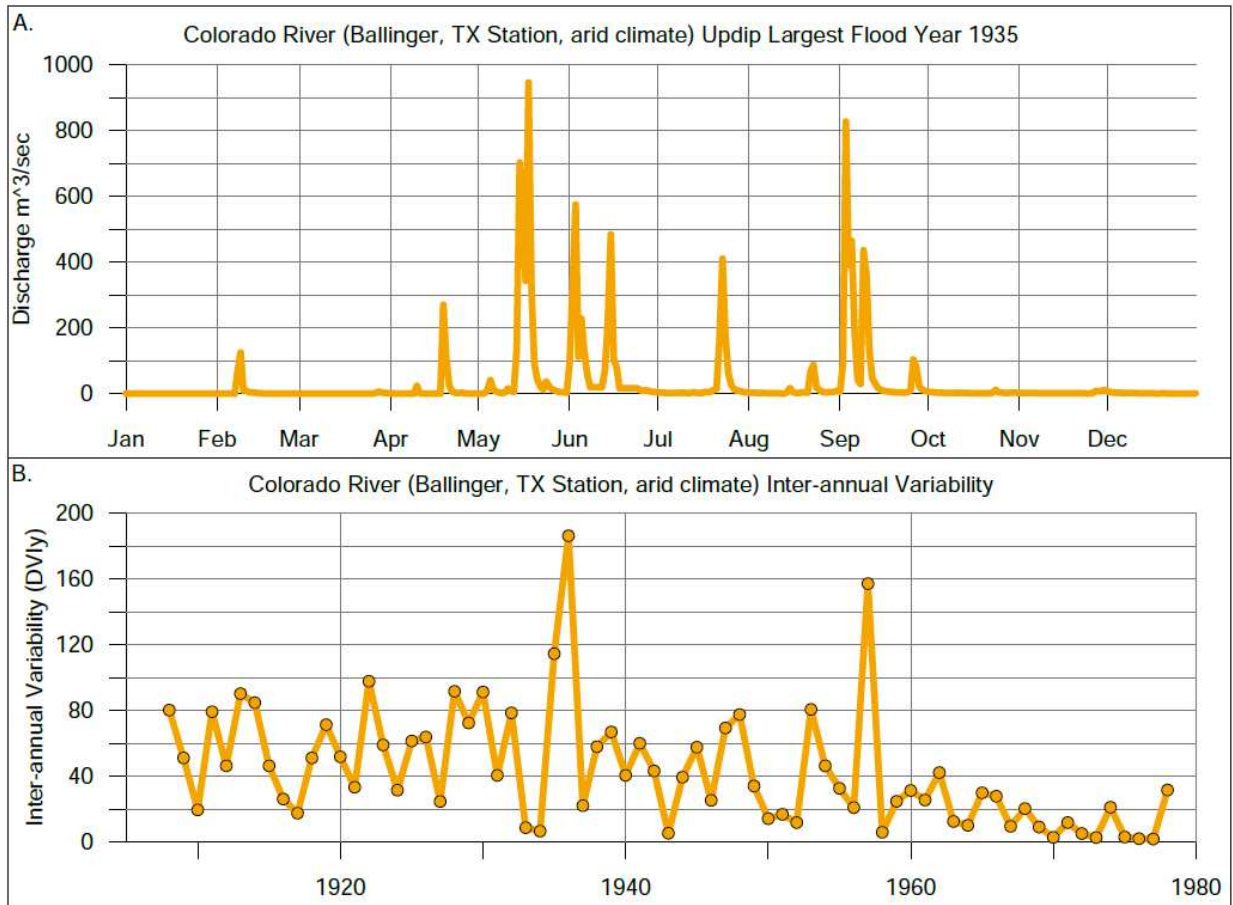


Figure 2.4: Colorado River Hydrographs (A) Colorado River (Ballinger, TX Station) 1935 hydrograph, the largest flood year demonstrates the binary character of flooding. (B) 70 years of discharge variability in the Colorado River indicate two large flood years and the significant reduction in discharge variability since late 1950s.

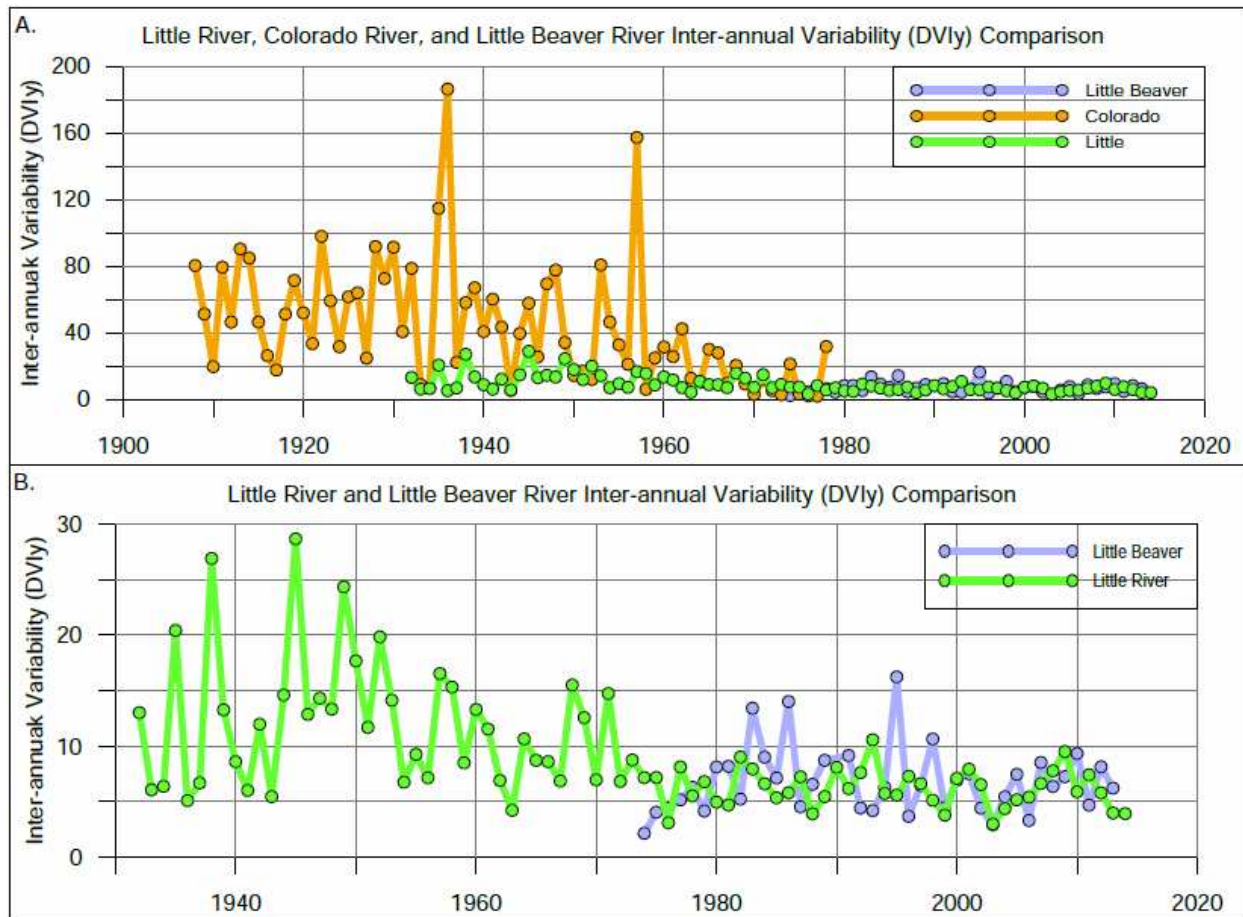


Figure 2.5: Comparison of inter-annual variability between (A) the Colorado River (arid), the Little River (temperate), and the Little Beaver River (polar). (B) Comparison of inter-annual variability between the Little River (temperate) and the Little Beaver River (polar).

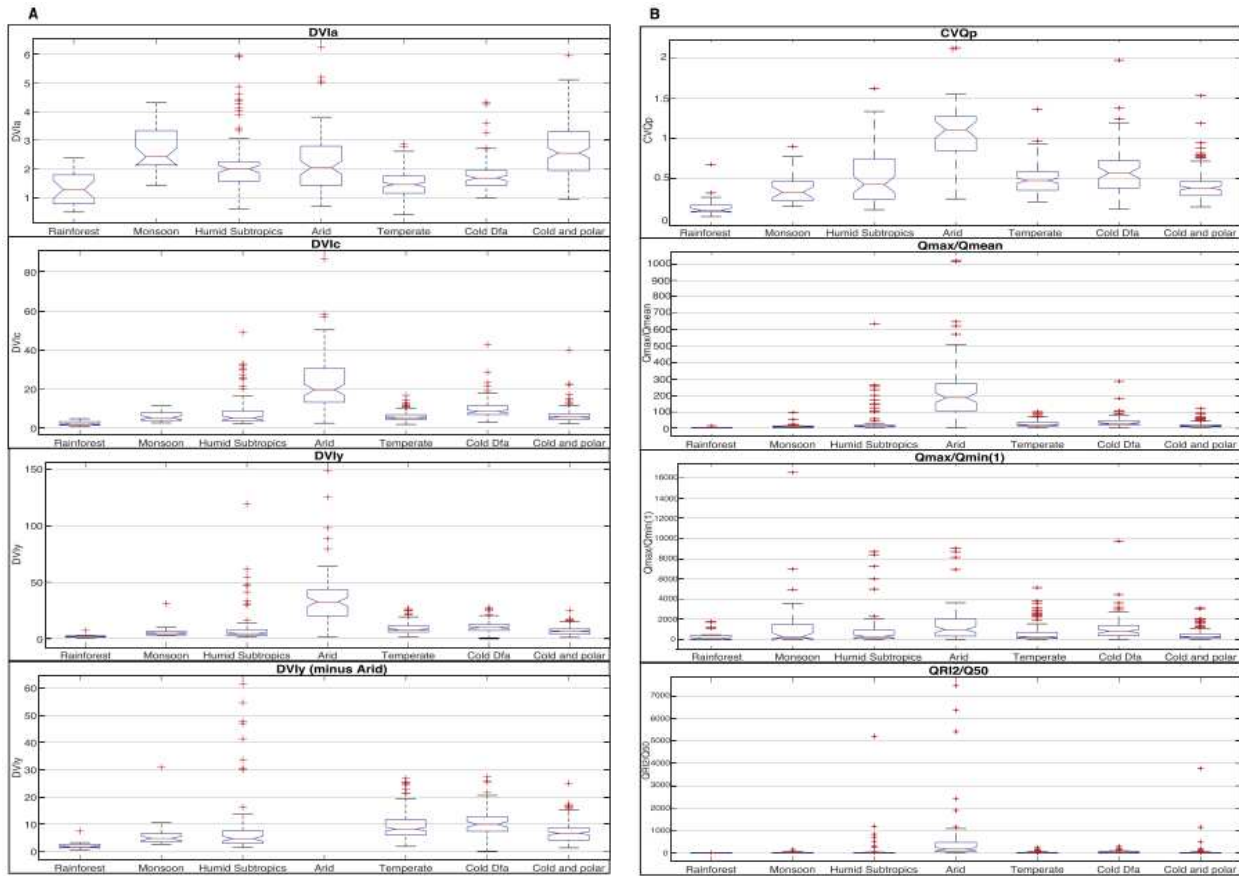


Figure 2.6: Discharge variability values of the 7 hydroclimate groups (A) Discharge variability values for DVI_a , DVI_c , DV_{ly} . The fourth box and whisker plot is a second plot of DV_{ly} with the Arid hydroclimate removed to better show the differences between the remaining six hydroclimates (B) Discharge variability values for CVQ_p , Q_{max}/Q_{mean} , $Q_{max}/Q_{min}(1)$, and QR_{12}/Q_{50} .

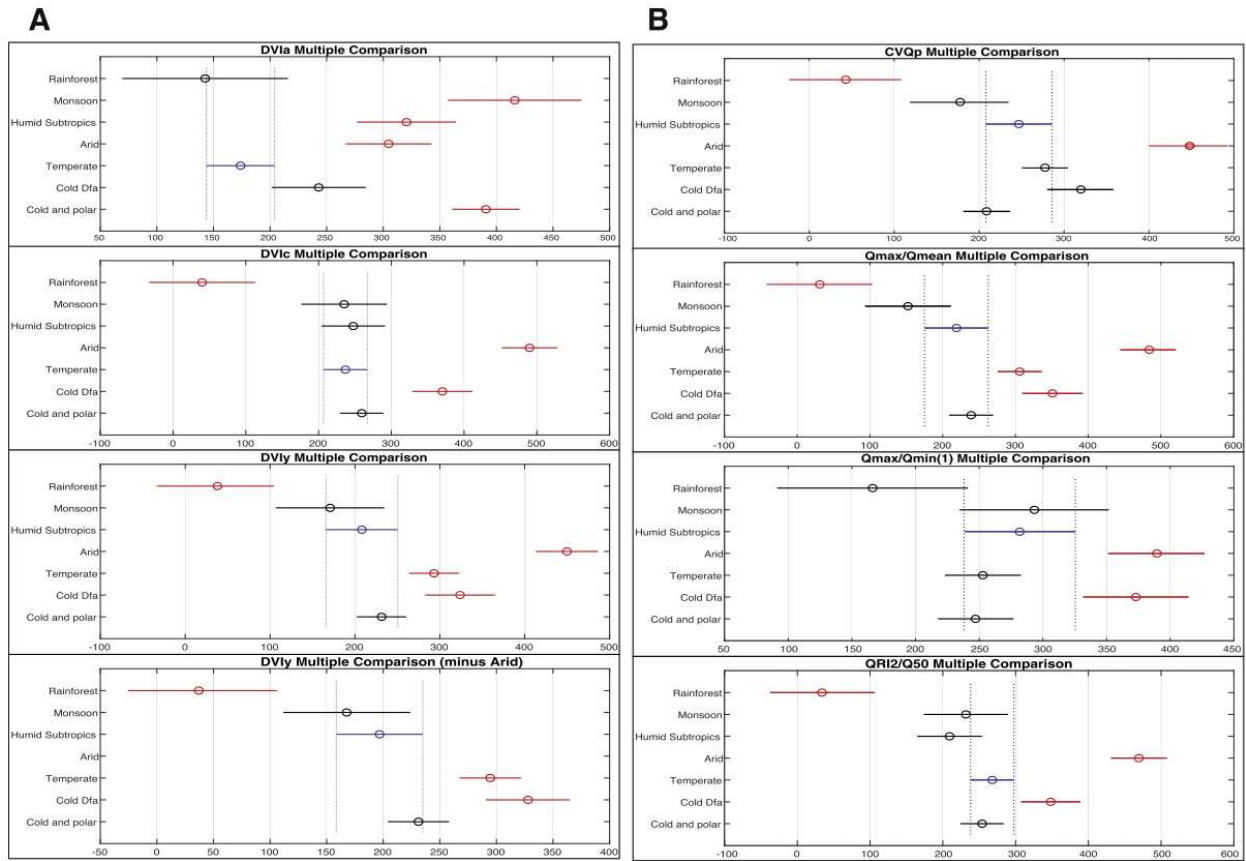
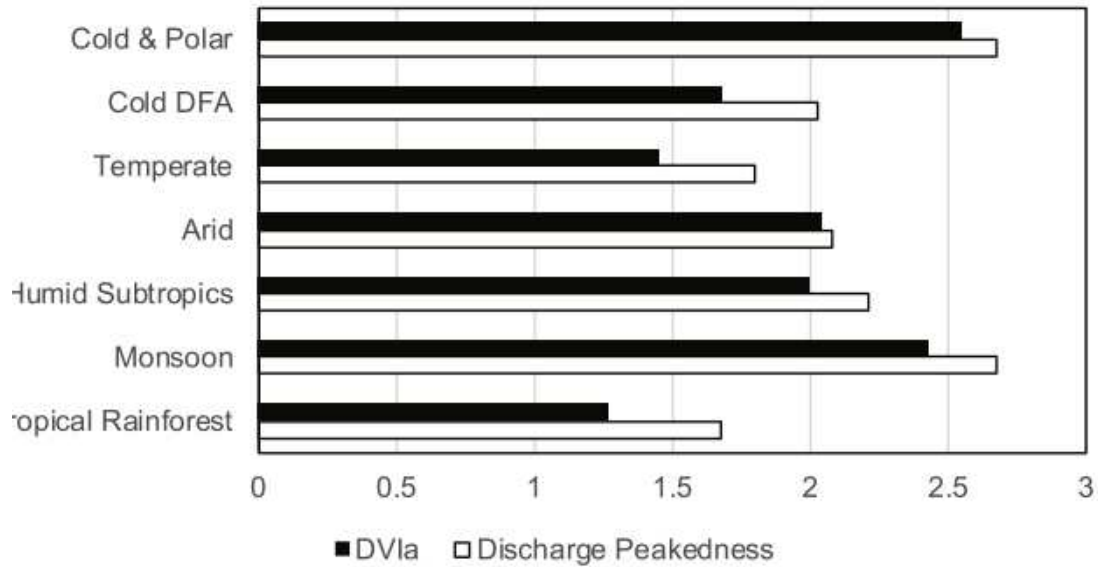


Figure 2.7: Multiple comparison tests on the Kruskal-Wallis test results. Hydroclimates that are statistically similar to the selected hydroclimate (blue) are shown in black, while hydroclimates that are statistically different are shown in red. The width of the line represents the range of ranks by the Kruskal-Wallis test. (A) Comparison for DVI_a , DVI_c , DVI_y . The fourth plot is a second plot of DVI_y with the Arid hydroclimate removed to better show the differences between the remaining six hydroclimates. (B) Comparison for CVQ_p , Q_{max}/Q_{mean} , $Q_{max}/Q_{min}(1)$, and Q_{RI2}/Q_{50} .

A Comparison of DVI_a and Discharge Peakedness



B

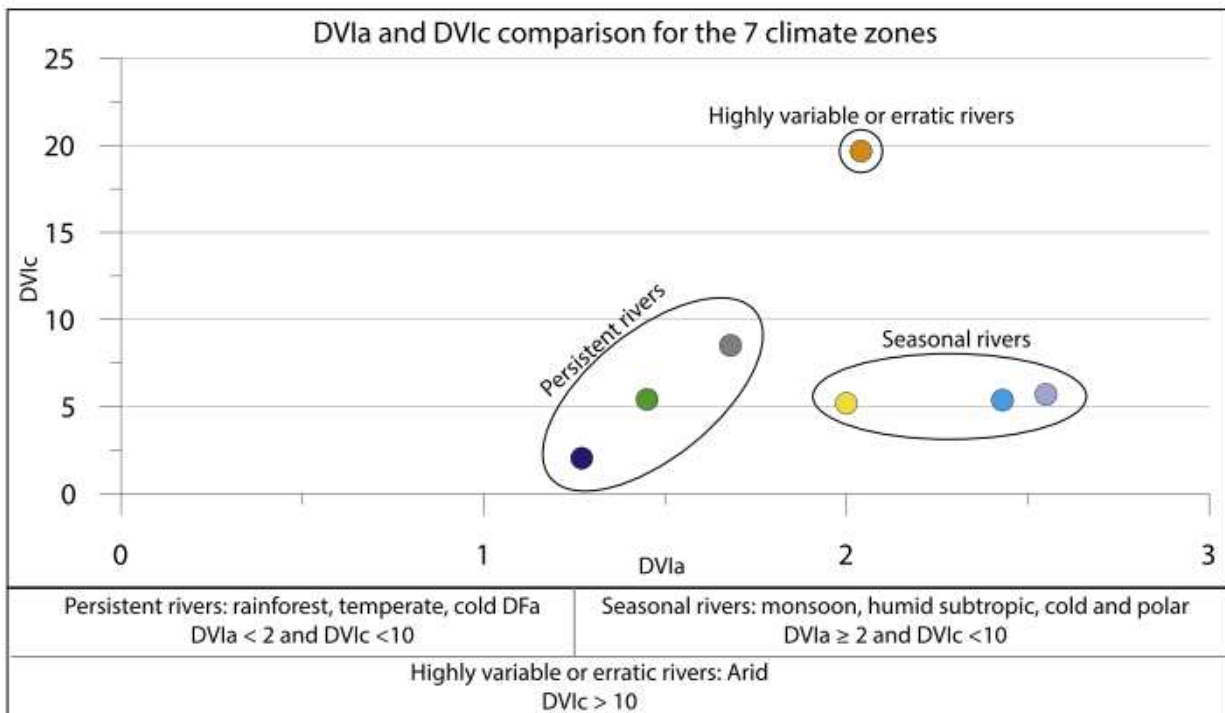


Figure 2.8: Discharge variability indexes grouping. (A) Comparison of DVI_a and Discharge Peakedness revealing similar results. (B) Using DVI_a and DVI_c together suggests three groups of rivers.

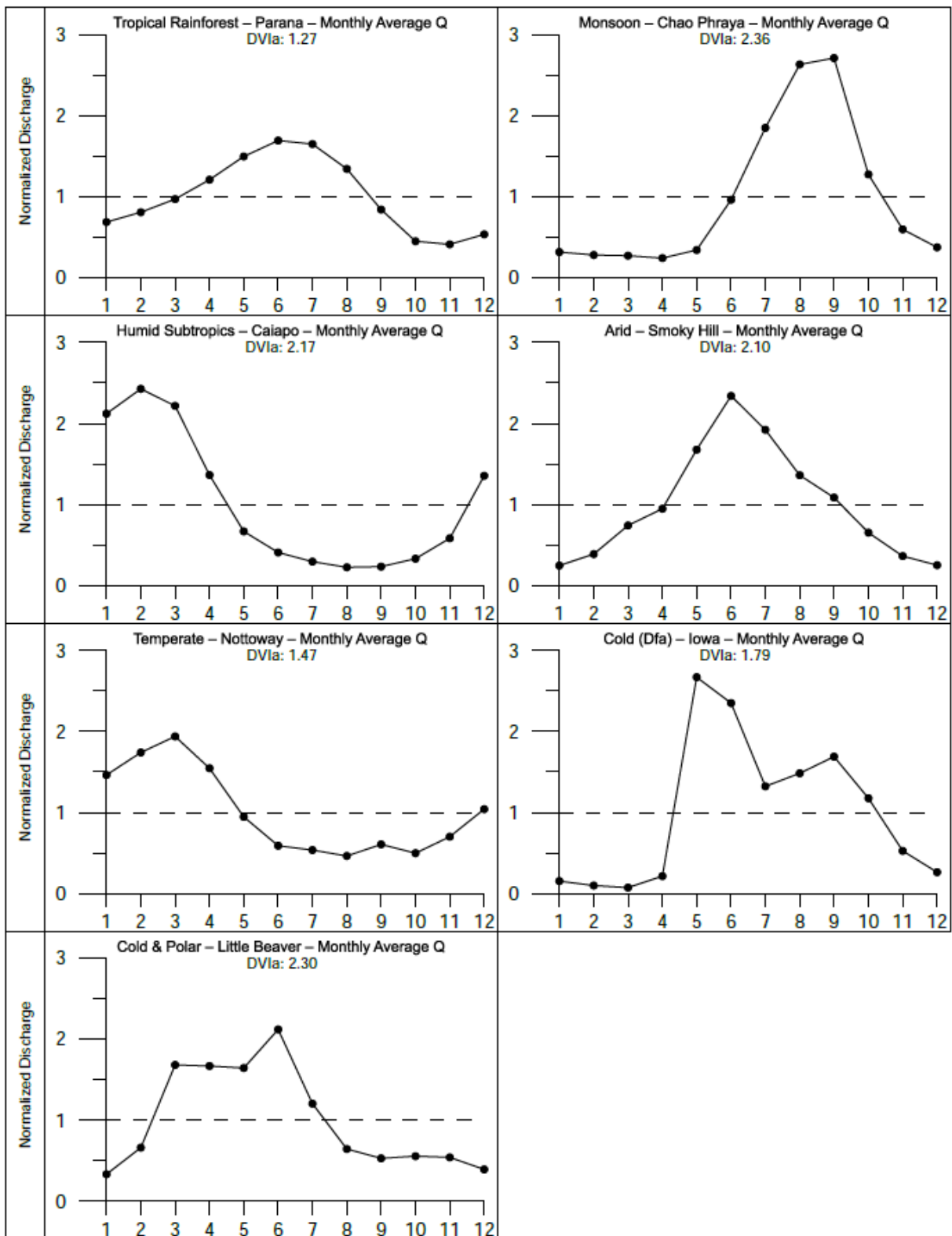


Figure 2.9: Normalized monthly average discharge graphs of the example rivers of the 7 climate types. Dashed line indicates 50th percentile discharge (Q_{50}).

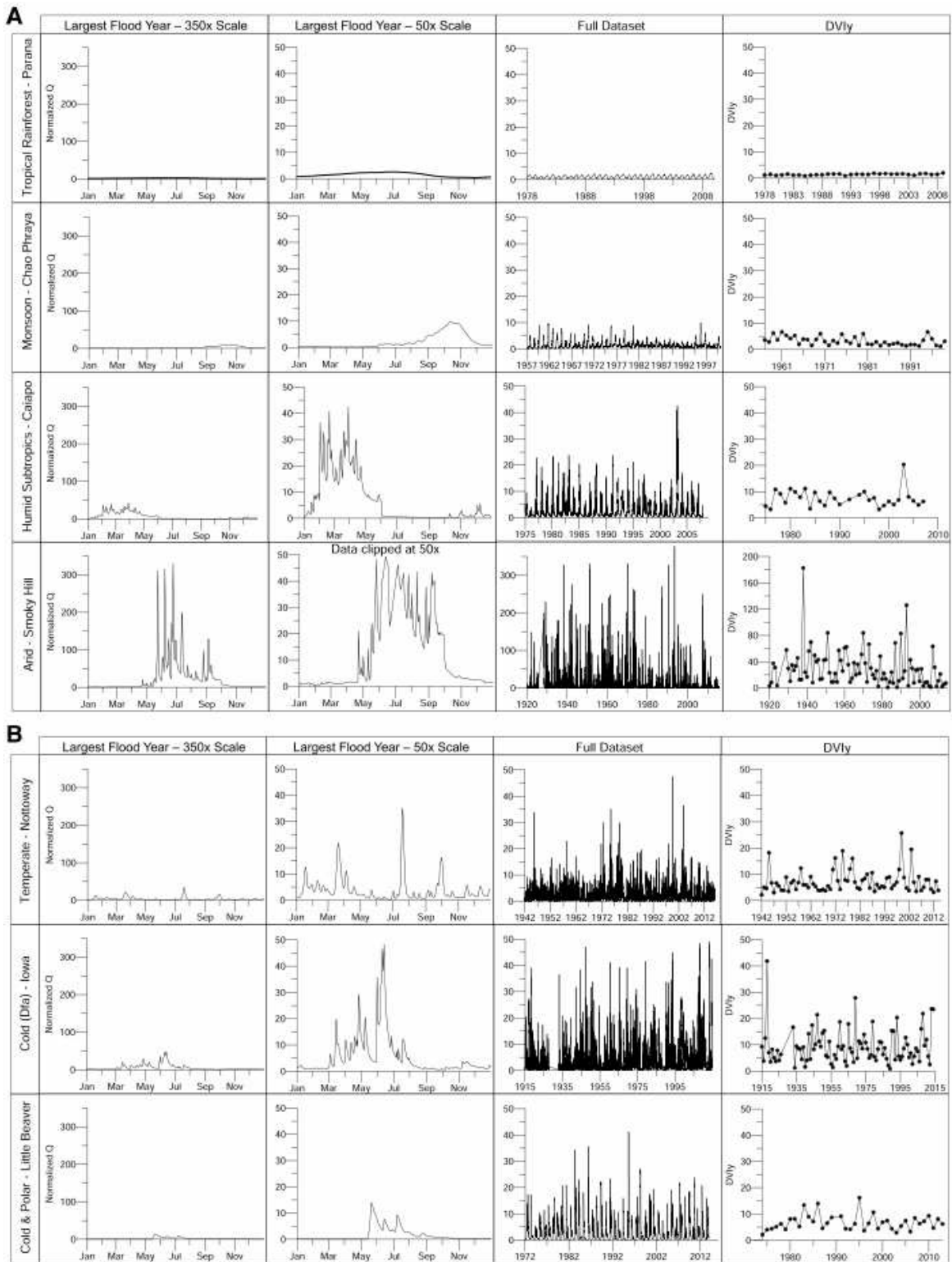


Figure 2.10: Largest flood examples for the representative rivers for each hydroclimate zone. Parana – Tropical Rainforest, Chao Phraya – Monsoon, Caiapo – Humid Subtropics, Smoky Hill – Arid, Nottoway – Temperate, Iowa – Cold (Dfa), Little Beaver – Cold & Polar.

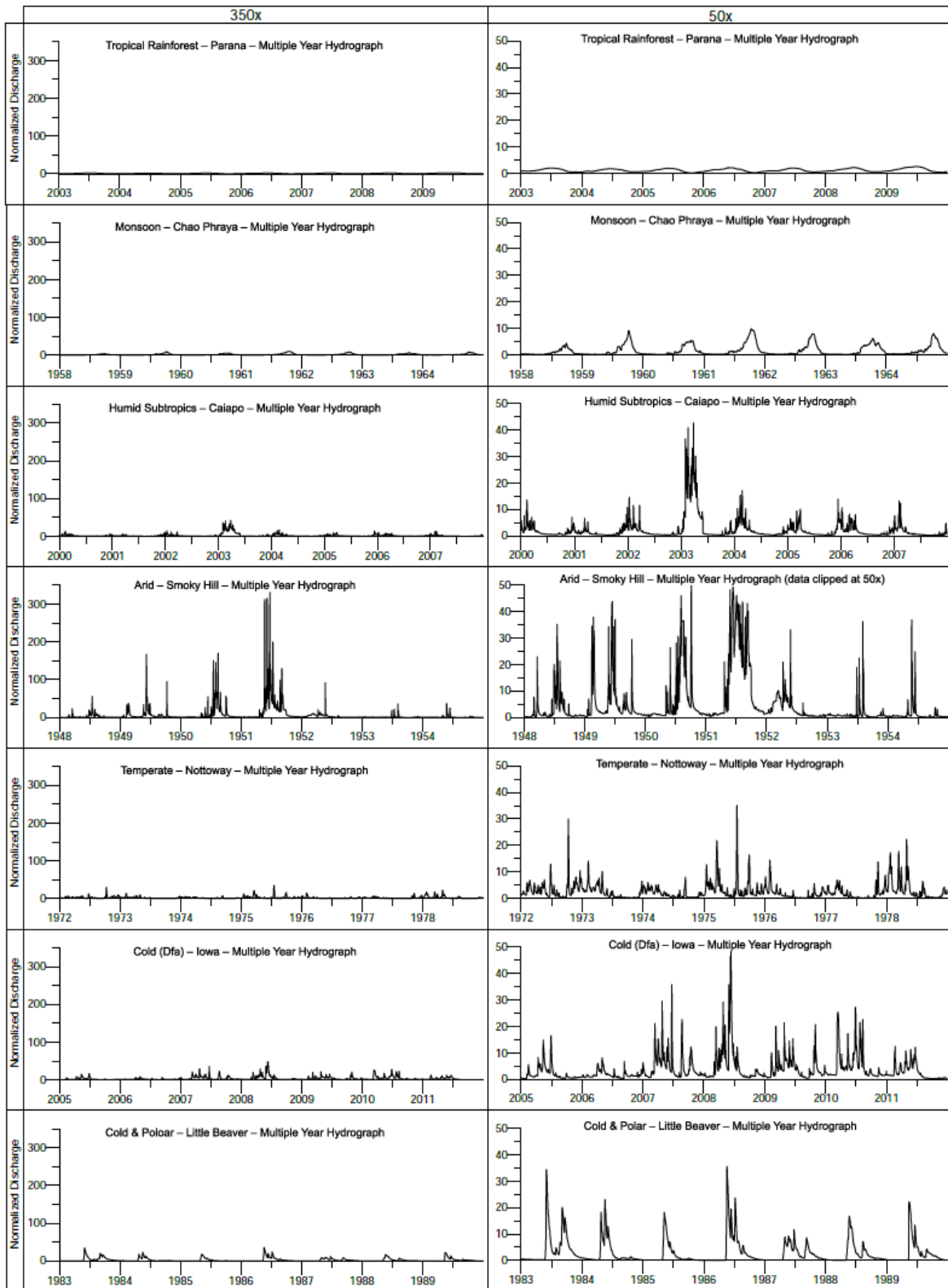


Figure 2.11: Multiple-year hydrographs (7 years) clustered around the largest flood year demonstrate flooding character in different systems as well as inter-annual variability

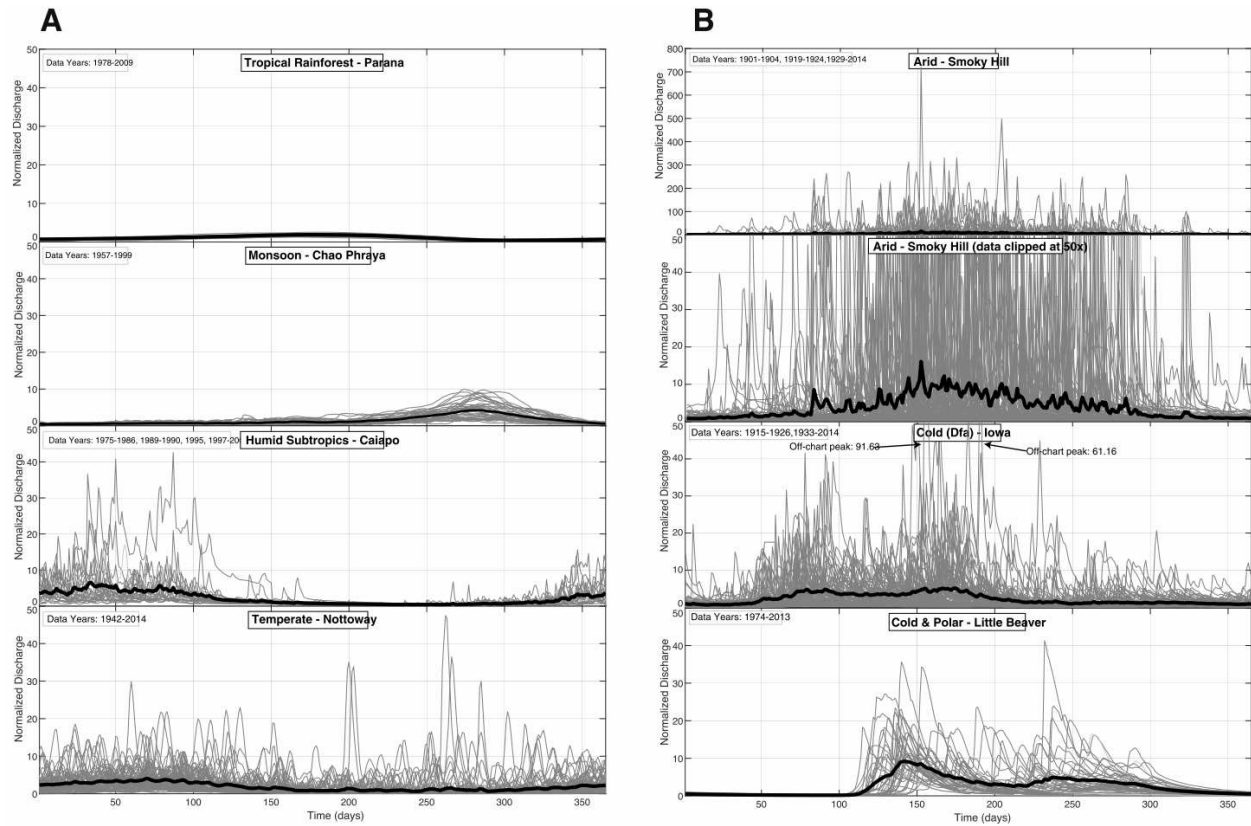


Figure 2.12: Hydrographs of the representative rivers for each hydroclimate zone. Each year of data is graphed individually as thin grey lines and the average discharge for each day is represented by the thick black line. Parana – Tropical Rainforest, Chao Phraya – Monsoon, Caiapo – Humid Subtropics, Smoky Hill – Arid, Nottoway – Temperate, Iowa – Cold (Dfa), Little Beaver – Cold & Polar.

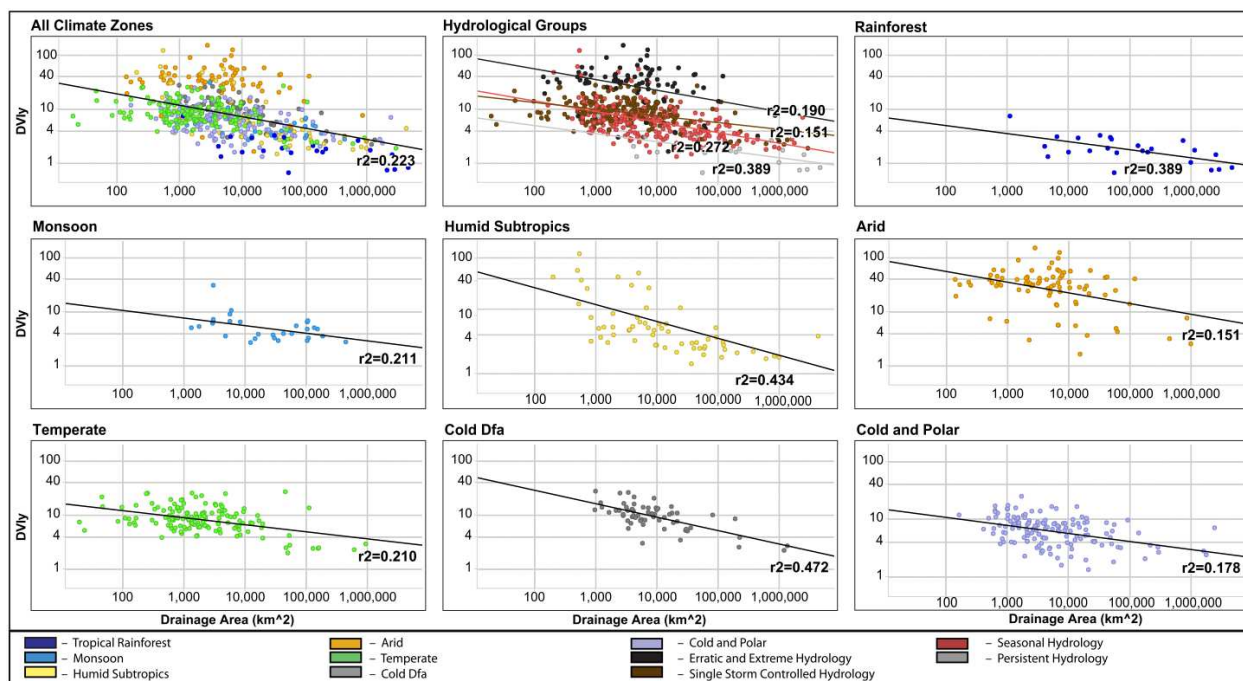


Figure 2.13: Relationship between drainage area and discharge variability (DVI_y) in the seven different hydroclimate zones and the four different hydrological groups (see text) indicate a weak correlation between increasing drainage area and decreasing discharge variability.

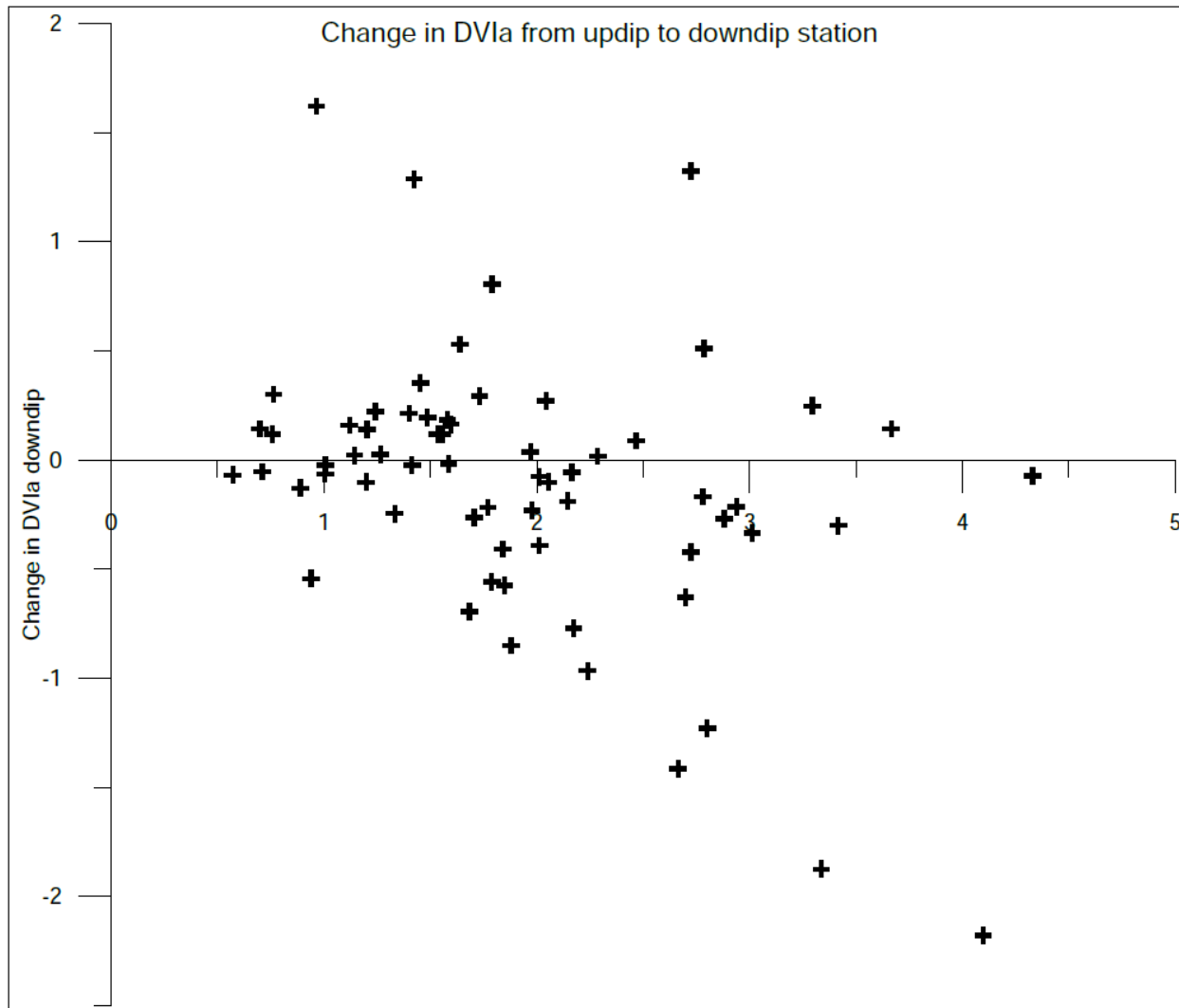


Figure 2.14: Change in DVI_a along a river from the updip station to the downdip station. The updip station's DVI_a is on the x-axis and the change in DVI_a to the downdip station is represented on the y-axis. An increase in DVI_a downdip results in positive change and a decrease in DVI_a downdip results in a negative change. No dominant trend was identified.

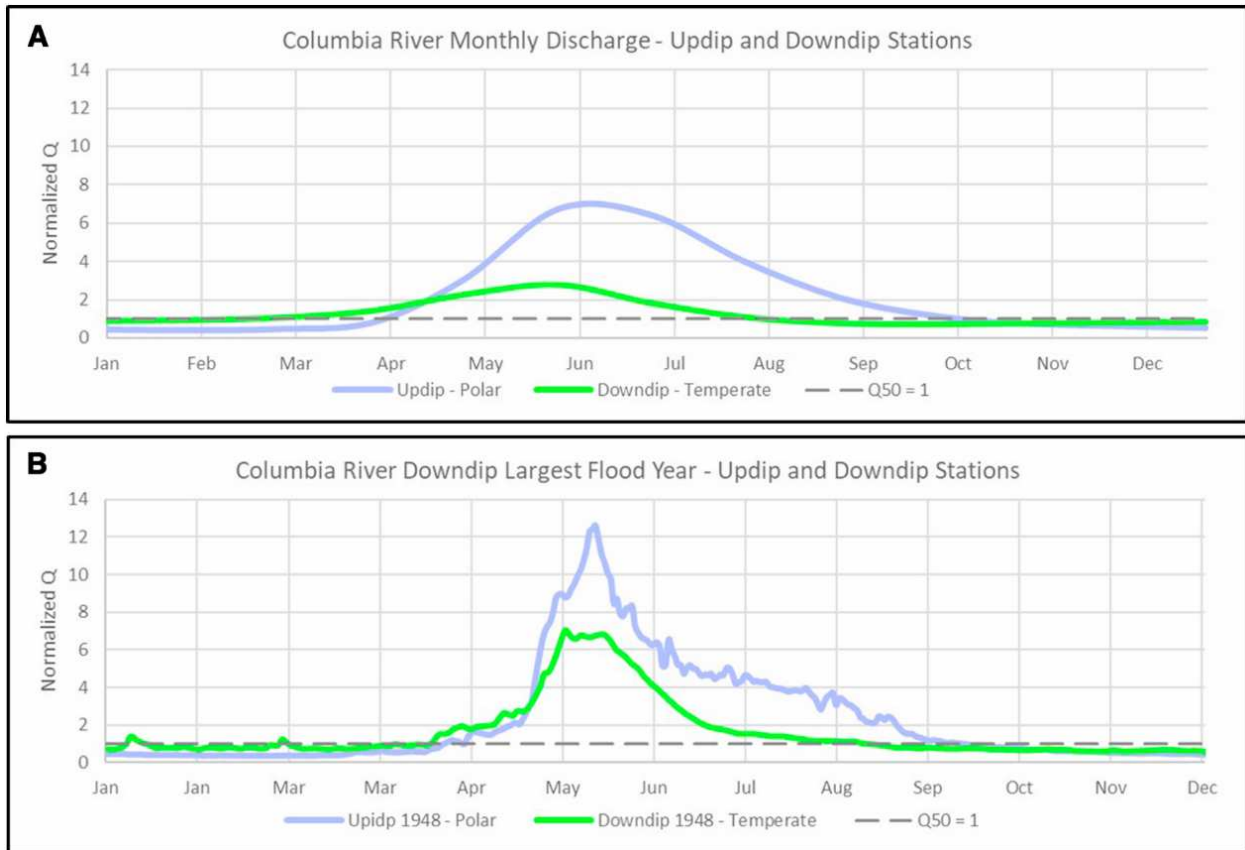


Figure 2.15: Columbia River hydrograph. (A) Columbia River initially starts as a cold and polar hydroclimate zone river in Canada, but as it travels South into the US, it moves into the temperate hydroclimate zone and the DVI_a correspondingly drops from 2.90 to 1.57. (B) This change in hydroclimate zone can be identified in each station's largest flood. The updip polar station has the characteristic cold and polar right-skewed discharge pattern with a sudden initial peak that then slowly tails off during the summer months, whereas the downdip temperate station has the characteristic more normal distribution of temperate rivers. The largest downdip flood occurred in 1948.

Table 2.1: Hydroclimate types defined by general precipitation patterns.

| | Hydroclimate type | Köppen-Geiger Climate Type | Definition |
|---|--------------------------|-----------------------------------|--|
| 1 | Tropical rainforest | Af | Perennial precipitation style with little seasonal variability and ever-wet conditions |
| 2 | Monsoonal | Am | Variable and highly seasonal precipitation |
| 3 | Humid subtropical | Aw | Similar to monsoon climate, but dry season precipitation tends to be lower and inter-annual variability considerably higher |
| 4 | Arid | BWh, BWk, BSh, BSk | Highly variable precipitation and sustained aridity |
| 5 | Temperate | Cs, Cw, Cfa, Cfb, Cfc | Relatively low seasonal precipitation variability, with the annual precipitation range as compared with the annual mean characteristically low |
| 6 | Cold and polar | Ds, Dw, Dfb, Dfc, Dfd, ET, EF | High seasonal variability in temperature and surface water availability |
| 7 | Cold Dfa | Dfa | Low seasonal precipitation variability |

Table 2.2: Discharge variability metrics and equations

| Metrics | Equations |
|--|---|
| Discharge Peakedness | $Q_{Peak} = Q_{Average\ of\ Wettest\ Month} / Q_{Mean}$ |
| Average Discharge Variability (DVI _a) | $\frac{Discharge\ of\ Average\ Wettest\ Month - Discharge\ of\ Average\ Driest\ Month}{Average\ Discharge}$ |
| Cumulative Discharge Variability (DVI _c) | $\frac{Average\ Discharge\ of\ Wettest\ Month\ of\ Record - Average\ Discharge\ of\ Driest\ Month\ on\ Record}{Average\ Discharge}$ |
| Yearly Discharge Variability (DVI _y) | $\frac{\sum \frac{Maximum\ Daily\ Discharge\ of\ Year\ X - Minimum\ Daily\ Discharge\ for\ Year\ X}{Average\ Discharge}}{n\ years}$ |

Table 2.3: Discharge variability metrics for the 7 hydroclimate types

| Climate Zones | Median | Average | Mode | q1-q3 |
|-----------------------------|---------------|----------------|-------------|--------------|
| <i>DVI_a</i> | | | | |
| Tropical rainforest | 1.27 | 1.30 | 0.76 | 0.79-1.79 |
| Monsoon | 2.43 | 2.65 | 3.43 | 2.14-3.31 |
| Humid subtropics | 2.00 | 2.31 | 1.64 | 1.58-2.24 |
| Arid | 2.04 | 2.21 | 1.73 | 1.42-2.79 |
| Temperate | 1.45 | 1.47 | 1.40 | 1.15-1.75 |
| Cold Dfa | 1.68 | 1.79 | 1.94 | 1.42-1.94 |
| Cold and polar | 2.55 | 2.63 | 2.56 | 1.94-3.30 |
| <i>Discharge Peakedness</i> | | | | |
| Tropical rainforest | 1.68 | 1.77 | 2.15 | 1.47-2.11 |
| Monsoon | 2.68 | 2.79 | 2.87 | 2.39-3.35 |
| Humid subtropics | 2.21 | 2.55 | 2.34 | 1.95-2.43 |
| Arid | 2.08 | 2.48 | 1.82 | 1.78-2.93 |
| Temperate | 1.80 | 1.83 | 1.80 | 1.59-2.03 |
| Cold Dfa | 2.03 | 2.15 | 2.03 | 1.81-2.24 |
| Cold and polar | 2.68 | 2.82 | 1.89 | 2.15-3.42 |
| <i>DVI_c</i> | | | | |
| Tropical rainforest | 2.03 | 2.43 | 2.00 | 1.59-3.30 |
| Monsoon | 5.37 | 6.04 | 3.80 | 4.01-7.37 |
| Humid subtropics | 5.18 | 9.26 | 4.21 | 3.61-8.66 |
| Arid | 19.67 | 26.73 | 19.6 | 13.58-30.58 |
| Temperate | 5.41 | 6.01 | 4.94 | 4.27-6.90 |
| Cold Dfa | 8.51 | 10.25 | 9.79 | 7.03-11.40 |
| Cold and polar | 5.69 | 6.69 | 4.56 | 4.60-7.45 |
| <i>DVI_y</i> | | | | |
| Tropical rainforest | 1.72 | 2.07 | 1.60 | 1.40-2.68 |
| Monsoon | 4.81 | 5.90 | 4.80 | 3.53-6.54 |
| Humid subtropics | 4.73 | 11.96 | 4.21 | 3.08-7.79 |
| Arid | 32.67 | 35.05 | 39.80 | 20.67-43.26 |
| Temperate | 8.21 | 9.43 | 6.77 | 6.05-11.62 |
| Cold Dfa | 10.01 | 10.67 | 9.73 | 7.75-12.80 |
| Cold and polar | 6.70 | 7.14 | 3.15 | 4.16-8.66 |
| <i>CVQ_p</i> | | | | |
| Tropical rainforest | 0.11 | 0.16 | 0.10 | 0.09-0.18 |
| Monsoon | 0.33 | 0.37 | 0.37 | 0.23-0.46 |
| Humid subtropics | 0.43 | 0.52 | 0.19 | 0.25-0.75 |
| Arid | 1.12 | 1.09 | 1.26 | 0.90-1.27 |
| Temperate | 0.48 | 0.49 | 0.31 | 0.36-0.59 |
| Cold Dfa | 0.57 | 0.61 | 0.57 | 0.39-0.72 |
| Cold and polar | 0.39 | 0.42 | 0.42 | 0.29-0.47 |

Table 2.3: Continued.

| Climate Zones | Median | Average | Mode | q1-q3 |
|----------------------|---|----------------|-------------|--------------|
| | $Q_{99.863}/Q_{50}$ (<i>Single value</i>) | | | |
| Tropical rainforest | | 2.53 | | |
| Monsoon | | 14.04 | | |
| Humid subtropics | | 11.49 | | |
| Arid | | 176.22 | | |
| Temperate | | 17.60 | | |
| Cold Dfa | | 31.99 | | |
| Cold and polar | | 18.93 | | |

Table 2.4: Discharge variability metrics for representative rivers of the seven hydroclimate zones

| Example Rivers | Hydroclimate Type | DVI_a | Q Peakedness | DVI_c | DVI_y | CVQ_p |
|-----------------------|--------------------------|------------------------|---------------------|------------------------|------------------------|------------------------|
| Parana | Tropical rainforest | 1.27 | 1.69 | 2.14 | 1.42 | 0.14 |
| Chao Phraya | Monsoonal | 2.36 | 2.70 | 6.21 | 3.25 | 0.46 |
| Caiapo | Humid subtropical | 2.17 | 2.34 | 11.38 | 7.52 | 0.44 |
| Smoky Hill | Arid | 2.10 | 2.34 | 27.20 | 29.69 | 0.95 |
| Nottoway | Temperate | 1.47 | 1.94 | 6.79 | 7.27 | 0.60 |
| Iowa | Cold Dfa | 1.79 | 1.69 | 10.42 | 9.30 | 0.70 |
| Little Beaver | Cold and polar | 2.60 | 2.67 | 7.96 | 6.80 | 0.44 |

| Example Rivers | Hydroclimate Type | Q_{Max}/Q_{Min} | Q_{Max}/Q_{Mean} | Q_{99.863}/Q₅₀ |
|-----------------------|--------------------------|--|---|--|
| Parana | Tropical rainforest | 1.27 | 1.69 | 2.53 |
| Chao Phraya | Monsoonal | 2.36 | 2.70 | 14.04 |
| Caiapo | Humid subtropical | 2.17 | 2.34 | 11.49 |
| Smoky Hill | Arid | 2.10 | 2.34 | 176.22 |
| Nottoway | Temperate | 1.47 | 1.94 | 17.60 |
| Iowa | Cold Dfa | 1.79 | 1.69 | 31.99 |
| Little Beaver | Cold and polar | 2.60 | 2.67 | 18.39 |

Table 2.5: Median discharge variability metrics for small (<25,000km²) and large (>25,000km²) rivers.

| | DVI_a | Q Peakedness | DVI_c | DVI_y | CVQ_p | Q_{Max}/Q_{Min} | Q_{Max}/Q_{Mean} | Q_{99.863}/Q₅₀ |
|---------------------|------------------------|---------------------|------------------------|------------------------|------------------------|--|---|--|
| Small Rivers | 1.81 | 2.11 | 6.70 | 8.65 | 0.50 | 373.59 | 23.20 | 24.51 |
| Large Rivers | 1.88 | 2.15 | 4.41 | 3.24 | 0.30 | 144.45 | 6.38 | 8.22 |

Table 2.6: Downriver increase and decrease in discharge variability.

| | DVI_a | | DVI_c | | Q Peakedness | | DVI_y | | CVQ_p | |
|---------------------------|------------------------|--------|------------------------|--------|---------------------|-----|------------------------|--------|------------------------|--------|
| Increase downriver | 30 | 46.15% | 28 | 43.08% | 26 | 40% | 23 | 35.94% | 30 | 46.88% |
| Decrease downriver | 35 | 53.85% | 37 | 56.98% | 39 | 60% | 41 | 64.06% | 34 | 53.12% |

CHAPTER 3
RIVER DISCHARGE VARIABILITY AS THE LINK BETWEEN CLIMATE AND
FLUVIAL FAN FORMATION

Mark R. Hansford¹ and Piret Plink-Björklund²

In submission with the Journal of *Geology*

3.1 Abstract

There are two contrasting hypotheses on whether fluvial fans need specific climate conditions to form. Deduction of climatic and tectonic signals from landscapes and the sedimentary record is a key aim in geology and geomorphology. It is thus of great interest to obtain recognition criteria of specific climate changes in the sedimentary record in general, and the fluvial fans in particular, because they may form the bulk of the continental fluvial record. The hypothesis that links fluvial fan occurrence to climate, specifically indicates precipitation variability as a key control, as it promotes streamflow variability, channel instability, and avulsions that are the key process of fluvial fan formation. Here we test this hypothesis by quantitative analyses of discharge patterns of 68 fan forming rivers that have a global distribution. Using an ensemble of dimensionless metrics we show that 75% of the fan-forming rivers in this dataset have a high discharge variability. We further analyze down-fan changes in discharge variability and discuss the nature of discharge variability in different hydroclimates as a function of intra- and inter-annual precipitation fluctuations. We examine the fan-forming rivers with moderate to low discharge variability and conclude that although river discharge variability strongly promotes fluvial fan formation, fluvial fans may also be formed by rivers with a moderate or low discharge variability if other favorable conditions that promote avulsions occur.

¹Primary author, graduate student, Colorado School of Mines

²Associate Professor, Colorado School of Mines

3.2 Introduction

Rivers have been regarded as sediment transfer or bypass zones in source to sink systems (Allen, 2008). Recognition of fluvial fans (also known as fluvial megafans, distributive fluvial systems) that are low gradient ($\sim .03^\circ$ - 0.001°), fan-shaped fluvial deposystems built by nodal river avulsions in fan apex (Fig. 3.1), introduces a new type of fluvial systems able to build significant stratigraphic thicknesses that are important repositories for climatic and tectonic signals (Leier et al., 2005; Chakraborty et al., 2010; Latrubesse, 2015; Weissmann et al., 2015; Ventra and Clarke, 2018). Deduction of climatic and tectonic signals from the landscapes and the sedimentary record is a key aim in geomorphology and sedimentology, and ambiguous because climate, tectonics, and the landscapes are linked in a complex fashion and display nonlinear dynamics (Whipple, 2009). Deciphering climatic signals from topography is difficult due to non-unique and difficult-to-decode responses (Tucker, 2004). Therefore, in some cases, the sedimentary record is the best archive of landscape response to past climate (Allen, 2008; Armitage et al., 2011). It is thus of great interest to obtain recognition criteria of specific climate changes in the sedimentary record in general, and the fluvial fans in particular because they may form the bulk of the continental fluvial record (Weissmann et al., 2010).

Fluvial fan formation has been linked to large sediment and water discharges (DeCelles and Cavazza, 1999), and to fluctuations in discharge as a result of highly seasonal precipitation in climatic settings that promote marked seasonal and inter-annual hydrological changes leading to variable discharge regimes and exceptional flood events (Leier et al., 2005) (Fig. 3.2). This supposed correlation between seasonal precipitation and fan occurrence asserts significant climatic control on fan formation and reveals their potential as climate proxies. Precipitation is considered one of the primary controls on river discharge and sediment yields (Langbein and Schumm, 1958), and linked to river hydrology as mean annual precipitation (Syvitski and Milliman, 2007), or as the temporal distribution of precipitation that has a significant control on channel and floodplain processes through discharge variability and

the nature of river morphodynamics, sedimentary environments, and soil development (Lartrubesse et al., 2005; Plink-Björklund, 2015; Fielding et al., 2018). However, a fluvial fan dataset (Hartley et al., 2010), contradicts this climate-link hypothesis, as it documents global distribution of fluvial fans in “all climatic regimes”. It remains an open question why only a limited number of rivers form fluvial fans despite the multitude of sizeable rivers around the world that exit topographic highlands and enter basins - what is unique about these rivers (Leier et al., 2005)? Whether fluvial fans form only in certain climatic conditions has wide-ranging implications not just for understanding of Earth landscape evolution, but also for aquifer architecture (Van Dijk et al., 2016), hydrocarbon reservoirs (Moscariello, 2018), paleoclimate modeling (Carmichael et al., 2018) and even planetary and life evolutionary studies through climate reconstructions on Mars (Fawdon et al., 2018) and Saturn’s moon Titan (Radebaugh et al., 2018).

Here we present a quantitative assessment of the link between river discharge variability and fluvial fan occurrence. Our results show that river discharge variability strongly promotes fluvial fan formation, and there is a correlation between fan occurrence and the precipitation pattern. However, fluvial fans do occur globally and are not linked to specific climate regimes.

3.3 Data and Methods

3.3.1 Data

We use the Global Runoff Data Centre (GRDC) gauging station discharge data from the fan-forming rivers identified by Hartley et al. (2010), and examine the discharge patterns of 85 river gauging stations from 68 fans. Although gauging station data are available for only 16.4% of the 415 fans identified by Hartley et al., (2010), their global distribution represents the dataset well (Fig. 3.3). Fans were searched for globally (see Hartley et al., 2010) and their spatial distribution reflects their uneven global distribution (Fig. 3.3). There are 56 stations with daily and 29 stations with monthly discharge data. The mean station record length is 29.4 years. Drainage areas range from 8.5 km² to 1,950,000 km², as measured upstream from the location of the gauging station.

3.3.2 Methods

For quantitative assessment of river discharge variability we employ an ensemble of dimensionless metrics that collectively capture intra- (seasonal) and inter-annual variability (see Hansford et al., 2020) (Table 3.1). Average discharge variability index DVI_a (Plink-Björklund, 2015) and discharge peakedness Q_{peak} (Leier et al., 2005) metrics capture seasonal discharge variability and are calculated as mean discharge of the wettest month minus the mean discharge of the driest month over the mean annual discharge, and as the mean discharge of the wettest month over the mean annual discharge, respectively. Yearly discharge variability index DVI_y (Hansford et al., 2020), flood intensity Q_{max}/Q_{mean} , and discharge variability Q_{max}/Q_{10} metrics (Latrubesse et al., 2005) better capture the more erratic and extreme discharge variations, and measure the difference between the highest daily discharge in a year compared to the lowest daily discharge in the same year divided by the mean discharge, the highest discharge on record divided by mean discharge, and the highest discharge on record divided by 10th percentile discharge, respectively. We modified Q_{max}/Q_{min} of Latrubesse et al. (2005) to Q_{max}/Q_{10} because many rivers do not transmit discharge during low flow ($Q_{min}=0$). Annual peak discharge variance CVQ_p (Fielding et al., 2018) is the standard deviation of the annual peak discharge divided by the mean annual peak flood discharge and measures inter-annual variability. The cutoff values for high, moderate and low discharge variability for DVI_a and DVI_y are based on outcomes of Hansford et al. (2020), and for CVQ_p on Fielding et al. (2018). For assessment of down-fan discharge variability gauging stations were assigned one of four positions: upstream of apex (n=33), apex (n=21), mid fan (n=23), and toe of fan (n=8). We follow Hartley et al. (2010) and Leier et al. (2005) and assign climate types by the gauging station location using the hydroclimates established by Hansford et al. (2020). River discharge primarily reflects precipitation conditions in the drainage area that may differ from precipitation patterns of the fan.

3.4 Results

3.4.1 Quantitative Assessment of Discharge Variability

High intra- and inter-annual discharge variability is indicated by $DVI_a > 2$, $DVI_y > 10$, or $CVQ_p > 0.6$ in 51 of 68 rivers (75%), or in 66 of the 85 (77.65%) gauging stations (Fig. 3.4A). Moderate discharge variability is indicated by DVI_a ca 1-2, DVI_y ca 2-10, and CVQ_p 0.4-0.6 in 11 rivers (16.18%) and 15 stations (17.65%) (Figs. 3.4A, 3.4C). Low discharge variability as indicated by $DVI_a < 1$, $DVI_y < 2$, and $CVQ_p < 0.4$ values occurs in 4 rivers and 6 stations (Figs. 3.4A, 3.4C). Q_{peak} values corroborate these results with on average 0.22 higher values than their respective DVI_a for the same river, and with a tighter grouping with standard deviation of 1.32 for DVI_a and 1.16 for Q_{peak} . Q_{max}/Q_{10} and Q_{max}/Q_{mean} were calculated for 56 gauging stations with daily records (Fig. 3.4B), and indicate an extreme discharge variability with $Q_{max}/Q_{10} > 300$ or $Q_{max}/Q_{mean} > 10$ in 29 gauging stations (51.79%), and moderate discharge variability with Q_{max}/Q_{10} 20-300 or Q_{max}/Q_{mean} 2.5-15 in 22 gauging stations (39.26%). Low discharge variability as indicated by $Q_{max}/Q_{10} < 10$ and $Q_{max}/Q_{mean} < 2.5-15$ occurs in 3 gauging stations (5.36%). CVQ_p indicates that inter-annual discharge variability is high or very high in 25 of 86 gauging stations (29.07%), moderate in 23 of 86 gauging stations (26.74%), and low or very low in 36 gauging stations (41.86%) (Fig. 3.4C). Based on the above discharge variability metrics, we show that 75% of the fan-forming rivers in this dataset have a high discharge variability.

3.4.2 Down-Fan Changes in Discharge Variability

Two different trends in down-fan discharge variability emerge (Fig. 3.4D). Metrics that measure the maximum range of discharge and thus capture the flashy or erratic behavior, such as DVI_y and Q_{max}/Q_{mean} indicate down-fan decrease in discharge variability, whereas metrics that measure seasonal discharge variability, such as DVI_a and Q_{peak} are consistent across the fan (Fig. 3.4D), indicating that the peak values of yearly or total maxima are moderated down-fan, whereas mean monthly flood discharge is not.

3.4.3 Discharge Variability and Hydroclimates

Further analyses of discharge patterns and comparison to the hydroclimates show that 39 stations (45.88%) on 29 rivers (42.65%) display a highly seasonal, but a relatively low inter-annual discharge variability with $DVI_a > 2$, $DVI_y < 10$, and a low to moderate CVQ_p (Figs. 3.4A, 4C). Rivers with such discharge variability patterns occur in the monsoonal and sub-humid subtropical hydroclimates, characterized by intense wet-season monsoon precipitation and a distinct dry season, or in cold and polar climates with a seasonal snow-melt pattern. Out of the 56 daily stations on 43 rivers, 17 stations (30.36%) on 17 rivers (39.53%) display erratic and both inter- and intra-annually variable discharge with $DVI_y > 10$, $Q_{max}/Q_{mean} > 20$, and high to very high CVQ_p (Figs. 3.4A-C). Most such rivers occur in arid hydroclimates and some in sub-humid subtropics. Arid subtropics, as well as some sub-humid subtropics experience highly variable precipitation patterns, where intense rainfall events are linked to extreme monsoon seasons and tropical cyclones and provide inter- as well as intra-annual highly variable surface water supply. Seven stations (8.24%) on 5 rivers (7.35%) with $DVI_a < 1$, $DVI_y < 10$, and very low to low CVQ_p indicate perennial discharge patterns with low variability (Figs. 3.4A, 3.4C). Such rivers occur in the tropical rainforest hydroclimate.

3.5 Discussion

3.5.1 Link Between River Discharge Variability and Fluvial Fan Formation

In this dataset 75% of the fan-forming rivers (51 of 68) have high discharge variability (Fig. 3.4), suggesting a correlation between fan formation and discharge variability, corroborating the hypothesis of Leier et al. (2005). This tendency of rivers with large fluctuations in discharge to construct fans is related to channel instability and avulsions (Leier et al., 2005), triggered by channel bed super-elevation as a function of channel bed aggradation (Bryant et al., 1995; Hajek and Wolinsky, 2012). Incisional avulsions also occur (Hajek and Wolinsky, 2012), and in both cases large fluctuations in river discharge are avulsion-triggering events (Jones and Schumm, 1999). This link between river discharge variability

and fluvial fan formation has further been corroborated by the documented fan activation and deactivation cycles, and changes in deposition rates, avulsion frequency, and fluvial fan aggradation and progradation in response to monsoon intensity and precipitation pattern changes (Assine et al., 2014; Fontana et al., 2014). For example, the Chaco fans formed at 60-28 ka in pleniglacial conditions with a more seasonal precipitation pattern (Latrubesse et al., 2012). Southern Alpine fans experienced major deposition at 26-19 ka during the Last Glacial Maximum, followed by incision and inactivity at 19-17 ka when sediment delivery decreased (Fontana et al., 2014). Furthermore, globally the high spatial clustering of fans in certain regions correlates with more variable precipitation patterns (Fig. 3.3).

3.5.2 Low Discharge Variability Fans

There are 19 stations on 13 rivers that have moderate or low discharge variability (Fig. 3.4), which raises the question whether there are additional or alternative conditions that promote fluvial fan formation. Two thirds (9 of 13) of these fans occur in wetlands, such as in the Pantanal wetlands of South America with five of these low to moderate discharge variability fans. The most studied Pantanal fan, the Taquari fan, is formed by the Taquari River with DVI_a 0.68, Q_{peak} 1.43, DVI_y 1.76, Q_{max}/Q_{mean} 4.64, Q_{max}/Q_{10} 3.48, and CVQ_p 0.36. Despite low discharge variability metrics, the Taquari River has a seasonality signature due to a sub-humid subtropical climate with seasonally variable precipitation (Assine, 2005). Another wetland fan, the Okavango fan is DVI_a 1.58, Q_{peak} 2.02, DVI_y 1.76, Q_{max}/Q_{mean} 3.29, Q_{max}/Q_{10} 3.97, and CVQ_p 0.26. Although moderate, the discharge is distinctly seasonal, and the fan occurs in a semi-arid climate (Stanistreet and McCarthy, 1993).

Some of the fans in this group may be currently inactive, as indicated by river incision into the fan surface (e.g. Fontana et al., 2014). The Taquari River is currently incising in the upper portion of the fan but also depositing in the lower portion (Assine, 2005), and is the only fan in this dataset with documented incision. Current inactivity has been documented in other fans, not included in this dataset as they lack gauging stations, such as the Chaco fans (Latrubesse et al., 2012) and the São Lourenço fan (Assine et al., 2014)

in South America, the Lannemezan fan (Mouchené et al., 2017) of the French Pyrenees, and fans of the southern Alpine piedmont (Fontana et al., 2014).

Some fans may further be controlled by unique external processes. For example, the Santa Clara fan (not included in Hartley et al., 2010 database) is controlled by volcanic rather than climatic processes (Galve et al., 2016). The volcanic processes mobilize sediment by destroying vegetation cover, destabilizing slopes, and concentrating rainfall due to the orographic barrier (Galve et al., 2016).

In summary, although discharge variability seems to strongly promote fluvial fan formation, there is increased likelihood for fluvial fan formation wherever avulsion frequency is increased, provided there is sufficient lateral space (see North and Warwick, 2007). For example adjacent to orogenic belts with high sediment supply, or wetlands with lush vegetation or high water tables that increase deposition rates. However, as fan formation is controlled by nodal avulsions at apex (e.g. Chakraborty et al., 2010), their formation is insensitive to water table or presence of a lake or marine basin at the fan toes only, and requires perched water tables or water tables high enough to affect the formative discharges at the apex.

3.6 Conclusions

We conclude that both the Leier et al. (2005) and Hartley et al. (2010) hypotheses are partially correct. Our analyses support Leier et al. (2005) in that river discharge variability promotes fluvial fan formation and there is a correlation between fan occurrence and the precipitation pattern. However, fluvial fans do occur globally and are not linked to specific climate regimes as suggested by Hartley et al. (2010). The link to climate is not well defined by specific climate regimes, as variable precipitation patterns or snow-melt conditions occur across multiple climate types. Our analyses further support that any conditions that promote avulsions increase the likelihood for fluvial fan formation, provided there is lateral space available. Thus, fluvial fans are likely proxies for climates with seasonal or variable precipitation patterns, but do not indicate specific climate types, and corroborating evidence is needed for conclusive assessment.

3.7 Acknowledgements

We thank the Global Runoff Data Centre, 56068 Koblenz, Germany for discharge data. We thank reviewers Dario Ventra, Gary Weissmann, and Mario Assine for their constructive criticism.

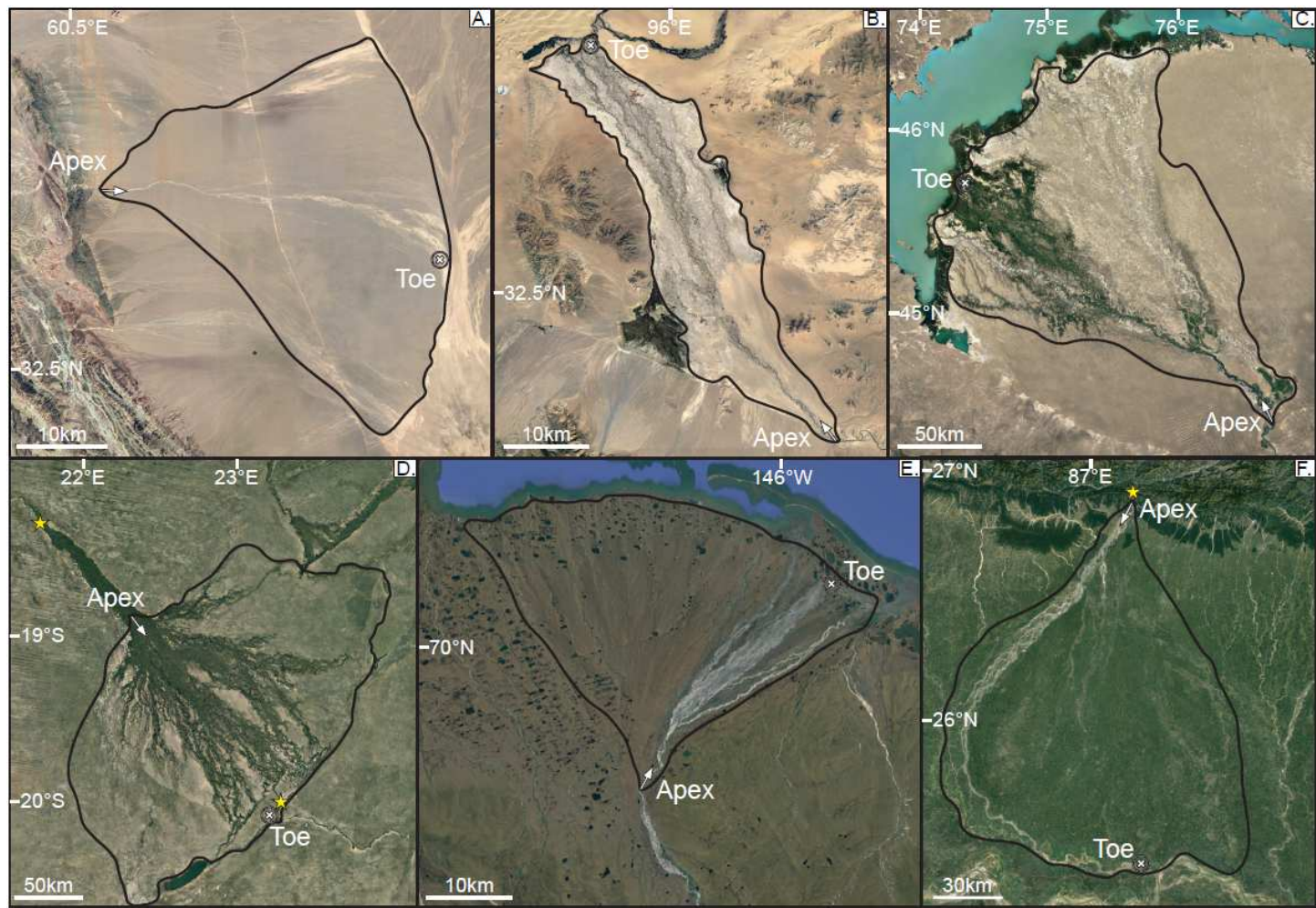


Figure 3.1: Examples of fluvial fans. A. Arid fan in Iran (22). B. Partially laterally confined fan in Mongolia (10). C. Fan in Kazakhstan with small deltas at the fan termination (02). D. Okavango fan in Botswana (01). E. Alaska (04) fan with a “classic” fan shape. F. Kosi fan in India (05). Star denotes a gauging station. North is up in all images. Fan numbers refer to the database (Suppl. Table 3.2).

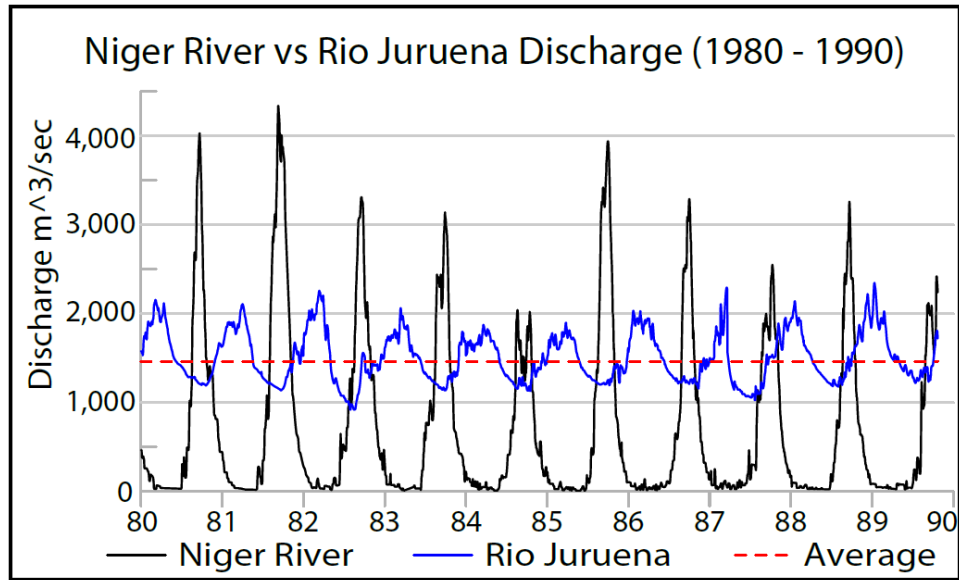


Figure 3.2: Streamflow hydrographs illustrating low (Rio Juruena, DVIa 0.49) vs high (Rio Niger, DVIa 3.33) discharge variability for two rivers with similar mean annual discharge (red line).

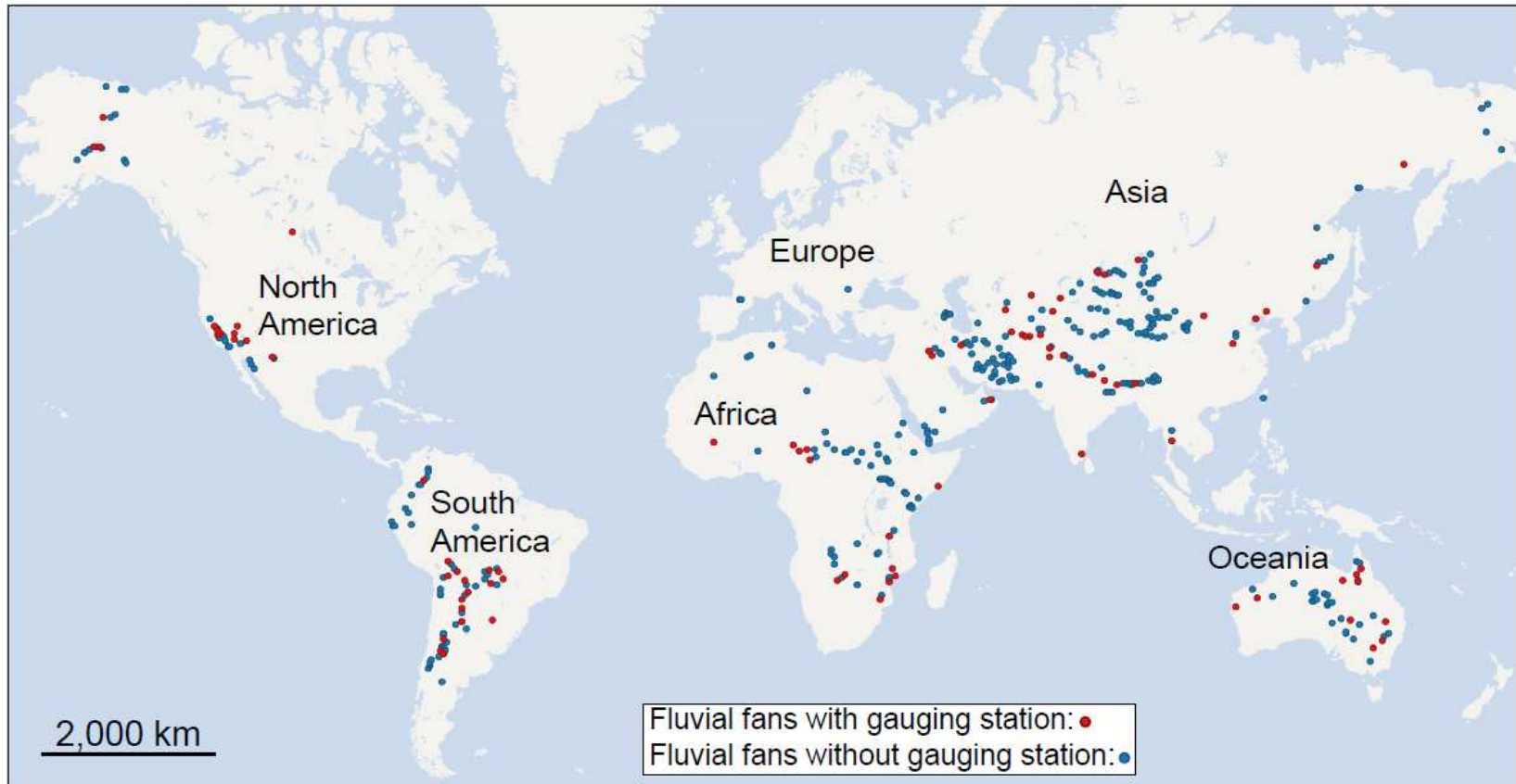


Figure 3.3: Map of fluvial fan locations (apex indicated by dots) and river discharge gauging stations used in this study.

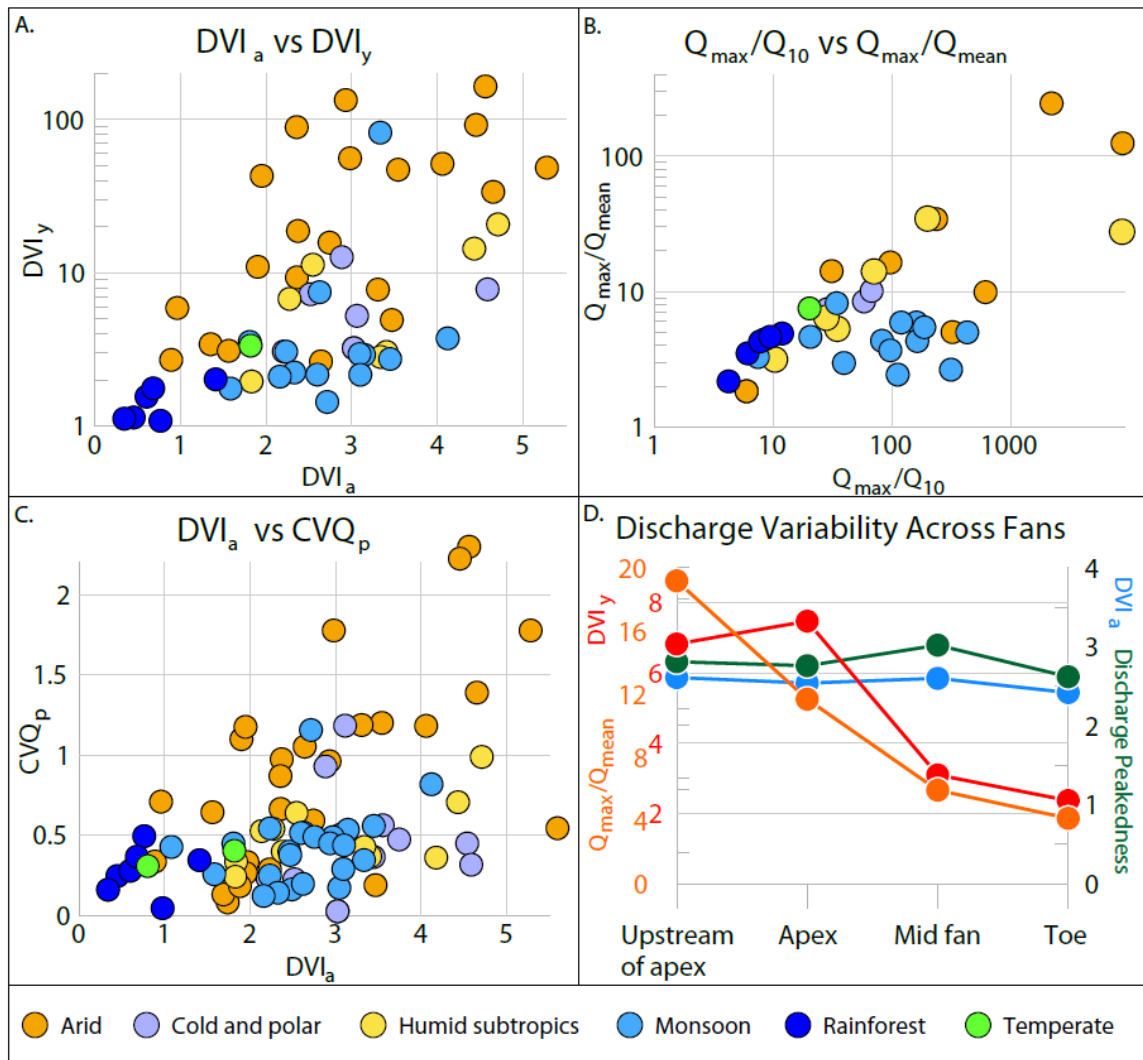


Figure 3.4: Discharge variability in fan forming rivers, expressed by dimensionless metrics of DVI_a vs DVI_y (A), Q_{max}/Q_{10} vs Q_{max}/Q_{mean} (B), DVI_a vs CVQ_p (C), and downstream discharge variability changes from apex to toe measured by DVI_a , DVI_y , Q_{max}/Q_{mean} and Q_{peak} (D).

Table 3.1: Discharge variability metrics

| Discharge Variability Metric | Equation | Reference |
|---|------------------------------------|--|
| Q_{peak} : discharge peakedness | Q_{WMmax}/Q_{mean} | Leier et al., 2005 |
| Q_{max}/Q_{10} : discharge variability | Q_{max}/Q_{10} | modified from Q_{max}/Q_{min} of Latrubesse et al., 2005 |
| Q_{max}/Q_{mean} : flood intensity | Q_{max}/Q_{mean} | Latrubesse et al., 2005 |
| DVI_a : average discharge variability index | $(Q_{WMmax} - Q_{WMmin})/Q_{mean}$ | Plink-Björklund, 2015 |
| DVI_y : yearly discharge variability index | $(Q_{Dmax} - Q_{min})/Q_{mean}$ | Hansford et al., 2020 |
| $Q_{99.863}/Q_{50}$: Flood magnitude | $Q_{99.863}/Q_{50}$ | Hansford et al., 2020 |
| CVQ_p : annual peak discharge variance | $(\sigma Q_{Ymax})/Q_{Ymean}$ | Fielding et al., 2018 |

Table 3.1: Discharge variability metrics used in this study. Measures of discharge (Q): Q_{mean} – mean; Q_{max} - maximum; Q_{min} - minimum; Q_{50} - 50th percentile; Q_{10} - 10th percentile; $Q_{99.863}$ – 99.863th percentile (equivalent to 2-year flood (Elliott and Capesius, 2009); Q_{WMmax} – maximum of wettest month; Q_{WMmin} – minimum of wettest month; Q_{Dmax} - daily maximum of a year; Q_{Dmin} - daily minimum of the same year; σQ_{Ymax} – standard deviation of the annual peak; Q_{Ymean} - mean annual peak flood.

CHAPTER 4

GEOMORPHOMETRIC SCALING RELATIONSHIPS IN FLUVIAL FANS

Mark R. Hansford¹ and Piret Plink-Björklund²

A paper to be submitted to *Sedimentology*

4.1 Abstract

Fluvial fans are a relatively newly accepted sedimentological concept and their formation is not yet fully understood. Studying their scaling relationships gives insight to the controls exerted on fluvial fans and the architectural development of these terrestrial systems. We combine daily and monthly discharge from 85 river gauging stations with satellite imagery of 415 fluvial fans to quantitatively test different scaling relationships between fan size and channel width with river discharge, discharge variability, drainage area, climate type, and tectonic setting. We identified a number of relationships governing system behavior and evolution by comparing various morphological parameters between fluvial fans. The results suggest that discharge, channel width, and drainage area are inter-related, while fan size is not. Fan size is controlled by both tectonic and climatic regimes, but further study is needed to fully understand these controls. Fan size is positively skewed with a long tail, with median fan size of 1,085 km² while average fan size is 5,818 km². In approximately three-quarters of fluvial fans (72.5%) river channels narrow from apex to toe and their width scales with 99.863th percentile flow (bankfull flow) in fan apex, and with 50th percentile flow at the toes. As opposed to alluvial fans that occur adjacent to mountain fronts, fluvial fans occur up to more than 500 km distance from their mountainous hinterlands, implying different controls on fan formation. Application of these morphological relationships will be useful for fluvial fan recognition and reconstruction, source to sink analysis, and reservoir modeling.

¹Primary author, graduate student, Colorado School of Mines

²Associate Professor, Colorado School of Mines

4.2 Introduction

Fluvial fans (fluvial megafans, distributive fluvial systems) are low gradient ($\sim 0.03^\circ$ - 0.001°), fan-shaped fluvial deposystems built by nodal river avulsions at fan apex (Figure 4.1) (North and Warwick, 2007; Chakraborty et al., 2010). Fluvial fans are relatively newly acknowledged fluvial systems able to build significant stratigraphic thicknesses that are important repositories for climatic and tectonic signals (Leier et al., 2005; Chakraborty et al., 2010; Latrubesse, 2015; Weissmann et al., 2015; Ventra and Clarke, 2018). Fluvial fans are of particular interest as they may form the bulk of the continental fluvial record (Weissmann et al., 2010).

Facies models have been proposed for different types of fan-shaped bodies built by riverine and floodplain processes, such as terminal fans (Friend, 1978; Kelly and Olsen, 1993), fluvial distributary systems (Nichols 1987; Nichols and Hirst, 1998; Nichols and Fisher, 2007), fluvial megafans (e.g. Gohain and Parkash, 1990; Singh et al., 1993; Shukla et al., 2001; Chakraborty et al., 2010), losimean fans (Stanistreet and McCarthy, 1993), and distributive fluvial systems (Weissman et al., 2010; Hartley et al., 2010). These facies models present significant similarities, such as downfan decrease in the proportion of channel vs floodplain deposits, downfan decrease in channel size, degree of channel amalgamation and grain size. However, many open questions remain about how fluvial fans form and what the controls are on their formation, or what are the key characteristics of their geomorphology, hydrology and sedimentology (Ventra and Clarke, 2018).

Sufficient lateral space together with discharge or environment conditions that promote avulsion have been suggested as key controls of fluvial fan formation (North and Warwick, 2007). Accordingly, large sediment and water discharges (DeCelles and Cavazza, 1999), and large fluctuations in discharge as a result of highly seasonal precipitation in climatic settings that promote marked seasonal and inter-annual hydrological changes leading to highly variable discharge regimes and exceptional flood events (Leier et al., 2005), and low gradients (North and Warwick, 2007) have been suggested to promote fan formation. As

fluvial fan formation is controlled by nodal avulsions at the apex (e.g. North and Warwick, 2007; Chakraborty et al., 2010), their formation is insensitive to water table or presence of a lake or marine basin at the fan toes. It follows that quantifying the morphology and hydrology of fluvial fans is essential for understanding the underlying controls (Pike et al., 2009).

Satellite imagery is the main tool used to measure fluvial fans. The first global study (Hartley et al, 2010) scanned 724 modern continental sedimentary basins and identified 415 fluvial fans. They documented the apex location, toe location, apex-to-toe length, gradient, planform, termination type, tectonic setting, and climatic setting for each identified fluvial fan. This was the first study to identify more than a handful of fluvial fans and was instrumental in suggesting the possibility that fluvial fans make up the bulk of the fluvial record (Weissmann et al., 2010). There are two, follow-up complementary studies to Hartley et al. (2010). The first, Davidson et al. (2013) focused on 36 of the 415 identified fluvial fans and measured channel width and channel sinuosity at five locations on each fluvial fan leading to the creation of depositional models with recognizable geomorphic elements. The second, Davidson and Hartley (2014) focused on the 182 fluvial fans in endorheic basins and suggested strong relationships between the drainage area (contributing drainage located above the apex) and the area of the fluvial fan. These scaling relationships are important for source to sink reconstructions and prediction of sediment flux.

Scaling relationships provide insight into the properties and processes of depositional systems (Sømme et al., 2009; Milliken et al., 2012; Pettinga et al., 2018). The above studies described the morphology of fluvial fans, examining the scaling relationships which control the formation of fluvial fans, but up until now, no study has incorporated discharge values. The inclusion of discharge to these scaling relationships will fill the knowledge gap by investigating, in unison, the formative flows and the resulting deposits. This new knowledge will further constrain the interpretation and reconstruction of fluvial fans.

Here we present results of morphometric scaling relationships in fluvial fans, with the aim to provide quantitative data for improved fluvial fan facies and morphodynamic models. We use satellite imagery for 415 fluvial fans and river discharge data from 85 river gauging stations and test different scaling relationships between fan size and channel width with river discharge, discharge variability, drainage area, climate type, and tectonic setting. We go beyond average discharge and consider multiple discharge magnitudes for each river. We further quantify downfan change in channel width and their scaling relationships with river discharge, and the fan location in relation to the mountainous orogenic belts in their hinterland. The latter aspect is motivated by that fluvial fans, as opposed to alluvial fans, may form hundreds of kilometers from mountain fronts, but some fluvial fan models consider the transition from laterally confined catchments/valleys to open plains or broader valleys the ultimate reason underlying the construction of fan-shaped alluvial landforms (e.g. Ventura and Clark, 2018).

4.3 Data and Methods

4.3.1 Satellite Imagery Data

We utilize Google Earth for fan area and channel width measurements, based on the apex and toe locations provided by Hartley et al. (2010) in their study of 415 fans (Figure 4.2). Hartley et al. (2010) measured the straight-line apex-to-toe distance. We were able to measure outlines for 385 of these fans. The area of each fluvial fan was measured using the polygon function in Google Earth that provides an estimate limited by resolution of the satellite imagery as well as agricultural or infrastructural modifications of fans. Where two fans are directly adjacent to each other, the outline for each fan was traced abutting against each other with no overlap and drawn where channels intersect. The fan outlines are available for download as .kmz files in Supplementary Database 1.

Channel widths were measured at for each fluvial fan at the apex and toe locations identified by Hartley et al., (2010). We took three measurements at each apex and toe location, and measured the narrowest, the widest channel width, and an intermediate channel

width at each location (see Figure 4.3). We were able to collect measurements for 353 channels at the apex and for 211 channels at the toe, due to variable satellite imagery quality. Channel width measurements are available for download in Supplementary Database 2. Channel width was measured to approximate the width at bankfull discharge, even if the river was at low flow conditions on the satellite images, by measuring from vegetation edge to vegetation edge (see Figure 4.3a). For single-thread river channels, such as straight, meandering, or braided channels, width was measured across the single thread. For multi-thread channel types, such as anabranching or anastomosing channels, width was measured either at a point where the channel became a single-thread or at the widest section that captured the majority of the flow (see Figure 4.3b).

For 49 of the fans, only a single measurement was taken at the toe because the small size of channels was below the image resolution. This is most common for fluvial fans in more arid climates, where the fan terminates and the channel width is below image resolution. In more extreme cases, measurements were only taken at the apex of the fan and these fans were excluded from down-fan channel narrowing analysis. Where possible, we utilized older satellite imagery with higher resolution or lower cloud cover. Since the original analysis was done for this study, more satellite imagery has become available that will be useful for future studies.

We evaluate the fan apex adjacency to the confining mountain front with a simple “yes/no” and only estimate the maximum distance of the fans from their hinterland mountain front.

4.3.2 Discharge Data

We examine daily and monthly discharge data from the Global Runoff Data Centre (GRDC), using 85 river gauging stations on 68 fluvial fans. Although discharge data are available for only 16.4% of the 415 fans identified by Hartley et al. (2010), their global distribution covers the dataset well (Figure 4.2). There are 56 stations with daily discharge data and 29 stations with monthly discharge data. The mean record length is 29.4 years per

station and the median length is 24 years. Drainage area ranges from 8.5 km² to 1,950,000 km², as measured upstream from the location of the gauging stations.

In order to test the scaling relationships, we go beyond average discharge and consider different discharge magnitudes, ranging from the 10th percentile (Q_{10}), to the maximum recorded discharge for the gauging station (Q_{max}). In addition we calculate the bankfull flow discharge defined as the discharge equivalent to the 2-year recurrence interval flood or the 99.863th percentile flow ($Q_{99.863}$) (Elliott and Capesius, 2009).

For quantitative assessment of river discharge variability we employ an ensemble of dimensionless metrics that collectively capture intra- (seasonal) and inter-annual variability (see Hansford et al., 2020) (Table 4.1). Average discharge variability index DVI_a (Plink-Björklund, 2015) and discharge peakedness Q_{peak} (Leier et al., 2005) metrics capture seasonal discharge variability and are calculated as mean discharge of the wettest month minus the mean discharge of the driest month over the mean annual discharge, and as the mean discharge of the wettest month over the mean annual discharge, respectively. Yearly discharge variability index DVI_y (Hansford et al., 2020), flood intensity Q_{max}/Q_{mean} , and discharge variability Q_{max}/Q_{10} metrics (Latrubesse et al., 2005) better capture the more erratic and extreme discharge variations, and measure the difference between the highest daily discharge in a year compared to the lowest daily discharge in the same year divided by the mean discharge, the highest discharge on record divided by mean discharge, and the highest discharge on record divided by 10th percentile discharge, respectively. We modified Q_{max}/Q_{min} of Latrubesse et al. (2005) to Q_{max}/Q_{10} because many rivers do not transmit discharge during low flow ($Q_{min}=0$). Annual peak discharge variance CVQ_p (Fielding et al., 2018) is the standard deviation of the annual peak discharge divided by the mean annual peak flood discharge and measures inter-annual variability. The cutoff values for high, moderate and low discharge variability for DVI_a and DVI_y are based on outcomes of Hansford et al. (2020), and for CVQ_p on Fielding et al. (2018).

Each gauging station was assigned a position on the fan: upstream of apex (n=33), apex (n=21), mid fan (n=23) and toe of fan (n=8). Drainage area, as provided by gauging station data, is calculated from the point of the discharge gauging station, and is thus dependent on the gauging station position of the fan. We follow Hartley et al. (2010) and Leier et al. (2005) and assign climate types by the gauging station location using the hydroclimates established by Hansford et al. (2020). There is a limited number of data points for most hydroclimates, arid and monsoonal have the most at n=23 and n=18, respectively, whereas humid subtropics n=7, cold and polar n=5, rainforest n=5, and temperate n=2. River discharge primarily reflects precipitation conditions in the drainage area that may differ from precipitation patterns of the fan.

4.4 Results

4.4.1 Channel Width and Discharge

The relationship between river discharge and channel size underpins the basics of fluvial geomorphology first outlined by Leopold and Maddock (1953), and understanding the relationship between discharge and channel width is important for paleohydraulic reconstruction of fluvial fans. We find that the channel width in fan apex correlates best with the calculated bankfull discharge $Q_{99.863}$ with $r^2=0.820$ (Figure 4.4). There is a significant improvement in correlation from 50th to 99th percentile flow with $r^2=0.391$ for Q_{50} , $r^2=0.507$ for Q_{90} , and $r^2=.708$ for Q_{99} (Figure 4.4). At discharge levels above $Q_{99.863}$, correlation is weaker, with $r^2=0.575$ for maximum discharge Q_{max} . Average discharge Q_{avg} has also a relatively weak correlation with $r^2=0.601$.

Channel width at the fan toe correlates best with Q_{50} with $r^2=0.733$ (Figure 4.5). All discharge values below Q_{50} , ranging from Q_{min} to Q_{50} , have weaker correlations with r^2 values around 0.6. Correlation also weakens towards higher magnitude flows, where for Q_{90} $r^2=0.523$, Q_{99} $r^2=0.357$, and $Q_{99.863}$ $r^2=.301$ (Figure 4.5). Average discharge Q_{avg} has a relatively weak correlation with $r^2=0.426$.

Testing the relationship of discharge variability to channel width, using multiple discharge variability metrics (see Hansford et al., 2020) show no correlation with r^2 values of 0.005 to 0.091 (Figure 4.6). These findings do not corroborate previous studies (Robinson and McCabe, 1997; Gibling, 2006; Powell, 2009) that have suggested that increased discharge variability leads to higher aspect ratios (width/thickness).

4.4.2 Fan Size

Fan size in our dataset ranges from 108 km² to 219,123 km², with a median size of 1,085 km² and an average that is five times larger at 5,818 km². The distribution of fan size is positively skewed with a long tail (Figure 4.7), with the average fan size more than 1,500 km² larger than the third quartile fan size of 4,129 km², and the first quartile fan size of 575 km². Fan area strongly correlates with apex-to-toe distance (data from Hartley et al., 2010) with $r^2=0.845$ (Figure 4.8).

There is a very weak correlation between the fan area and discharge with r^2 values ranging from 0.110 to 0.245 for different discharge magnitudes (Figure 4.9). The correlation between fan size and channel width is even weaker with r^2 values from 0.002 to 0.211 (Figure 4.10).

Testing the relationship between fan size and tectonic setting (as defined in Hartley et al., 2010) shows that cratonic tectonic regimes have the largest median fan sizes at 2,161 km², while in compressional (foreland and piggy-back basins), extensional (rifts, rift shoulders, and passive margins), and strike-slip tectonic regimes median fan sizes are 1,085 km², 1,073 km², 1,052 km², and 883 km², respectively (Figure 4.11). Compressional and cratonic basins have the largest outlier fans with maximum sizes of 219,123 km² and 82,360 km², respectively (Figure 4.11). Strike-slip settings have significantly smaller maximum fan sizes with a maximum fan size of 6,711 km² despite the only marginal difference in median fan size (Figure 4.11). These data suggest that fan size is dependent on tectonic setting.

Testing the relationship between hydroclimate and fan size shows that monsoonal fluvial fans have a significantly larger median size than arid fluvial fans at 21,949 km² vs 1,305 km² (Figure 4.12). This difference in size is also reflected by difference in Q_{99} discharge at 2,449

m³/sec vs 36m³/sec (Figure 4.13). This difference is particularly interesting as we did not find a strong correlation between discharge and fan size (Figure 4.9), suggesting interdependency between fan size, discharge and hydroclimate. Hartley et al. (2010) also suggested a climatic control in that the gradient of fans was related to their ability to maintain flow across a basin and thus fans in drylands or arid settings may not be limited by horizontal accommodation, but by discharge.

4.4.3 Drainage Area

Research in geology, geomorphology, and hydrology has found drainage area to be a key control on river discharge, such as the widely used BQART model that utilizes the scaling relationship between drainage area and average discharge (Milliman and Syvitski, 1992; Syvitski et al., 2003; Syvitski and Milliman, 2007).

Testing the relationship between drainage area and discharge reveals the strongest correlation between drainage area and the calculated bankfull discharge $Q_{99.863}$ with $r^2=0.602$ (Figure 4.14). The correlation improves from lower to higher flow magnitudes, from Q_{30} with $r^2=0.347$, Q_{50} with $r^2=0.438$, and Q_{90} with $r^2=0.484$ (Figure 4.14). Average discharge Q_{avg} has a correlation of $r^2=0.593$.

We thus report a weaker correlation between drainage area and discharge compared to the BQART model that reported r^2 value of 0.71 between drainage area and mean annual discharge based on 488 rivers (Syvitski and Milliman, 2007).

4.4.4 Down-Fan Channel Width Change

Numerous datasets (Nichols, 1987; Kelly and Olsen, 1993; Nichols and Fisher, 2007; Weissmann et al., 2010; Davidson et al., 2013; Wang and Plink-Björklund, 2020) have described down-fan channel width decrease as a key recognition criterion for fluvial fans. Based on measurements of channel width at the apex and toe from 206 fluvial fans, we show that in 153 (72.5%) fluvial fans rivers narrow from the apex to the toe (Table 4.2). There are 84 fluvial fans in arid climates that terminate at the toe and the channel width was not

resolvable in the available satellite imagery resolution. In the fans where channels narrow down-fan, 45 (29.4%) have a toe channel width that is >50% of the apex channel width, 52 (34%) have a toe channel width 20-50% of the apex channel width, and 56 (36.6%) have a toe channel width <20% of the apex channel width (Table 4.2, Figure 4.15).

However, 58 of the 206 (27.5% of total) fluvial fans have channels that widen down-fan (Table 4.2, Figure 4.15). 22 (37.9%) of the 58 channels that widen have a toe channel width of <150% of the apex channel width, 24 (41.4%) have a toe width 150-300% of the apex channel width, and 12 (20.7%) have a toe width 300-1,000% of the apex width (Table 4.2, Figure 4.15).

4.4.5 Fan Adjacency to Mountainous Topography

In this dataset 150 fans (36%) are directly adjacent to high confining topography and 265 fans (64%) occur tens to up to more than 500 km away. These findings contradict Ventra and Clarke (2018) in that the transition from laterally confined catchments/valleys to open plains or broader valleys is the ultimate reason underlying the construction of fluvial fans.

Furthermore, there is a relationship between river discharge, fan size, and apex adjacency to mountain front. Fans that are not directly adjacent to their confining topography have median fan area and Q_{max} values (1,679 km² and 1,219 m³/sec) that are approximately double as compared to the fans that are directly adjacent to their confining topography (863 km² and 550 m³/sec) (Figures 4.16 and 4.17). Despite these differences in fan area and Q_{max} values, there is no significant difference in channel width between fans that are directly adjacent and fans that are not.

4.5 Discussion

4.5.1 Channel Forming Discharge

A unique aspect of this fluvial fan study is the combination of hydrological and geomorphological scaling relationships, by inclusion of river discharge data. A key outcome of this comparison is that drainage area as well as channel width at the fan apex scale most

strongly with the calculated bankfull discharge ($Q_{99.863}$) rather than with average discharge. The difference in r^2 values is largest for the channel width and discharge comparison with 0.820 for bankfull flow and 0.426 for average discharge. Drainage area and discharge correlation results in r^2 values of 0.602 for bankfull flow and 0.593 for average discharge. Moreover, only apex channel width has a strong correlation with the calculated bankfull discharge ($Q_{99.863}$), as channel width at fan toes scales most strongly with 50th percentile discharge (Q_{50}) with r^2 values of 0.733. In comparison $r^2=0.426$ for average discharge to toe channel width correlation.

These data indicate the inefficiency of average discharge in scaling relationships and corroborate the significance of bankfull flow as channel-forming discharge (Leopold and Maddock, 1953; see also Matthai, 1990; Davidson and North, 2009; Jones, 2017). However, as 72.5% of the analyzed fan-forming rivers narrow down-fan, only the apex channel widths have a strong scaling relationship with the bankfull flow. This down-fan narrowing has been documented in many datasets and used as a criterion for proximal vs distal fan recognition in ancient settings (Friend, 1978; Kelly and Olsen, 1993; Nichols and Fisher, 2007; Weissmann et al., 2010; Davidson et al., 2013; Wang and Plink-Björklund, 2019). Accordingly, vertical stratigraphic transitions from small to large channels have been interpreted as indicator of fluvial fan progradation (DeCelles and Cavazza, 1999; Uba et al., 2005; Chakraborty et al., 2010; Weissmann et al., 2013; Rittersbacher et al., 2014; Sinha et al., 2014; Owen et al., 2015, 2017; Chesley and Leier, 2018). Our data suggest that down-fan channel narrowing is a strong criterion (72.5%), but it does not occur in every fan. Our results are corroborated by Davidson et al. (2013) who show that in 94.4% of their studied 36 fluvial fans channels narrow downfan. Since over a quarter of fan-forming rivers in this dataset (27.5%) widen down-fan, additional criteria, such as the degree of channel amalgamation that characteristically decreases down-fan can be used as supportive evidence in the ancient sedimentary record (Kelly and Olsen, 1993; Singh et al., 1993; Shukla et al., 2001; Nichols and Fisher, 2007; Chakraborty et al., 2010; Weissmann et al., 2010, 2013; Fielding et al., 2012; Hajek

and Wolinsky, 2012; Davidson et al., 2013).

While it remains unclear why such a large proportion of fan-forming rivers widen down-fan in our dataset, down-fan narrowing has been assigned to discharge losses to floodplain processes, infiltration into the loose sediments of the fan, and evapotranspiration (DeCelles and Cavazza, 1999; Horton and DeCelles, 2001; Hartley et al., 2010; Weissmann et al., 2010; Davidson et al., 2013). Channel widening may be related to changes in channel planform or aspect ratio, discharge contribution from groundwater, or discharge capture from adjacent rivers.

Our dataset does not indicate a link between channel width and discharge variability, in contrast to previous work that has suggested a link between discharge variability and channel aspect ratio as a function of overland or sheet flow and extensive bank erosion (Robinson and McCabe, 1997; Gibling, 2006; Powell, 2009). We suggest that this characteristic can be further studied by comparing rivers with similar average discharge or drainage basin size, but with different discharge variability.

4.5.2 Large Rivers Do Not Build Large Fans

This dataset indicates that fluvial fan area does not scale with river discharge, channel width or drainage area. This implies that large rivers may form small fans and small rivers may form large fans, and contrasts the controls of fluvial fan size with those of deltas and submarine fans that scale with the river size (Sømme et al., 2009). These results contrast with Davidson and Hartley (2014) who report a strong correlation between drainage area and fluvial fan size in endorheic basins (r^2 values ranging from 0.75 to 0.95). The lack of data presentation in Davidson and Hartley (2014) does not allow for quantitative comparison between the two datasets, but they calculated drainage area using a Geographic Information System (GIS) platform as the area above the apex of the fan, whereas in this study we use the drainage area data provided with river discharge data that includes drainage area upstream of the gauging station. Their focus on endorheic basins also provides a dataset where sediment is not transferred out of the basin, and there is perhaps a more direct relationship between

source and sink. However, both studies have access to fan size data only and the fan volumes are unknown.

In our dataset fan size scales with tectonic setting and climate type (Figures 4.11 and 4.12). The former suggests a strong link between fan size and available lateral space (see North and Warwick, 2007; Hartley et al., 2010), whereas the interdependency with climate remains unclear. Hartley et al. (2010) suggested that fans in drylands or arid settings may not be limited by horizontal accommodation, but by discharge, and Davidson et al. (2013) showed that geomorphic elements and floodplain soils of fluvial fans are climate dependent. Climate thus seems a significant forcing factor on how fans form and build, and there is inter-dependency between fan size, tectonic setting and climate.

These findings imply that ancient fan size cannot be estimated from channel width or paleo-drainage size. For example, fluvial fan Australia (36) in arid hydroclimate and in an extensional basin has an apex channel width of 450 m and a fan area of 1,704 km², fluvial fan China (06) in monsoonal hydroclimate and in a compressional basin has an apex channel width of 466 m and a fan area of 12,098 km², and the Taquari fluvial fan Brazil (02) in rainforest hydroclimate and in a compressional basin has an apex channel width of 467 m and a fan area of 50,023 km².

4.5.3 Comparison of Modern and Ancient Channel Widths

Here we compare modern and ancient channel width from fluvial fans, motivated by the difficulty to measure channel widths on modern satellite imagery and in outcrops. In order to measure channel width at outcrops several elements are needed for good data quality: large outcrop size, minimal cover, knowledge of paleoflow direction as related to outcrop orientation, and access to tools, such as a laser range finder. Given these constraints, very few studies have measured channel width in detail. Two recent studies (Jones, 2017; Zellman, 2019) report channel widths from two different ancient fluvial fans (Figure 4.18). Comparison with our data show that the outcrop-measured channel widths are consistently wider (Figure 18), however Zellman (2019) reports that a high degree of channel amalgamation complicated

measurements in certain intervals.

Davidson et al. (2013) measured 36 fluvial fans and found channel widths that are generally narrower than in our considerably larger dataset (Figure 4.18). A quantitative comparison of rivers included in both datasets shows that 55% of their measurements were narrower, 28% were wider, and 17% were similar. This suggests that Davidson et al. (2013) may have used different measuring methods that resulted in generally narrower channel lengths, but lack of a methods section in their paper does not allow for further comparison.

4.5.4 Adjacency to Mountainous Hinterland

Our data show that 64% of the fans occur tens to more than 500 km away from their mountainous hinterlands. This implies that exit from confinement is not a critical control on fluvial fans, in contrast to alluvial fans that always occur adjacent to a mountain front (e.g. Blair and McPherson, 1994). This further signifies that the distribution of fluvial fans is considerably wider than that of alluvial fans which are limited to basin margins. It appears that greater discharge values increase the likelihood that a fluvial fan will form away from confinement, however this is not always the case as there are large rivers that form fluvial fans directly adjacent to confinement.

4.6 Conclusions

Scaling relationships based on the intrinsic properties of fluvial fans can be used to constrain the recognition, interpretation and reconstruction of fluvial fans. We compared fluvial fan size, channel width at the apex and the toe, and discharge in modern fluvial fans. We found that channel width at the apex best correlates to $Q_{99.863}$, while channel width at the toe best correlates to Q_{50} discharge. We also show that discharge correlates with drainage area. Approximately three quarters of fluvial fans (72.5%) have main channels that narrow from apex to toe. Fan size is controlled by both tectonic and climatic regime, but further study is needed to fully understand these interlinked controls. Fan size is positively skewed with a long tail, median fan size is 1,085 km², and average fan size is 5,818 km².

Our dataset indicates no link between fan area and discharge or fan area and channel width, or between channel width and discharge variability. We conclude that alluvial and fluvial fans have different formative controls, as the former are linked to exit from confinement at mountain fronts, whereas the latter are interdependent on available lateral space together with discharge characteristics as defined by hydroclimate types. However, this conclusion needs to be further tested for interdependency with sediment supply that was outside of the scope of this work.

4.7 Acknowledgments

We would like to thank our undergraduate research assistant Julia Payne for her hard work making measurements in Google Earth. We would also like to thank the Global Runoff Data Centre (GRDC), 56068 Koblenz, Germany for providing discharge data.

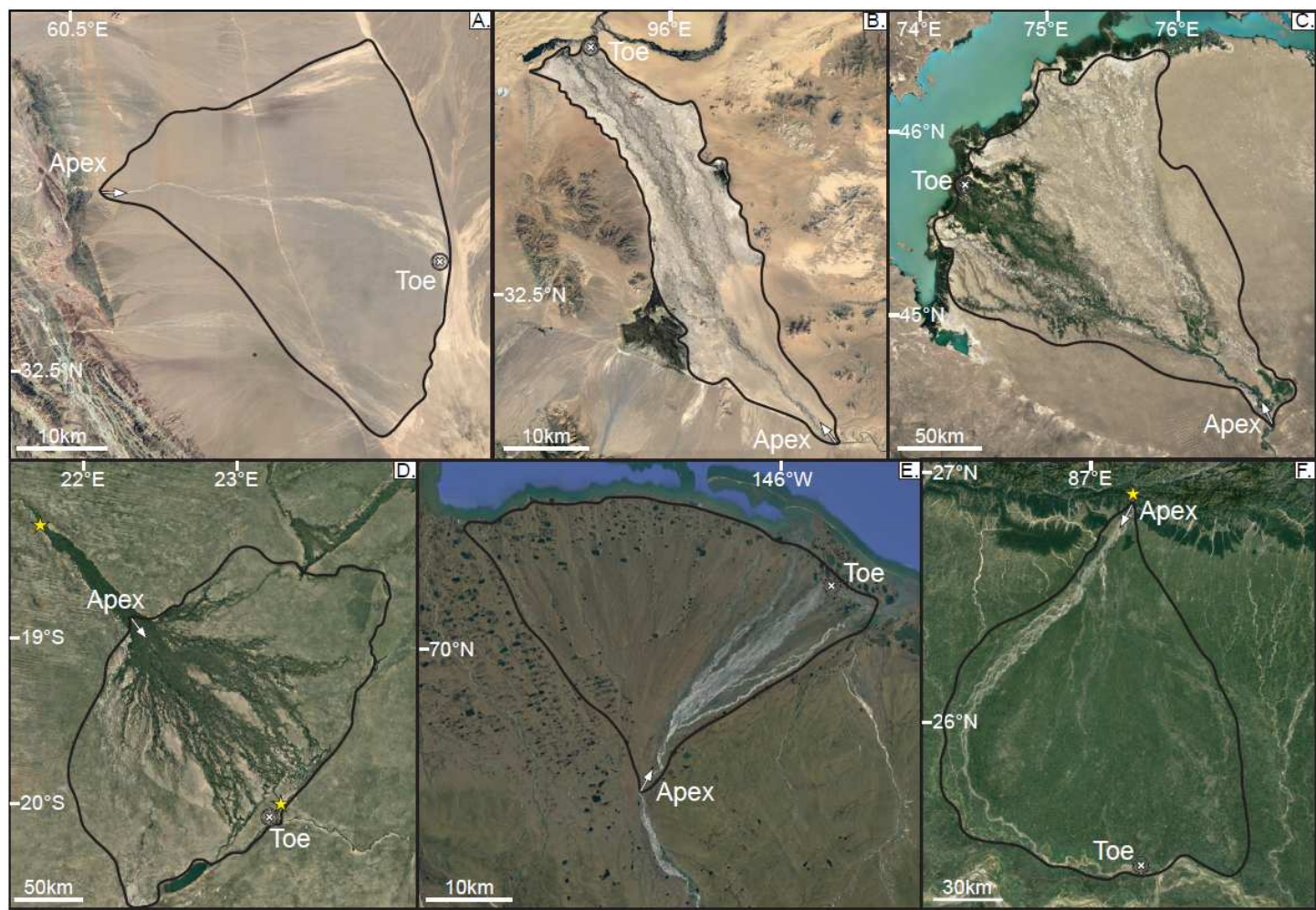


Figure 4.1: Examples of fluvial fans. A. Arid fan in Iran (22). B. Partially laterally confined fan in Mongolia (10). C. Fan in Kazakhstan with small deltas at the fan termination (02). D. Okavango fan in Botswana (01). E. Alaska (04) fan with a “classic” fan shape. F. Kosi fan in India (05). Star denotes a gauging station. North is up in all images. Fan numbers refer to the database (Suppl. Table 3.2).

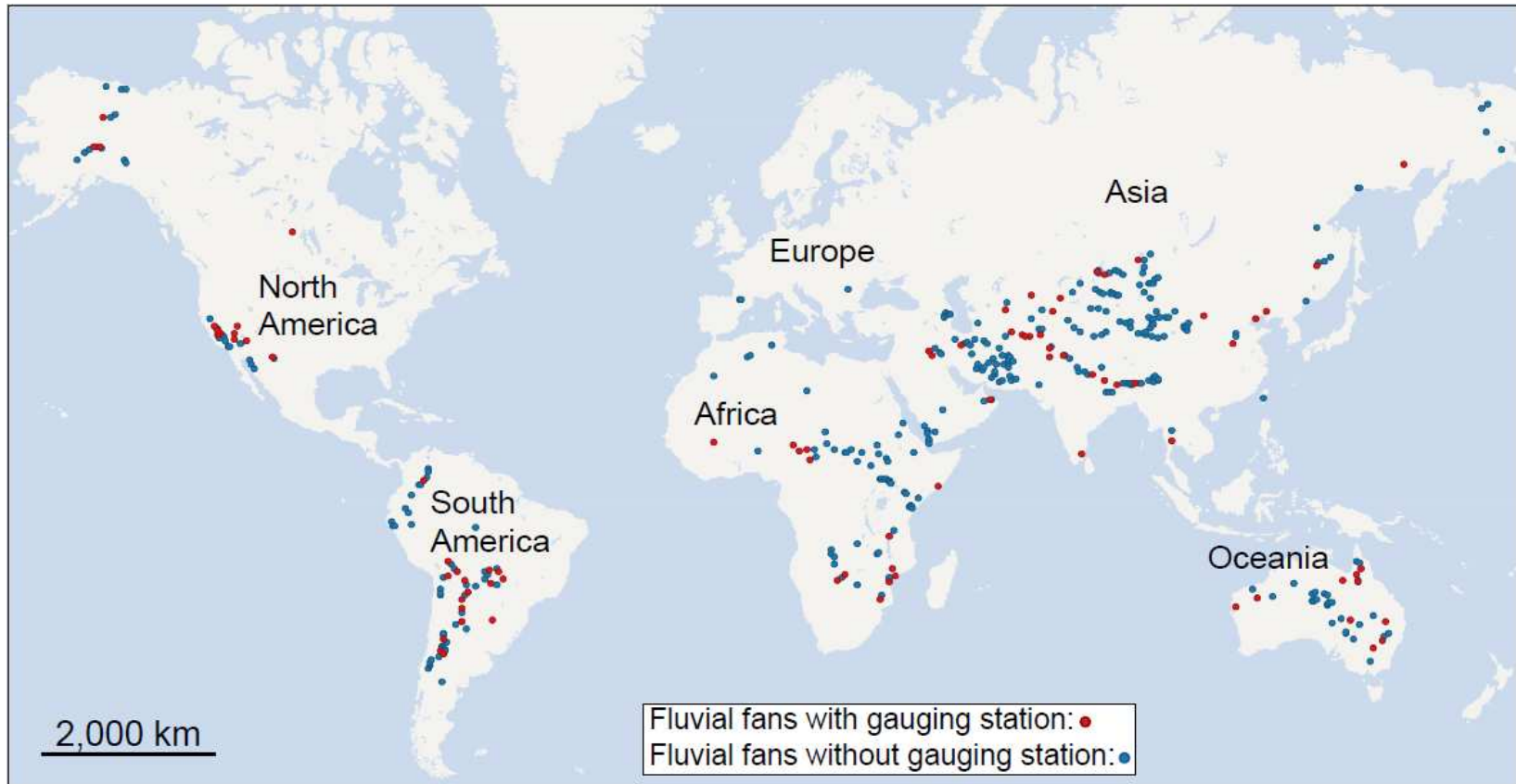


Figure 4.2: Map of fluvial fan locations (apex indicated by dots) and river discharge gauging stations used in this study.

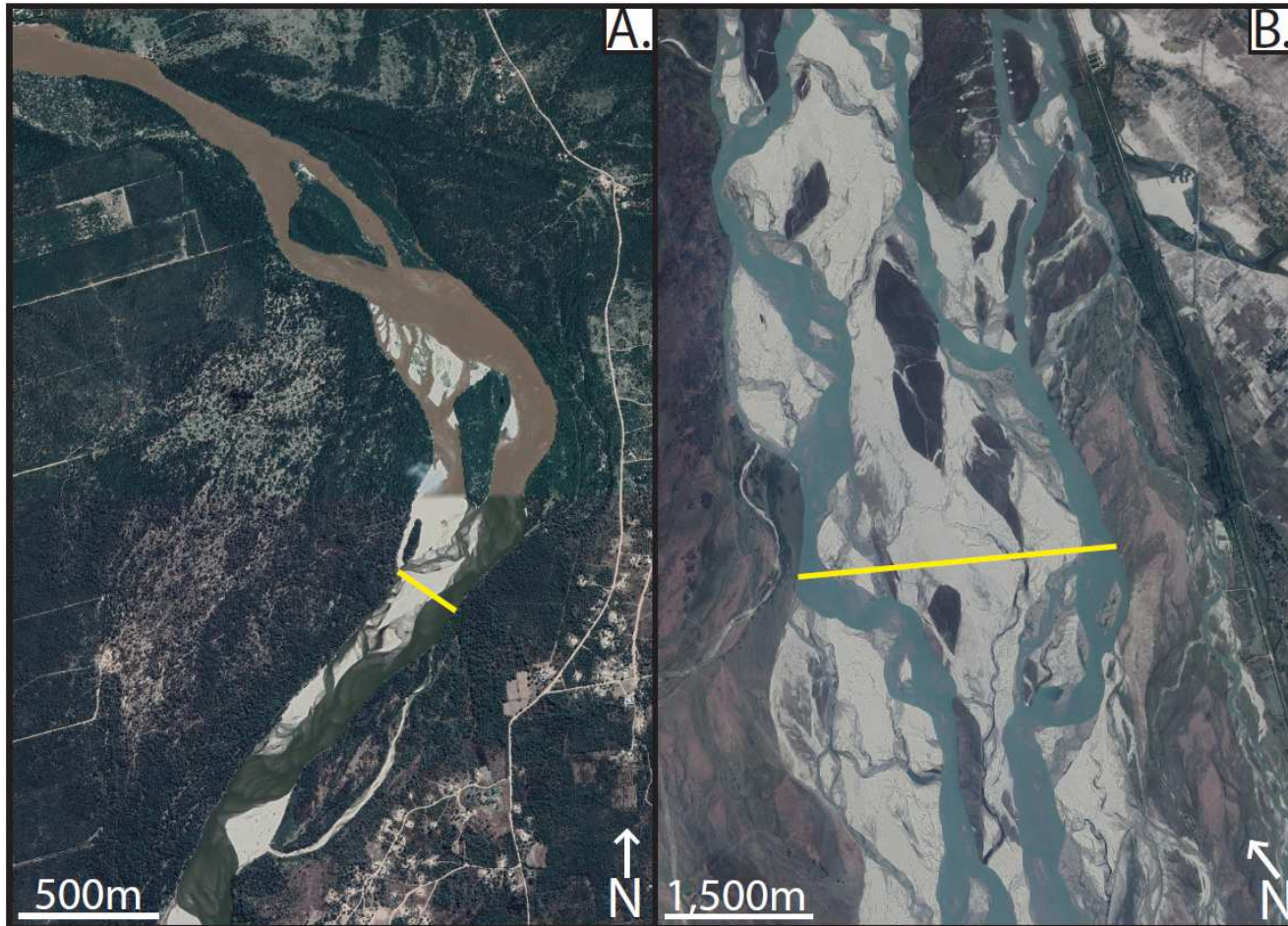
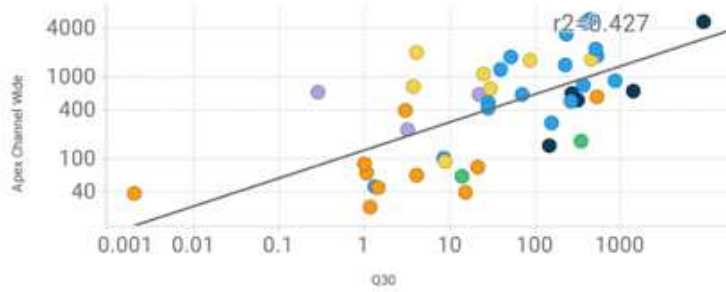
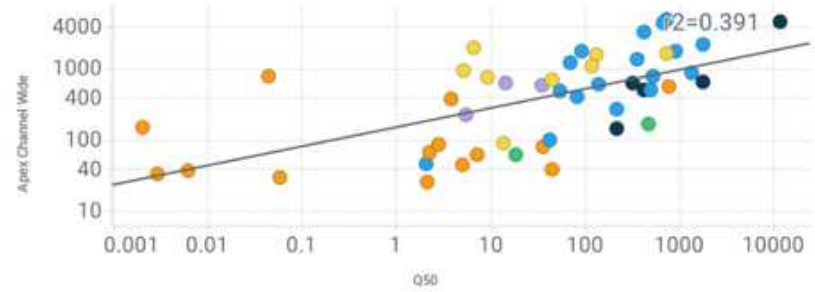


Figure 4.3: Channel width measurements examples for single-thread and multi-thread rivers. A) Fluvial Fan ARG04. The image is a composite from two different satellite images (top half vs bottom half) at two different flow conditions. This image illustrates the difficulty in measuring channel width bankfull flow. The discharge levels in the top half are much higher and are a better visual representation of bankfull flow. B) Fluvial Fan IN05. Multi-thread channels are inherently more difficult to measure, we measured from channel margin to channel margin while trying to avoid vegetated or potentially more permanent in channel bars.

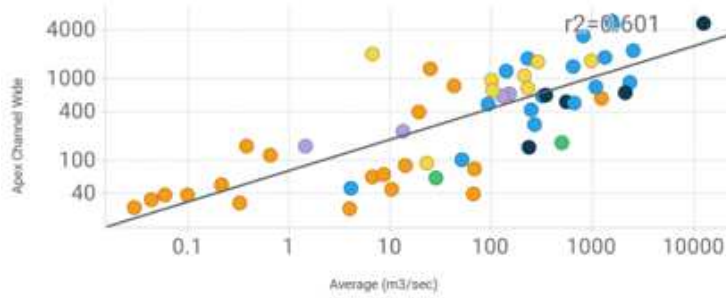
Apex Channel Wide vs. Q30



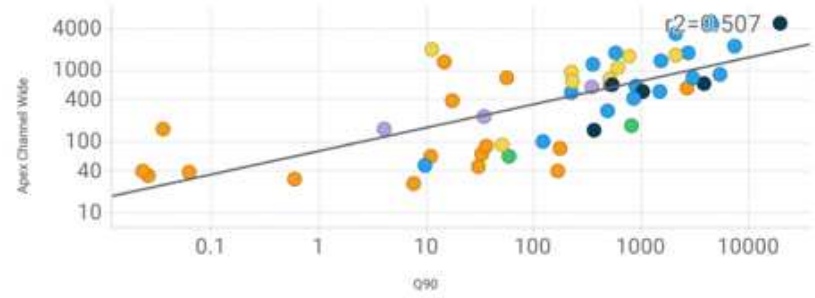
Apex Channel Wide vs. Q50



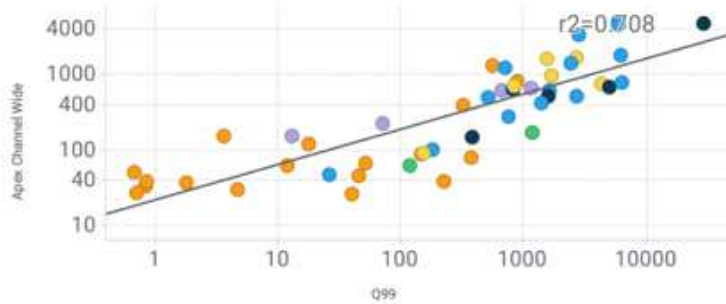
Apex Channel Wide vs. Average (m3/sec)



Apex Channel Wide vs. Q90



Apex Channel Wide vs. Q99



Apex Channel Wide vs. QR12

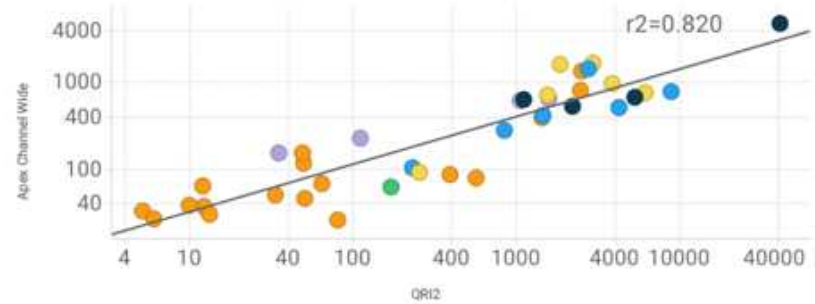


Figure 4.4: Apex channel width and discharge correlations. Apex channel (wide) best correlates with Q99.863 at $r^2=0.820$. There is a significant increase in correlation as discharge increases.

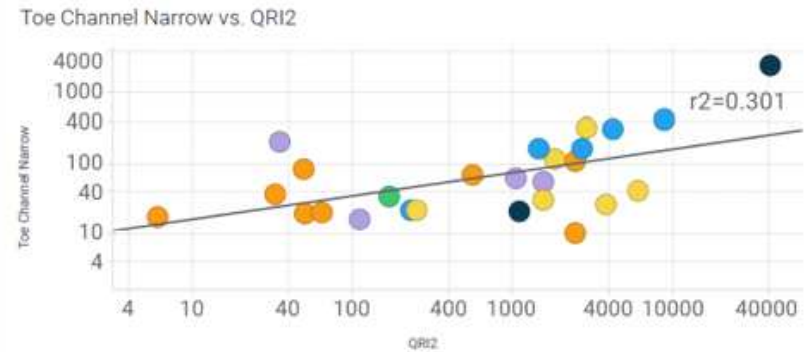
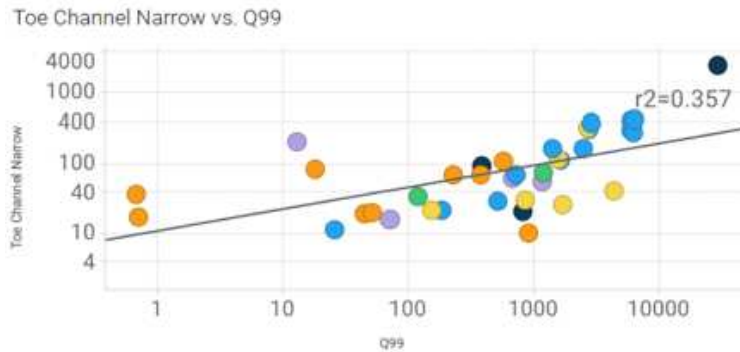
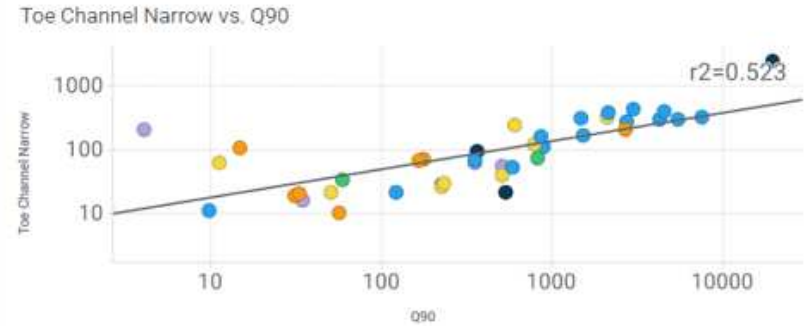
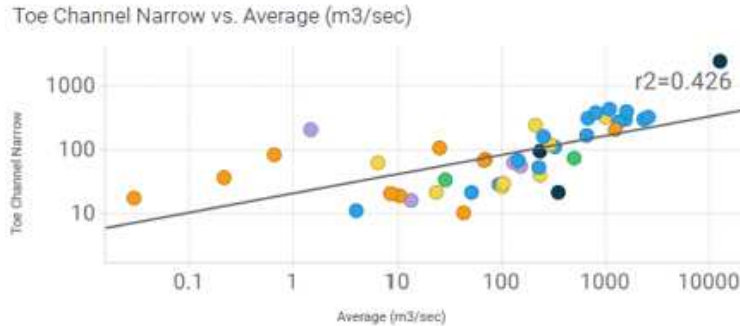
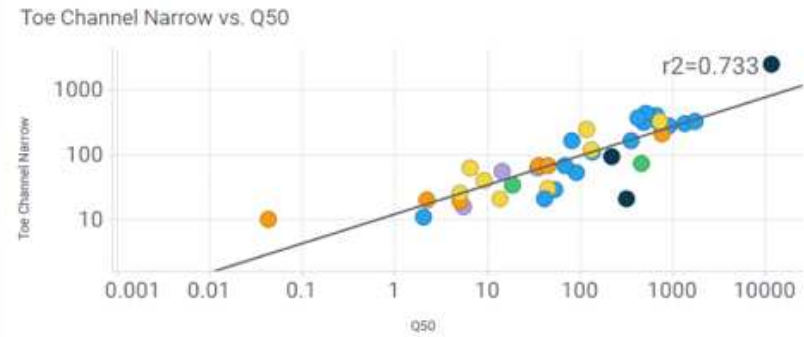
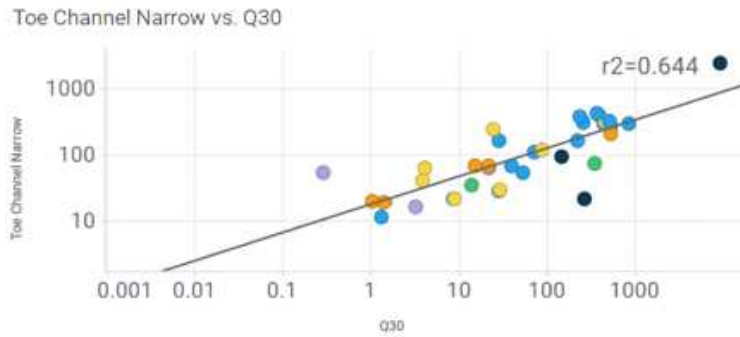
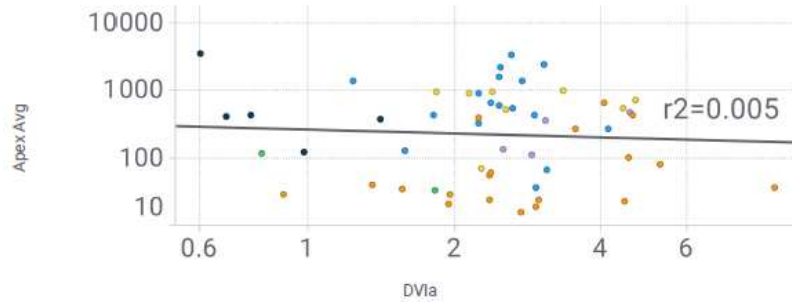
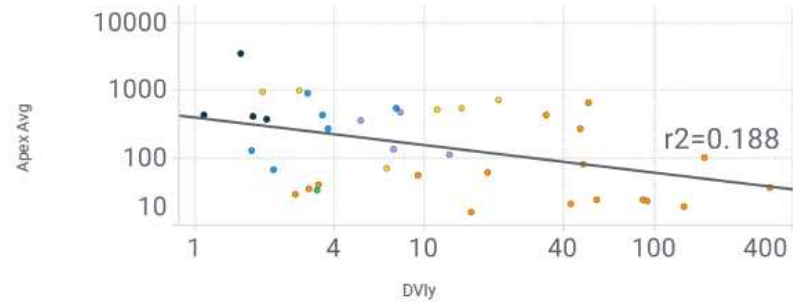


Figure 4.5: Toe channel width and discharge correlations. Toe Channel (narrow) best correlates with Q50 at $r^2=0.733$. Correlation gets worse below Q50 at values such as Q30. Correlation steadily gets worse at discharge values above Q50.

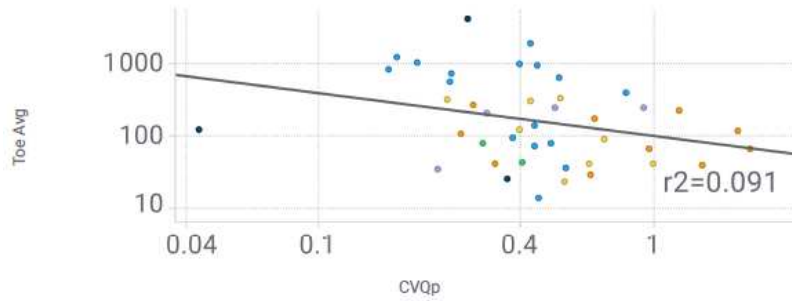
Apex Avg vs. DVla



Apex Avg vs. DVly



Toe Avg vs. CVQp



Toe Avg vs. Q99.863/Q50

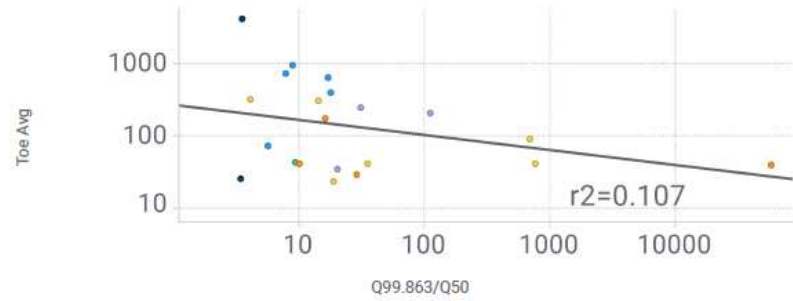


Figure 4.6: Channel width and discharge variability metrics. Nonexistent to very weak correlation of r^2 values that range from 0.005 to 0.091 between any of the discharge variability metrics and channel width.

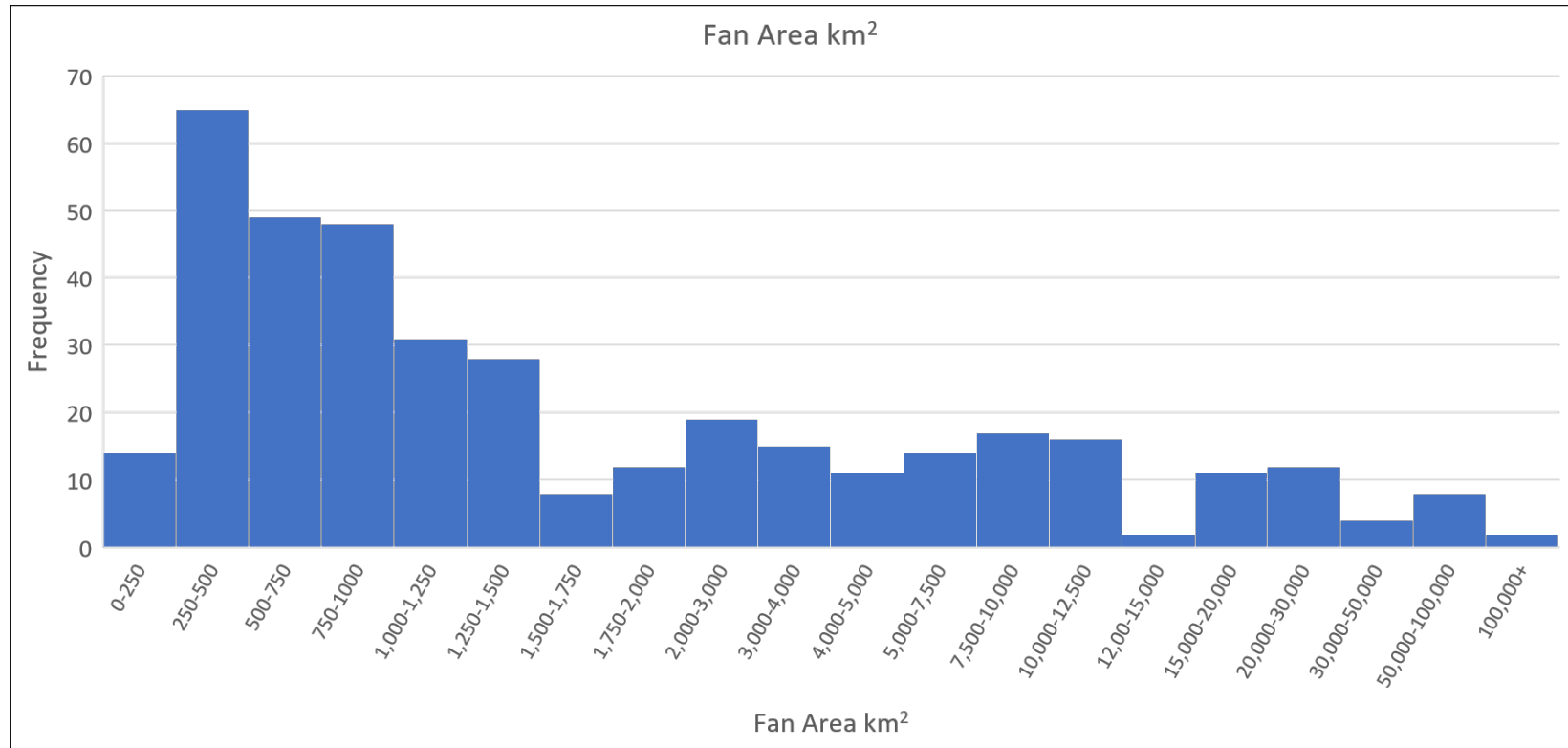


Figure 4.7: Binned frequency histogram of fan area. Fan area is positively skewed with a long tail. Median fan size is 1,085km² and average fan size is 5,818km². Please note that the fan area bin sizes increases somewhat logarithmically.

Apex-toe dist (km) vs. Fan Area (km²)

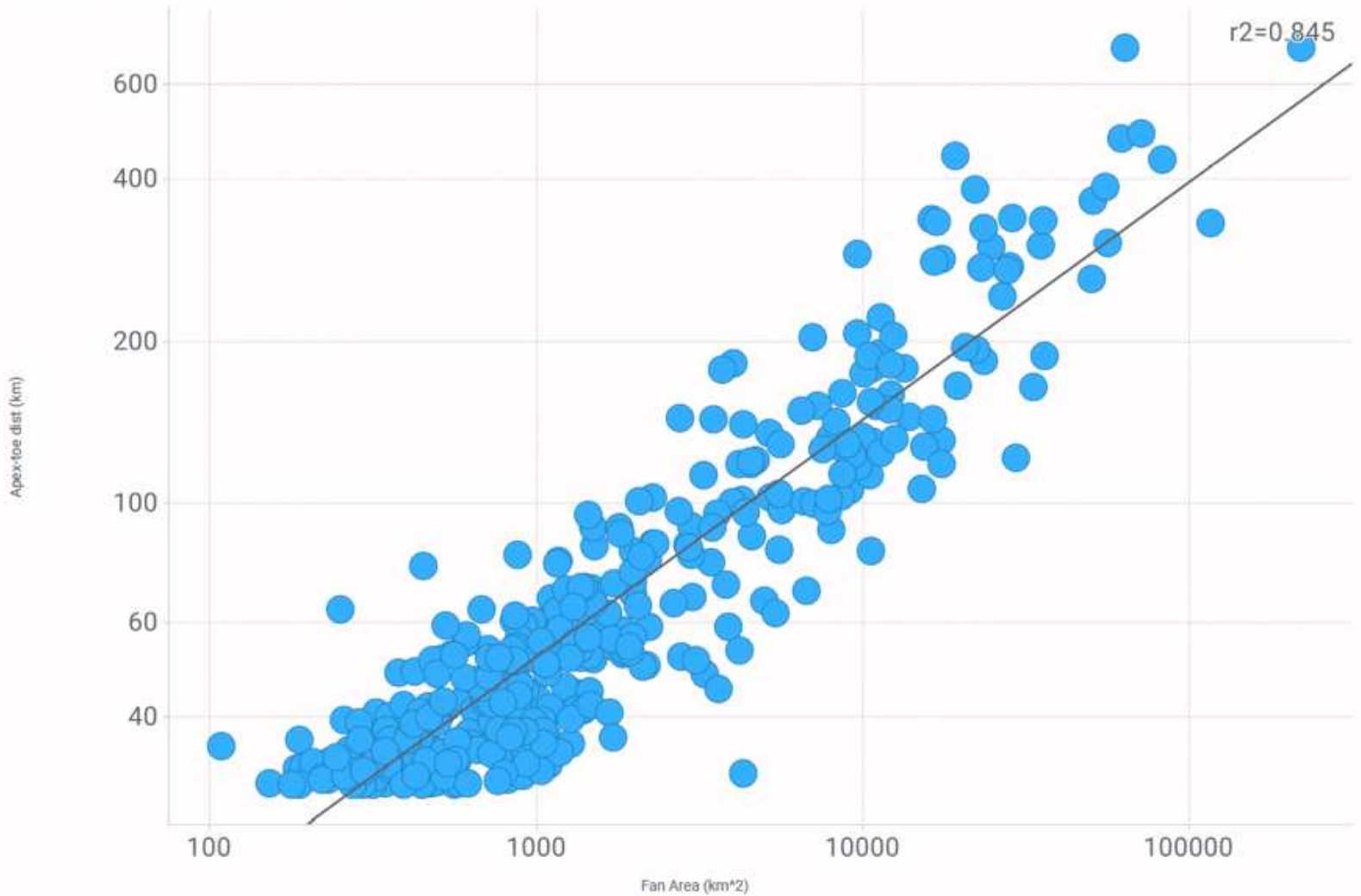


Figure 4.8: Fan area vs apex-to-toe distance. Strong correlation ($r^2 = 0.845$) between fan area (this study) and apex-to-toe distance (data from Hartley et al., 2010).

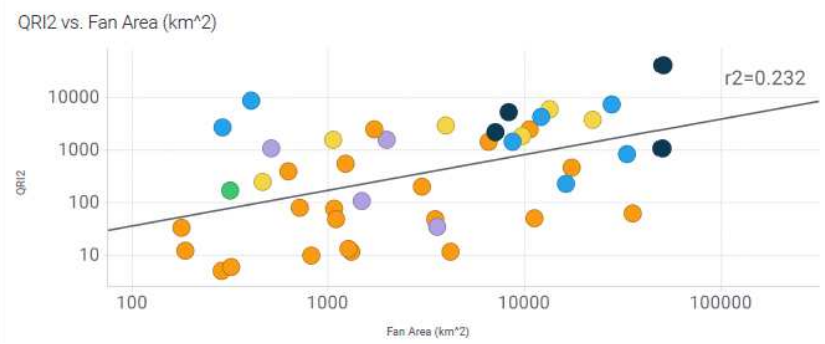
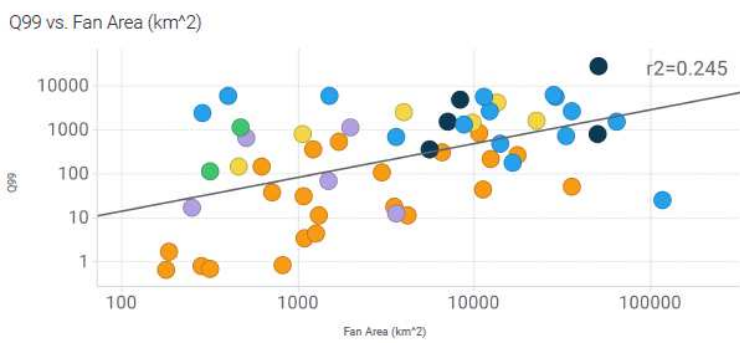
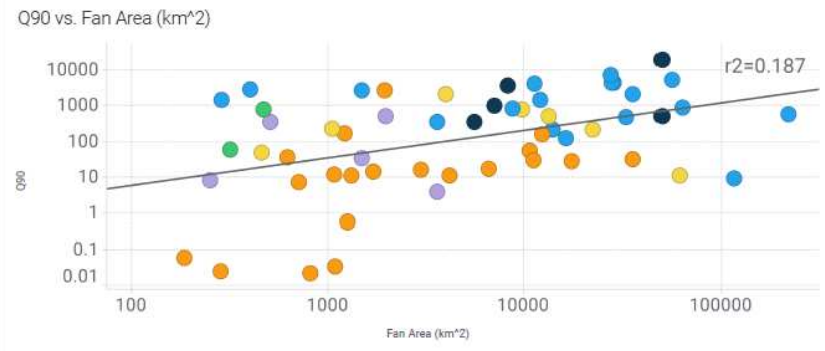
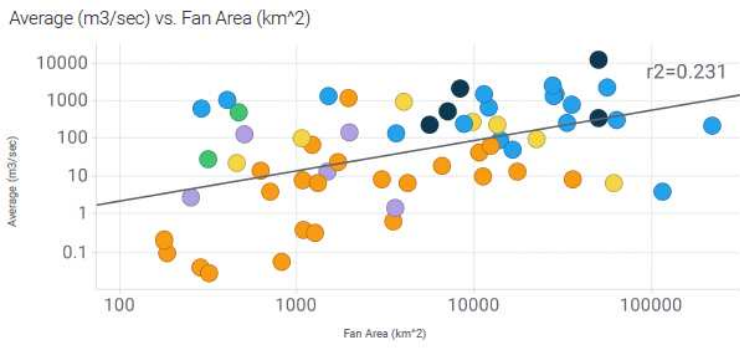
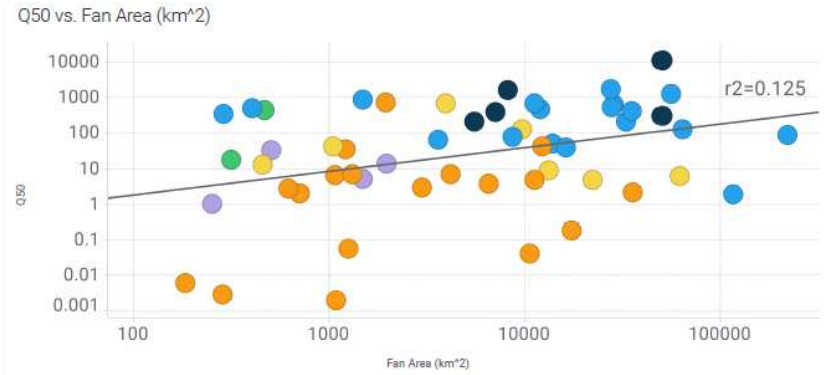
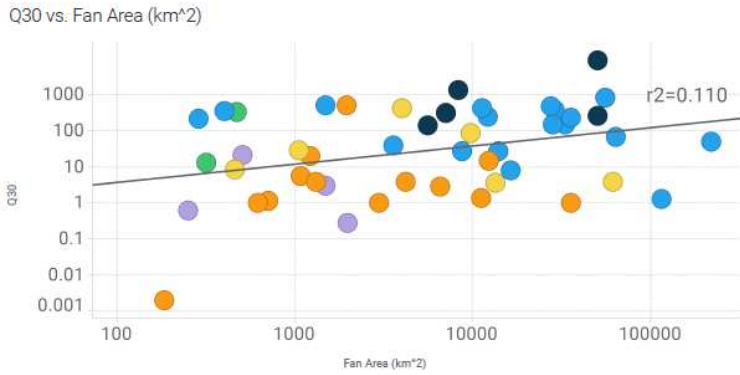
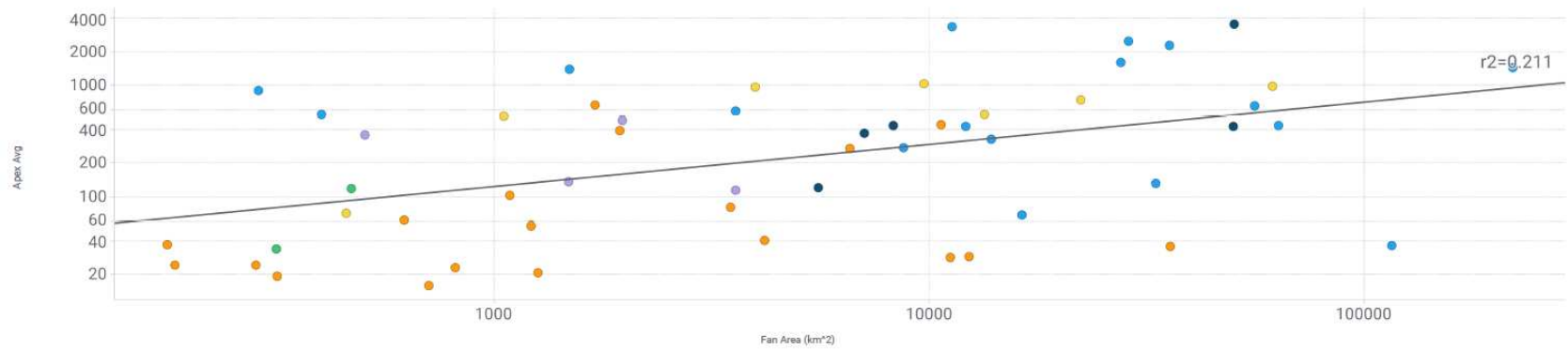


Figure 4.9: Fluvial fan size and discharge. Fan area has a very weak correlation to discharge with r² values ranging from 0.110 to 0.245.

Apex Avg vs. Fan Area (km²)



Toe Avg vs. Fan Area (km²)

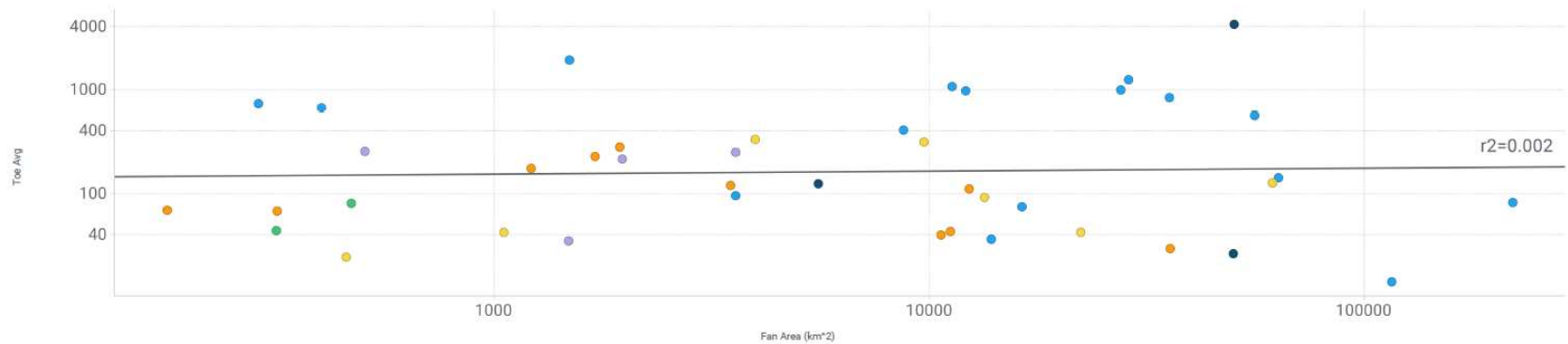


Figure 4.10: Fluvial fan size and channel width. Fan size has a very weak correlation to channel width with r^2 values ranging from 0.002 to 0.211.

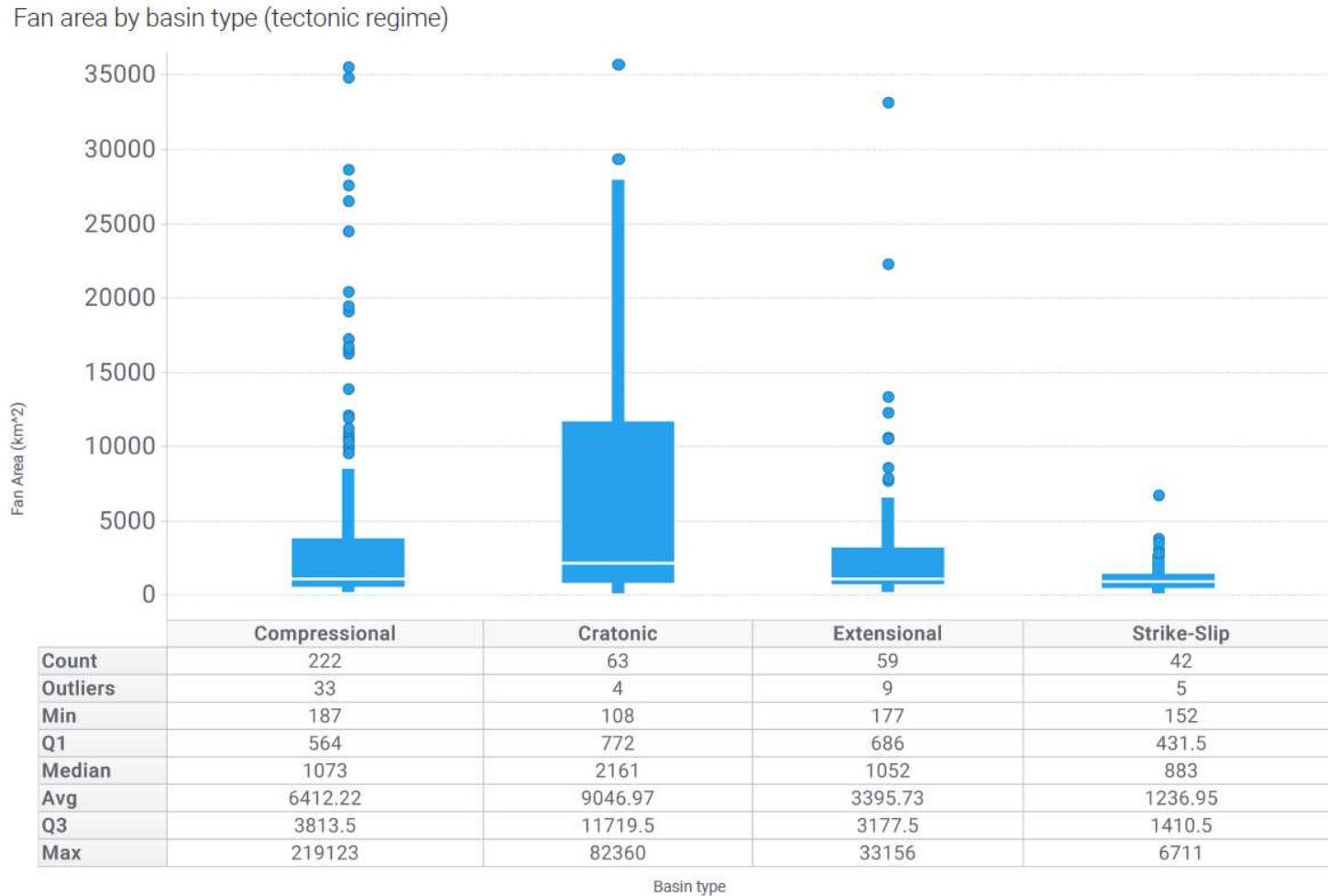


Figure 4.11: Tectonic regime controls on fluvial fan size. Compressional and cratonic basins have the largest fluvial fans. Cratonic basin fluvial fans have a much larger range of fluvial fan areas compared to the other three tectonic settings which tend to cluster around the median fan size of 1,085km². Strike-slip basin fluvial fans have a very narrow size range with no extremely large fans. Note: Extreme outliers have been cut off for image legibility, please refer to the supplemental table for fans larger than 35,000km².

Fan area by hydroclimate

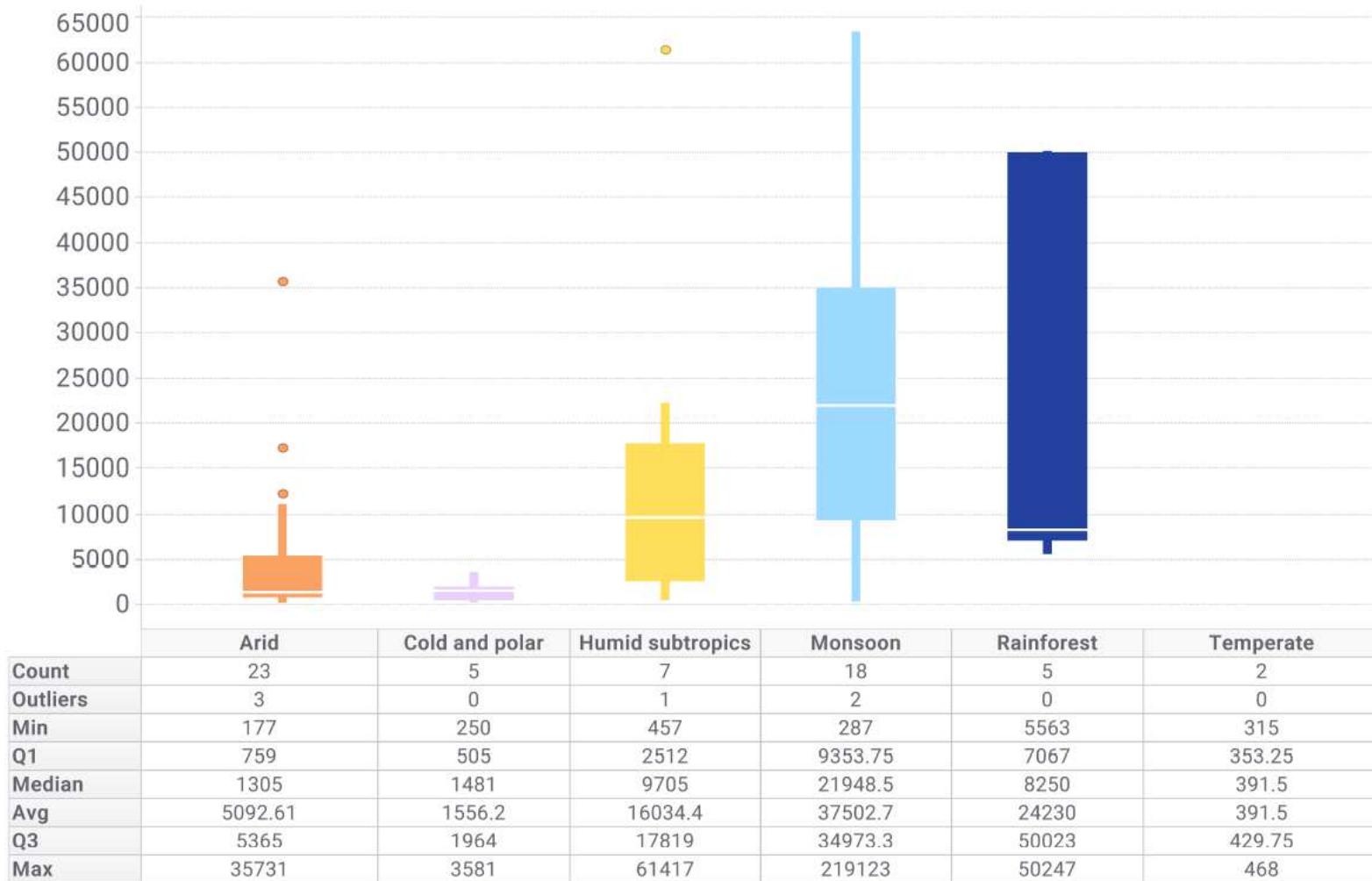


Figure 4.12: Climatic controls on fluvial fan size. There is a limited number of data points for most hydroclimates, with only arid and monsoonal hydroclimates having more than 10 data points, making comparisons difficult. Monsoonal fans have a significantly larger median area than arid fans at 21,949km² vs 1,305km², respectively

Q99 and Hydroclimate

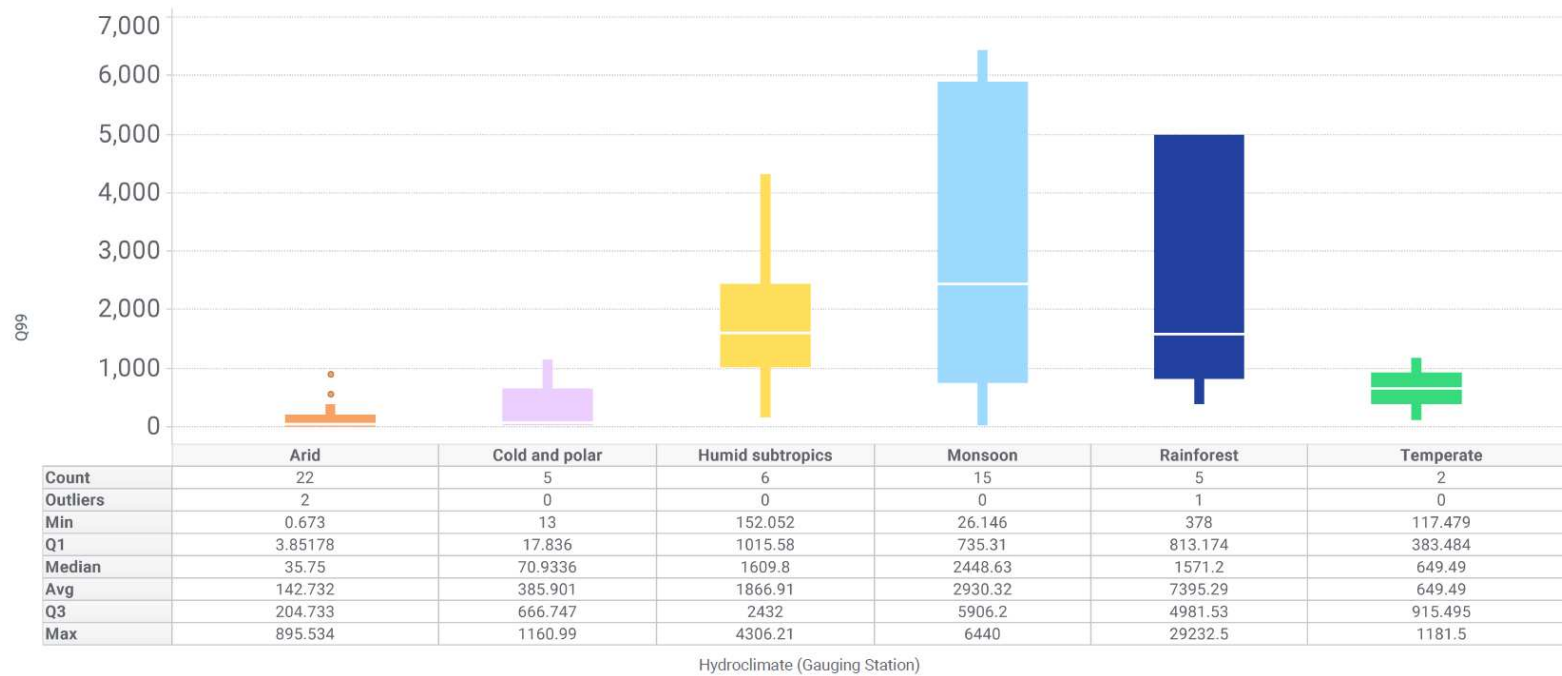


Figure 4.13: Climatic controls on Q_{99} discharge Monsoonal fans have a significantly larger median Q_{99} discharge than arid fans at $2,449\text{m}^3/\text{sec}$ vs $36\text{m}^3/\text{sec}$, respectively.

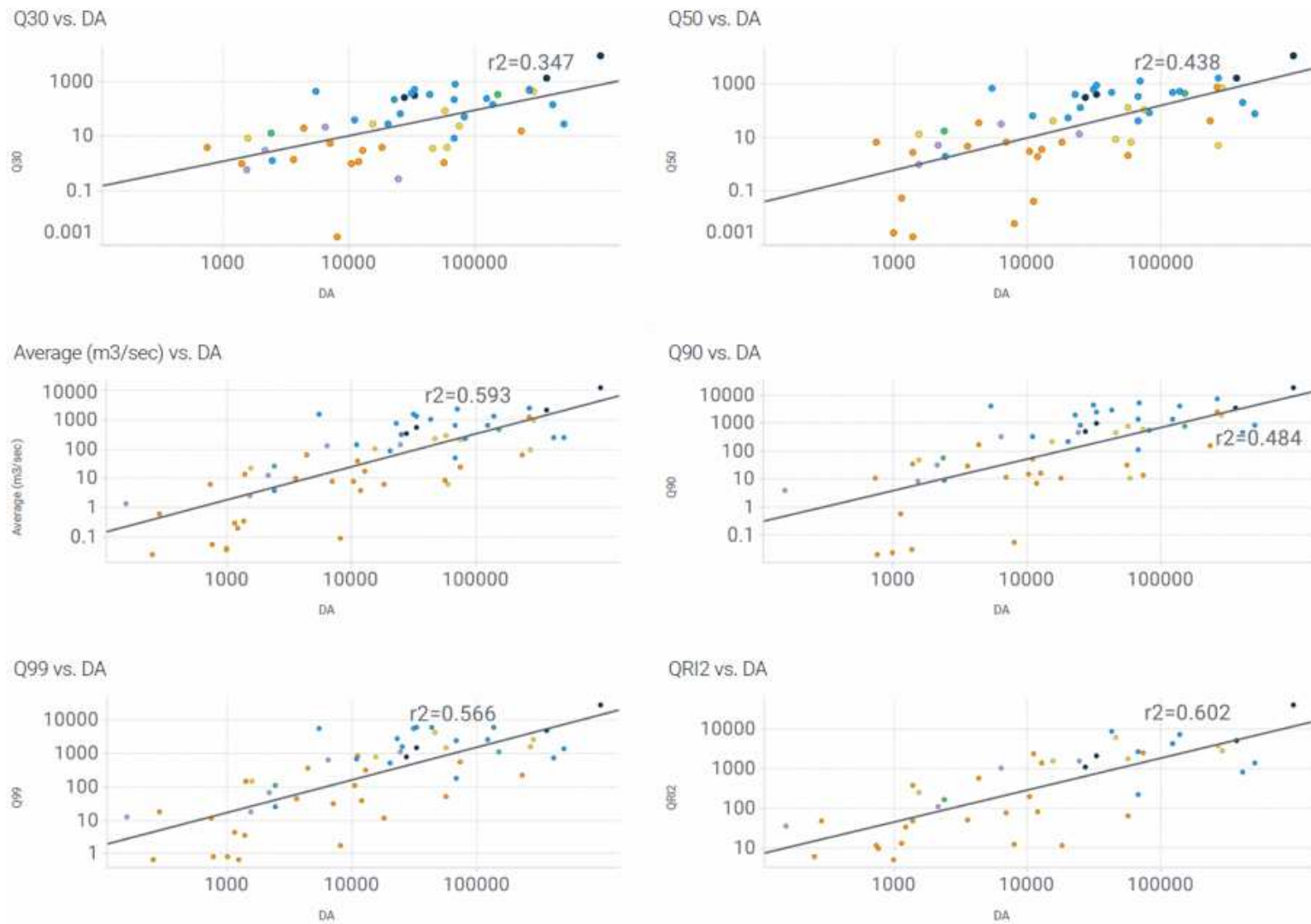


Figure 4.14: Drainage area and discharge correlations. Drainage Area best correlates with Q99.863 at $r^2=0.602$. This is not a particularly strong correlation, but steadily increases from lower discharge values indicating a positive trend.

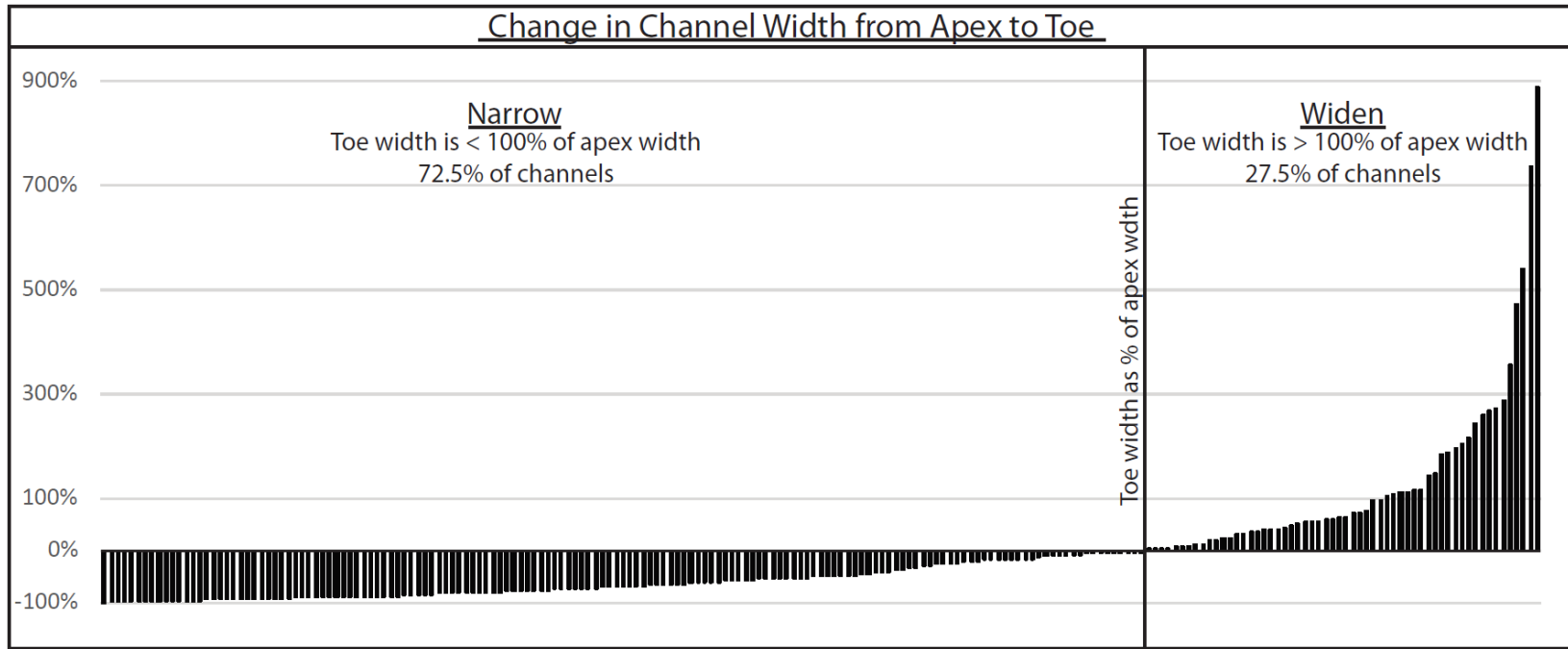


Figure 4.15: Changes in channel width from apex to toe. 72.5% of fluvial fans have channels that narrow from apex to toe. Each channel measured is represented by a vertical line, the length of which depicts the toe width as a % of apex width. Positive values on the right indicate that the channel is wider at the toe than at the apex, while negative values on the left indicate that the channel is narrower at the toe than at the apex.

Table 4.1: Discharge variability metrics

| Discharge Variability Metric | Equation | Reference |
|--|------------------------------------|--|
| Q_{peak} : discharge peakedness | Q_{WMmax}/Q_{mean} | Leier et al., 2005 |
| Q_{max}/Q_{10} : discharge variability | Q_{max}/Q_{10} | modified from Q_{max}/Q_{min} of Latrubesse et al., 2005 |
| Q_{max}/Q_{mean} : flood intensity | Q_{max}/Q_{mean} | Latrubesse et al., 2005 |
| DVI_a : average discharge variability index | $(Q_{WMmax} - Q_{WMmin})/Q_{mean}$ | Plink-Björklund, 2015 |
| DVI_y : yearly discharge variability index | $(Q_{Dmax} - Q_{min})/Q_{mean}$ | Hansford et al., 2020 |
| $Q_{99.863}/Q_{50}$: Flood magnitude | $Q_{99.863}/Q_{50}$ | Hansford et al., 2020 |
| CVQ_p : annual peak discharge variance | $(\sigma Q_{Ymax})/Q_{Ymean}$ | Fielding et al., 2018 |

Table 4.1: Discharge variability metrics used in this study. Measures of discharge (Q): Q_{mean} – mean; Q_{max} – maximum; Q_{min} – minimum; Q_{50} – 50th percentile; Q_{10} – 10th percentile; $Q_{99.863}$ – 99.863th percentile (equivalent to 2-year flood (Elliott and Capesius, 2009)); Q_{WMmax} – maximum of wettest month; Q_{WMmin} – minimum of wettest month; Q_{Dmax} – daily maximum of a year; Q_{Dmin} – daily minimum of the same year; σQ_{Ymax} – standard deviation of the annual peak; Q_{Ymean} – mean annual peak flood.

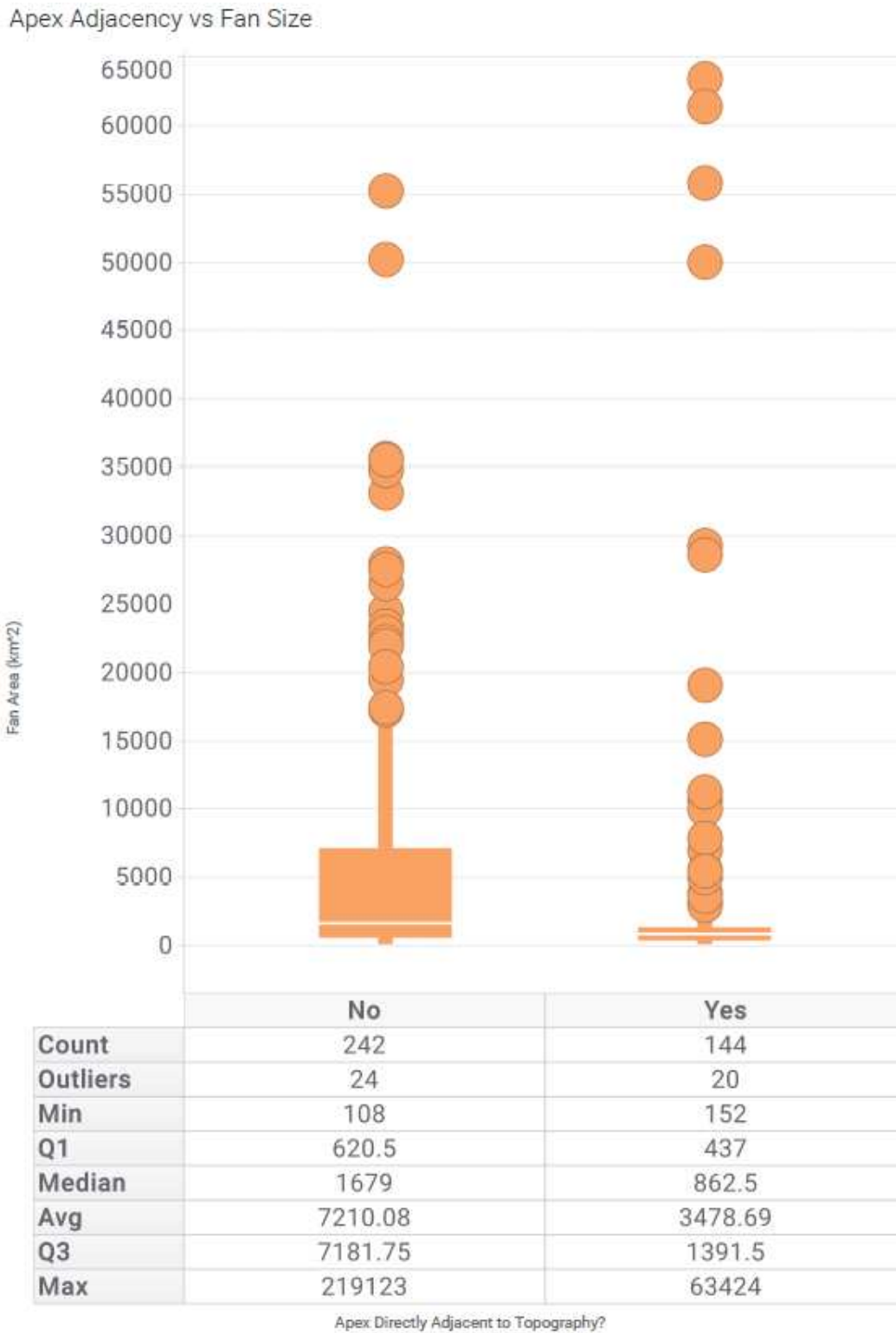


Figure 4.16: Fluvial fan size and apex adjacency. Fans that are not directly adjacent to their confining topography have median fans sizes that are approximately double fans that are directly adjacent.

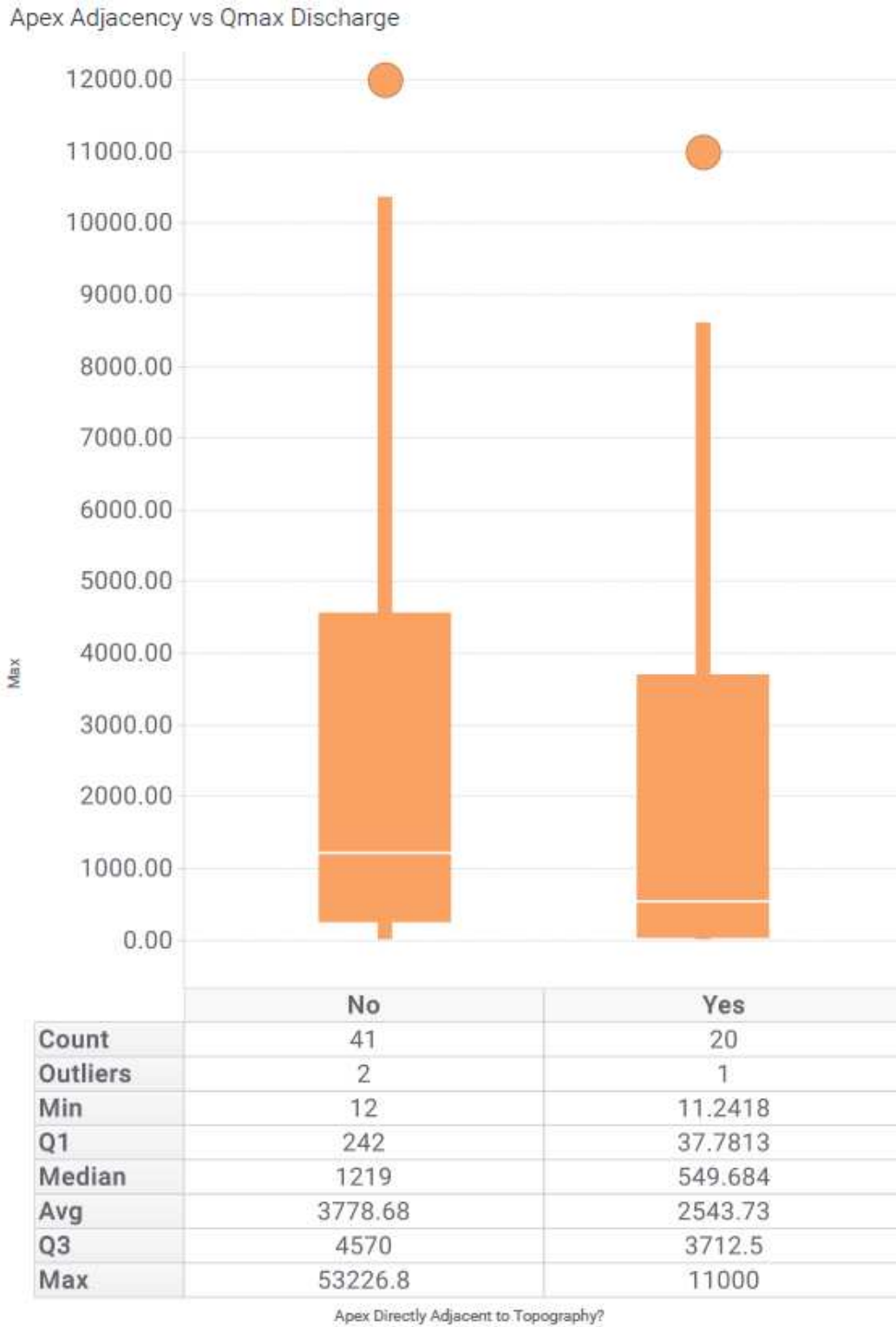


Figure 4.17: Fluvial fan maximum discharge and apex adjacency. Fans that are not directly adjacent to their confining topography have median maximum discharge values that are approximately double fans that are directly adjacent.

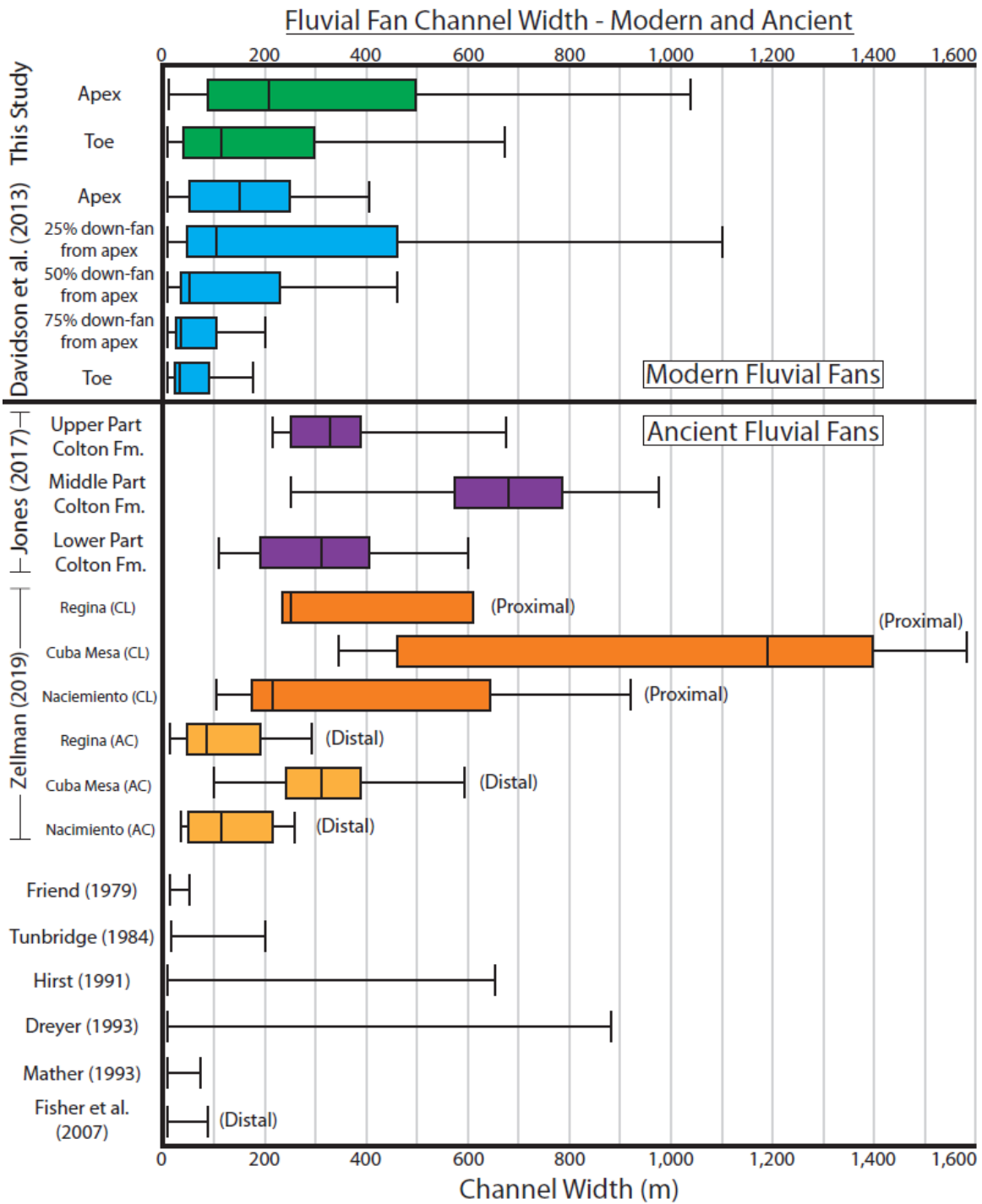


Figure 4.18: Channel width comparison between modern and ancient. Measurement locations noted where possible. Davidson et al. (2013) measured 36 modern fluvial fans in their study. Zellman (2019) measured the Early Eocene Regina and Cuba Mesa Members, which are part of the Jose Formation in the San Juan Basin, New Mexico. The Upper Paleocene Nacimiento Formation is also in the San Juan Basin, New Mexico. Jones (2017) measured the Late Paleocene to Early Eocene Formation in the Uinta Basin, Utah.

Table 4.2: Channel width change from apex to toe

| Channel width change from apex to toe | Count | % of total |
|--|------------|--------------|
| <hr/> | | |
| Widens (n=58) | 58 | 27.5% |
| Toe width 100% to 110% of apex | 7 | 3.3% |
| Toe width 110% to 125% of apex | 6 | 2.8% |
| Toe width 125% to 150% of apex | 9 | 4.3% |
| Toe width 150% to 200% of apex | 13 | 6.2% |
| Toe width 200% to 300% of apex | 11 | 5.2% |
| Toe width 300% to 500% of apex | 8 | 3.8% |
| Toe width > 500% of apex | 4 | 1.9% |
| <hr/> | | |
| Narrows (n=153) | 153 | 72.5% |
| Toe width 90% to 100% of apex | 15 | 7.1% |
| Toe width 80% to 90% of apex | 11 | 5.2% |
| Toe width 70% to 80% of apex | 7 | 3.3% |
| Toe width 60% to 70% of apex | 7 | 3.3% |
| Toe width 50% to 60% of apex | 5 | 2.4% |
| Toe width 40% to 50% of apex | 20 | 9.5% |
| Toe width 30% to 40% of apex | 15 | 7.1% |
| Toe width 20% to 30% of apex | 17 | 8.1% |
| Toe width 10% to 20% of apex | 25 | 11.8% |
| Toe width < 10% of apex | 31 | 14.7% |

CHAPTER 5

CONCLUSIONS

5.1 Summary Conclusions and Contributions

This dissertation contains three studies that collectively document: 1. Discharge variability and the climatic control in fluvial systems 2. How discharge variability controls the formation of fluvial fans and 3. Geomorphometric scaling relationships in fluvial fans. The key conclusions and contributions of each chapter are described below.

5.1.1 Chapter 2 Conclusions and Contributions

Chapter 2 developed a series of dimensionless metrics that quantitatively describes river discharge variability patterns. We found that a series of metrics captures the range of discharge variability better than any one metric. Analysis of the hydrograph shape is key for understanding discharge variability. Application of these metrics to 575 river gauging stations around the world shows that river discharge patterns fall into four statistically different and predictable groups as characterized by flood magnitude, hydrograph shape, and inter-annual variability. These hydrological groups occur in different hydroclimate types. Rivers with persistent hydrology occur in tropical rainforest zone. Rivers with single storm controlled hydrological variability occur in cold Dfa and temperate climates. Rivers with seasonal hydrology occur in monsoon zone, humid subtropics, and in cold and polar climates. Arid climate rivers have extreme and erratic hydrology.

Overall, this paper found a strong link between river hydrograph shapes and discharge variability patterns to hydroclimate and precipitation regimes. It also found that there is only a weak correlation between discharge variability and drainage basin size and that there is no simple relationship of downstream decrease in discharge variability.

5.1.2 Chapter 3 Conclusions and Contributions

Chapter 3 documents the control of discharge variability on the formation of fluvial fans. We found that river discharge variability promotes fluvial fan formation and that there is a correlation between fan occurrence and the precipitation pattern. Fluvial fans occur globally and are linked to discharge variability rather than specific climate zones. Our analysis shows that any conditions that promote avulsions increase the likelihood for fluvial fan formation, provided there is lateral space available. So while fluvial fans are likely proxies for climates with seasonal or variable discharge patterns, they do not exclusively indicate specific climate types.

5.1.3 Chapter 4 Conclusions and Contributions

Chapter 4 provides scaling relationships based on the intrinsic properties of fluvial fans that can be used to constrain the interpretation and reconstruction of fluvial fans. We compared fluvial fan size, channel width at the apex and the toe, and discharge in modern fluvial fans. We found that channel width at the apex best correlates to $Q_{99.863}$, while channel width at the toe best correlates to Q_{50} discharge. We also found that discharge correlates with drainage area. Approximately three-quarters of fluvial fans (72.5%) have main channels that narrow from apex to toe. Fan size is controlled by both tectonic and climatic regime, but further study is needed to fully understand these controls. Fan size is positively skewed with a long tail, median fan size is $1,085\text{km}^2$, and average fan size is $5,818\text{km}^2$. We were unable to find any correlation between channel width and discharge variability, however we may be lacking the data to appropriately examine this. We were also unable to find any correlation between fan area and discharge or fan area and channel width.

5.2 Future Work

This study was the first study since 1988 to quantify and describe the different patterns and controls on fluvial discharge. Since 1988, the global fluvial discharge record as well as computing power has greatly improved. However, we analyzed only a subset of the available

data. Significant advancement could be made by studying all available discharge data using machine learning and pattern recognition. Our work on fluvial discharge and magnitude needs to be advanced outside of the sedimentary community. Furthermore, the sedimentary community needs to study and discuss what flow regimes actually comprise the sedimentary record and discuss the impacts of different flow magnitude, duration, and intensity.

Despite having provided insight into fluvial discharge variability and the controls on fluvial fan formation, more study is needed. Our understanding of fluvial fans is still in its relative scientific and geologic infancy. This study has been one step closer to improving our understanding of fluvial fans, but there is still many more necessary steps. Here we have dived into the first steps of understanding the influence of climate, but it was only the first steps. Let alone the influence of tectonics, vegetation, bed rock, sediment source and supply, timing, gradient, etc. How significant are fluvial fans to the sedimentary record has yet to be scientifically tested.

We would like to see the quantitative scaling relationships found in fluvial fans compared to other quantitative studies. How do fluvial fans effect the source to sink model? Are fluvial fans fundamentally controlled by different scaling relationships than delta or submarine systems? Some of these studies already exist and it would be extremely interest to compare against them.

Hopefully the next phase of work undertaken by this research group will be studying how to differentiate between fluvial fans and fluvial deltas in the rock record, especially in a data limited environment. This has wide ranging implications not only for the better understanding of Earth's evolution paleoclimate modeling, but for planetary and life evolutionary studies through climate reconstructions on Mars and Saturn's moon Titan. The research group has found early promising results which will hopefully lead to a clearer understanding of whether the northern lowlands in Mars ever contained an oceanic body.

REFERENCES CITED

- Abdullatif, Osman Mahmoud. 1989. Channel-fill and sheet-flood facies sequences in the ephemeral terminal River Gash, Kassala, Sudan. *Sedimentary Geology*, **63**, 171–184.
- Alexander, Jan, Fielding, Christopher R, & Pocock, Geoff D. 1999. Flood behaviour of the Burdekin River, tropical north Queensland, Australia. *Geological Society of London Special Publications*, **163**, 27–40.
- Alfieri, Lorenzo, Bisselink, Berny, Dottori, Francesco, Naumann, Gustavo, Roo, Ad De, Salamon, Peter, Wyser, Klaus, & Feyen, Luc. 2017. Global projections of river flood risk in a warmer world. *Earth's Future AGU Publications*, 171–182.
- Allen, Jonathan P, Fielding, Christopher R, Rygel, Michael C, & Gibling, Martin R. 2013. Deconvolving signals of tectonic and climatic controls from continental basins: an example from the late Paleozoic Cumberland Basin, Atlantic Canada. *Journal of Sedimentary Research*, **83**, 847–872.
- Allen, Philip A. 2008. From landscapes into geological history. *Nature*, **451**(7176), 274–276.
- Amos, Kathryn J, Alexander, Jan, Horn, Anthony, Pocock, Geoff D., & Fielding, Chris R. 2004. Supply limited sediment transport in a high-discharge event of the tropical Burdekin River, North Queensland, Australia. *Sedimentology*, **51**, 145–162.
- Armitage, John J, Duller, Robert A, Whittaker, Alex C, & Allen, Philip A. 2011. Transformation of tectonic and climatic signals from source to sedimentary archive. *Nature Geoscience*, **4**, 231–235.
- Asadieh, Behzad, Krakauer, Nir Y, & Fekete, Balázs M. 2016. Historical Trends in Mean and Extreme Runoff and Streamflow Based on Observations and Climate Models. *Water*, **8**, 189.
- Assine, Mario Luis. 2005. River avulsions on the Taquari megafan, Pantanal wetland, Brazil. *Geomorphology*, **70**(3-4 SPEC. ISS.), 357–371.
- Assine, Mario Luis, Corradini, Fabrício Anibal, Pupim, Fabiano do Nascimento, & McGlue, Michael Matthew. 2014. Channel arrangements and depositional styles in the São Lourenço fluvial megafan, Brazilian Pantanal wetland. *Sedimentary Geology*, **301**, 172–184.
- Baker, Victor R. 1994. Geomorphological understanding of floods. *Geomorphology*, **10**, 139–156.

- Beckinsale, R.D. 1969. *River Regimes*. In: Chorley, R.J. (Ed.) *Water, Earth, and Man*.
- Benson, M.A. 1952. *Characteristics of frequency curves based on a theoretical 1,000-year record*. U.S. Geological Survey Open-File Report.
- Billi, Paolo. 2007. Morphology and sediment dynamics of ephemeral stream terminal distributary systems in the Kobo Basin (northern Welo, Ethiopia). *Geomorphology*, **85**, 98–113.
- Blair, Terence C, & McPherson, John G. 1994. Alluvial Fans and their Natural Distinction from Rivers Based on Morphology, Hydraulic Processes, Sedimentary Processes, and Facies Assemblages. *Journal of Sedimentary Research*, **64A**(3), 450–489.
- Blum, M., & Pecha, M. 2014. Mid-cretaceous to paleocene North American drainage reorganization from detrital zircons. *Geology*, **42**(7), 607–610.
- Bracken, Louise J, & Croke, Jacky. 2007. The concept of hydrological connectivity and its contribution to understanding runoff-dominated geomorphic systems. *Hydrological Processes*, **21**, 1749–1763.
- Bromley, Michael H. 1978. Variations in Fluvial Style as Revealed by Architectural Elements, Kayenta Formation, Mesa Creek, Colorado, USA: Evidence for both Ephemeral and Perennial Fluvial Processes.
- Bryant, Madeline, Falk, Peter, & Paola, Chris. 1995. Experimental study of avulsion frequency and rate of deposition. *Geology*, **23**, 365–368.
- Carmichael, Matthew J., Pancost, Richard D., & Lunt, Daniel J. 2018. Changes in the occurrence of extreme precipitation events at the Paleocene–Eocene thermal maximum. *Earth and Planetary Science Letters*, **501**, 24–36.
- Cecil, C B, Dulong, F T, Harris, R A, Cobb, J C, Gluskoter, H G, & Nugroho, H. 2003. Observations on climate and sediment discharge in selected tropical rivers, Indonesia. *Climate Controls on Stratigraphy*, **77**, 29–50.
- Cecil, C. Blaine, & Dulong, Frank T. 2003. Precipitation Models for Sediment Supply in Warm Climates. *SEPM Special Publication*, **77**(1958), 21–27.
- Chakraborty, Tapan, Kar, Rimpal, Ghosh, Parthasarathi, & Basu, Sounak. 2010. Kosi megafan: Historical records, geomorphology and the recent avulsion of the Kosi River. *Quaternary International*, **227**(2), 143–160.

- Clift, Peter D., Hodges, Kip V., Heslop, David, Hannigan, Robyn, Van Long, Hoang, & Calves, Gerome. 2008. Correlation of Himalayan exhumation rates and Asian monsoon intensity. *Nature Geoscience*, **1**(12), 875–880.
- Davidson, Stephanie K, & Hartley, Adrian J. 2014. A quantitative approach to linking drainage area and distributive fluvial system area in modern and ancient endorheic basins. *Journal of Sedimentary Research*, **84**, 1005–1020.
- Davidson, Stephanie K., & North, Colin P. 2009. Geomorphological regional curves for prediction of drainage area and screening modern analogues for rivers in the rock record. *Journal of Sedimentary Research*, **79**, 773–792.
- Davidson, Stephanie K, Hartley, Adrian J, Weissmann, Gary S, Nichols, Gary J, & Scuderi, Louis A. 2013. Geomorphic elements on modern distributive fluvial systems. *Geomorphology*, **180-181**, 82–95.
- DeCelles, P.G., & Cavazza, W. 1999. A comparison of fluvial megafans in the Cordilleran (Upper Cretaceous) and modern Himalayan foreland basin systems. *GSA Bulletin*, **111**, 1315–1334.
- Dingle, Elizabeth H, Paringit, Enrico C, Tolentino, Pamela L M, Williams, Richard D, Hoey, Trevor B, Barrett, Brian, Long, Hazel, Smiley, Crystal, & Stott, Eilidh. 2019. Decadal-scale morphological adjustment of a lowland tropical river. *Geomorphology*, **333**, 30–42.
- Eide, Christian Haug, Müller, Reidar, & Helland-Hansen, William. 2017. Using climate to relate water discharge and area in modern and ancient catchments. *Sedimentology*.
- Elliott, J.G., & Capesius, J.P. 2009. Geomorphic changes resulting from floods in reconfigured gravel-bed river channels in Colorado, USA. *The Geology Society of America Special Paper 451*, **451**, 173–198.
- Fawdon, Peter, Gupta, Sanjeev, Davis, Joel M., Warner, Nicholas H., Adler, Jacob B., Balme, Matthew R., Bell, James F. III, Grindrod, Peter M., & Sefton-Nash, Elliot. 2018. The Hypanis Valles delta: The last highstand of a sea on early Mars? *Earth and Planetary Science Letters*, **500**, 225–241.
- Fielding, Christopher R. 2006. Upper flow regime sheets, lenses and scour fills: Extending the range of architectural elements for fluvial sediment bodies. *Sedimentary Geology*, **190**, 227–240.
- Fielding, Christopher R, & Alexander, Jan. 1996. Sedimentology of the Upper Burdekin River of North Queensland, Australia-an example of a tropical, variable discharge river. *Terra Nova*, **8**, 447–457.

- Fielding, Christopher R, Allen, Jonathan P, Alexander, Jan, & Gibling, Martin R. 2009. Facies model for fluvial systems in the seasonal tropics and subtropics. *Geology*, **37**(7), 623–626.
- Fielding, Christopher R, Ashworth, Philip J., Best, James L., Prokocki, Eric W., & Smith, Gregory H. Sambrook. 2012. Tributary, distributary and other fluvial patterns: What really represents the norm in the continental rock record? *Sedimentary Geology*, **261-262**, 15–32.
- Fielding, Christopher R, Alexander, Jan, & Allen, Jonathan P. 2018. The role of discharge variability in the formation and preservation of alluvial sediment bodies. *Sedimentary Geology*, **365**, 1–20.
- Fielding, C.R., Allen, J.P., Alexander, J., Gibling, M.R., Rygel, M.C., & Calder, J.H. 2011. *From river to rock record*. In: Davidson, S.K., Leleu, S., North, C.P. (eds.), *The Preservation of Fluvial Sediments and Their Subsequent Interpretation* 97.
- Finlayson, B.L., McMahon, T.A., Srikanthan, R., & Haines, A. 1986. *World Hydrology: a New Data Base for Comparative Analysis*. Hydrology and Water Resources Symposium 1986. Institution for Engineers Australia, National Conference Publication.
- Fiorillo, Anthony R., McCarthy, Paul J., & Flaig, Peter P. 2010. Taphonomic and sedimentologic interpretations of the dinosaur-bearing Upper Cretaceous Strata of the Prince Creek Formation, Northern Alaska: Insights from an ancient high-latitude terrestrial ecosystem. *Palaeogeography, Palaeoclimatology, Palaeoecology*, **295**, 376–388.
- Fisher, J A, Nichols, G J, & Waltham, D A. 2007. Unconfined flow deposits in distal sectors of fluvial distributary systems: Examples from the Miocene Luna and Huesca Systems, northern Spain. *Sedimentary Geology*, **195**, 55–73.
- Flaig, P. P., Fiorillo, A. R., & McCarthy, P. J. 2014. Dinosaur-Bearing Hyperconcentrated Flows of Cretaceous Arctic Alaska: Recurring Catastrophic Event Beds on a Distal Paleopolar Coastal Plain. *Palaios*, **29**, 594–611.
- Foley, Michael G. 1978. Scour and fill in steep, sand-bed ephemeral streams. *GSA Bulletin*, **89**, 559–570.
- Fontana, Alessandro, Mozzi, Paolo, & Marchetti, Mauro. 2014. Alluvial fans and megafans along the southern side of the Alps. *Sedimentary Geology*, **301**, 150–171.
- François, B, Schlef, K E, Wi, S, & Brown, C M. 2019. Design considerations for riverine floods in a changing climate – A review. *Journal of Hydrology*, **574**, 557–573.

- Friend, P.F. 1978. Distinctive features of some ancient river systems. *Pages 531–542 of:* Miall, A.D. (ed), *Fluvial Sedimentology*.
- Frostick, Lynne E., & Reid, Ian. 1977. The origin of horizontal laminae in ephemeral stream channel-fill. *Sedimentology*, **24**, 1–9.
- Froude, Melanie J., Alexander, Jan, Barclay, Jenni, & Cole, Paul. 2017. Interpreting flash flood palaeoflow parameters from antidunes and gravel lenses: An example from Montserrat, West Indies. *Sedimentology*, **64**, 1817–1845.
- Gall, Ryan D, Birgeneheier, Lauren P, & Vanden Berg, Michael D. 2017. Highly Seasonal and Perennial Fluvial Facies: Implications For Climatic Control On the Douglas Creek and Parachute Creek Members, Green River Formation, Southeastern Uinta Basin, Utah, U.S.A. *Journal of Sedimentary Research*, **87**(9), 1019–1047.
- Galve, Jorge P., Alvarado, Guillermo E., Pérez-Peña, José Vicente, Mora, Mauricio M., Booth-Rea, Guillermo, & Azañón, José Miguel. 2016. Megafan formation driven by explosive volcanism and active tectonic processes in a humid tropical environment. *Terra Nova*, **28**(6), 427–433.
- Gentilli, J. 1952. *Seasonal river regimes in Australia*. 8th General Assembly and 17th International Congress Proceedings.
- Ghinassi, M, Moody, J, & Martin, D. 2018. Influence of extreme and annual floods on point-bar sedimentation: Inferences from Powder River , Montana , USA. *GSA Bulletin*, **131**, 71–83.
- Gibling, M. R. 2006. Width and Thickness of Fluvial Channel Bodies and Valley Fills in the Geological Record: A Literature Compilation and Classification. *Journal of Sedimentary Research*, **76**, 731–770.
- Gohain, K., & Parkash, B. 1990. Morphology of the Kosi Megafan. *Pages 151–178 of:* Rachocki, A.H., & Church, M. (eds), *Alluvial Fans—A Field Approach*. Chichester: John Wiley & Sons.
- Graf, W.L. 1988. *Fluvial Processes in Dryland Rivers*.
- Gupta, Vijay K, & Dawdy, David R. 1995. Physical interpretations of regional variations in the scaling exponents of flood quantiles. *Hydrological Processes*, **9**(September 1994), 347–361.
- Haines, A T, Finlayson, B I, & McMahon, T A. 1988. A global classification of river regimes. *Applied Geography*, **8**, 255–272.

- Hajek, Elizabeth A., & Wolinsky, Matthew A. 2012. Simplified process modeling of river avulsion and alluvial architecture: Connecting models and field data. *Sedimentary Geology*, **257-260**, 1–30.
- Hansford, Mark R, Plink-Björklund, Piret, & Jones, Evan R. 2020. Global quantitative analyses of river discharge variability and hydrograph shape with respect to climate types. *Earth-Science Reviews*, **200**, 1–20.
- Hartley, A. J., Weissmann, G. S., Nichols, G. J., & Warwick, G. L. 2010. Large Distributive Fluvial Systems: Characteristics, Distribution, and Controls on Development. *Journal of Sedimentary Research*, **80**(2), 167–183.
- Hayden, Bruce P. 1988. Flood Climates. *Chap. 1, pages 13–26 of:* Baker, Victor R., Kochel, Craig R., & Patton, Peter C. (eds), *Flood Geomorphology*. John Wiley & Sons.
- Hodgkins, Glenn A., Whitfield, Paul H., Burn, Donald H., Hannaford, Jamie, Renard, Benjamin, Stahl, Kerstin, Fleig, Anne K., Madsen, Henrik, Mediero, Luis, Korhonen, Johanna, Murphy, Conor, & Wilson, Donna. 2017. Climate-driven variability in the occurrence of major floods across North America and Europe. *Journal of Hydrology*, **552**, 704–717.
- Holbrook, J., & Wanas, H. 2014. A Fulcrum Approach To Assessing Source-To-Sink Mass Balance Using Channel Paleohydrologic Parameters Derivable From Common Fluvial Data Sets With An Example From the Cretaceous of Egypt. *Journal of Sedimentary Research*, **84**(5), 349–372.
- Horton, B.K., & DeCelles, P.G. 2001. Modern and ancient fluvial megafans in the foreland basin system of the central Andes, southern Bolivia: implications for drainage network evolution in fold-thrust belts. *Basin Research*, **13**, 43–63.
- Jones, C M. 1977. Effects of varying discharge regimes on bed-form sedimentary structures in modern rivers. *Geology*, **5**, 567–570.
- Jones, Evan Rhys. 2017. *Probabilistic Source-To-Sink Analysis of the Provenance of the California Paleoriver: Implications for the Early Eocene Paleogeography of Western North America*. Ph.D. thesis.
- Kale, Vishwas S. 2003. Geomorphic Effects of Monsoon Floods on Indian Rivers. *Natural Hazards*, **28**, 65–84.
- Kale, Vishwas S. 2007. Geomorphic effectiveness of extraordinary floods on three large rivers of the Indian Peninsula. *Geomorphology*, **85**, 306–316.

- Kale, Vishwas S, Ely, Lisa L, Enzel, Yehouda, & Baker, Victor R. 1994. Geomorphic and hydrologic aspects of monsoon floods on the Narmada and Tapi Rivers in central India. *Geomorphology*, **10**, 157–168.
- Keller, R. 1968. *Die Regime der Flüsse der Erde*. Freiburger Geographische Hefte.
- Kelly, Sean B., & Olsen, Henrik. 1993. Terminal fans-a review with reference to Devonian examples. *Sedimentary Geology*, **85**, 339–374.
- Knighton, D., & Nanson, G. 1952. *Distinctiveness, Diversity and Uniqueness in Arid Zone River Systems, Chapter 10*. Arid Zone Geomorphology, Process, Form and Change in Drylands.
- Langbein, W.B., & Schumm, S.A. 1958. Yield of Sediment in Relation to Mean Annual Precipitation. *Eos Transactions, American Geophysical Union*, **39**(6), 1076–1084.
- Langford, Richard, & Bracken, Bryan. 1987. Medano Creek, Colorado, a model for upper-flow-regime fluvial deposition. *Journal of Sedimentary Petrology*, **57**(5), 863–870.
- Latrubesse, E. M., Stevaux, J. C., & Sinha, R. 2005. Tropical rivers. *Geomorphology*, **70**, 187–206.
- Latrubesse, Edgardo M. 2015. Large rivers, megafans and other Quaternary avulsive fluvial systems: A potential "who's who" in the geological record. *Earth-Science Reviews*, **146**, 1–30.
- Latrubesse, Edgardo M., Stevaux, Jose C., Cremon, Edipo H., May, Jan Hendrik, Tatumi, Sonia H., Hurtado, Martín A., Bezada, Maximiliano, & Argollo, Jaime B. 2012. Late Quaternary megafans, fans and fluvio-aeolian interactions in the Bolivian Chaco, Tropical South America. *Palaeogeography, Palaeoclimatology, Palaeoecology*, **356-357**, 75–88.
- Leier, Andrew L., DeCelles, Peter G., & Pelletier, Jon D. 2005. Mountains, monsoons, and megafans. *Geology*, **33**(4), 289–292.
- Leopold, Luna B., & Maddock, Thomas. 1953. The Hydraulic Geometry of Stream Channels and Some Physiographic Implications. *U.S. Geological Survey, Professional Paper*, **252**, 57.
- Lvovich, M.I. 1945. *Elementy Vodnogo Regima Rek Zemnogo Shara (Elements of the hydrological regime of the world's rivers)*. In Russian.
- Matthai, Howard F. 1990. Floods. *Pages 97–120 of: Surface Water Hydrology*. Boulder: Geological Society of America.

- Mckee, E D, Crosby, E J, & Berryhill, H L. 1967. Flood Deposits, Bijou Creek, Colorado, June 1965. *Journal of S*, **37**, 829–851.
- McMahon, T. A., Finlayson, B. L., Haines, A., & Srikanthan, R. 1987. Runoff variability: a global perspective. *Pages 1–10 of: The Influence of Climate Change and Climatic Variability on the Hydrologic Regime and Water Resources (Proceedings of the Vancouver Symposium)*.
- McMahon, T.A., Finlayson, B.L., Haines, A.T., & Srikanthan, R. 1992. *Global Runoff. Continental Comparisons of Annual Flows and Peak Discharges*.
- Merz, R., & Blöschl, G. 2003. A process typology of regional floods. *Water Resources Research*, **39**(12), 1–20.
- Meybeck, M., Laroche, L., Dürr, H. H., & Syvitski, J. P.M. 2003. Global variability of daily total suspended solids and their fluxes in rivers. *Global and Planetary Change*, **39**, 65–93.
- Milliken, Kristy, Blum, Mike, & Martin, John. 2012. Scaling Relationships in Fluvial Depositional Systems. *AAPG ACE*, 23.
- Milliken, K.T., Anderson, J.B., Simms, A.R., & Blum, M.D. 2017. A Holocene record of flux of alluvial sediment related to climate: Case studies from the northern Gulf of Mexico. *Journal of Sedimentary Research*, **87**, 780–794.
- Milliman, John D., & Syvitski, James P.M. 1992. Geomorphic/Tectonic Control of Sediment Discharge to the Ocean: The Importance of Small Mountainous Rivers. *The Journal of Geology*, **100**(5), 525–544.
- Moscariello, A. 2018. Alluvial fans and fluvial fans at the margins of continental sedimentary basins: geomorphic and sedimentological distinction for geo-energy exploration and development. *Geological Society of London Special Publications*, **440**(2).
- Mouchené, Margaux, van der Beek, Peter, Mouthereau, Frédéric, & Carcaillet, Julien. 2017. Controls on Quaternary incision of the Northern Pyrenean foreland: Chronological and geomorphological constraints from the Lannemezan megafan, SW France. *Geomorphology*, **281**, 78–93.
- Nicholas, Andrew P., Sambrook Smith, Gregory H., Amsler, Mario L., Ashworth, Philip J., Best, James L., Hardy, Richard J., Lane, Stuart N., Orfeo, Oscar, Parsons, Daniel R., Reesink, Arnold J H, Sandbach, Steven D., Simpson, Christopher J., & Szupiany, Ricardo N. 2016. The role of discharge variability in determining alluvial stratigraphy. *Geology*, **44**(1), 3–6.

- Nichols, Gary J., & Hirst, J Philip. 1998. Alluvial Fans and Fluvial Distributary Systems, Oligo-Miocene, Northern Spain: Contrasting Processes and Products. *Journal of Sedimentary Research*, **68**(5), 879–889.
- Nichols, G.J. 1987. Syntectonic alluvial fan sedimentation, southern Pyrenees. *Geological Magazine*, **124**(2), 121–133.
- North, C. P., & Warwick, G. L. 2007. Fluvial Fans: Myths, Misconceptions, and the End of the Terminal-Fan Model. *Journal of Sedimentary Research*, **77**, 693–701.
- North, Colin P, & Taylor, Katy S. 1996. Ephemeral-Fluvial Deposits: Integrated Outcrop and Simulation Studies Reveal Complexity. *AAPG Bulletin*, **80**(6), 811–830.
- Owen, Amanda, Nichols, Gary J, Hartley, Adrian J, Weissmann, Gary S, & Scuderi, Louis A. 2015. Quantification of a distributive fluvial system: The Salt Wash DFS of the Morrison Formation, SW U.S.A. *Journal of Sedimentary Research*, **85**(2013), 544–561.
- Owen, Amanda, Nichols, Gary J, Hartley, Adrian J, & Weissmann, Gary S. 2017. Vertical trends within the prograding Salt Wash distributive fluvial system, SW United States. *Basin Research*, **29**, 64–80.
- Pardé. 1933a. *Fleuves et Rivières*.
- Pechlivanidis, I G, Arheimer, B, & Donnelly, C. 2017. Analysis of hydrological extremes at different hydro-climatic regimes under present and future conditions. *Climatic Change*, **141**, 467–481.
- Peel, M C, Finlayson, B L, & McMahon, T A. 2007. Updated world map of the Köppen-Geiger climate classification. *Hydrology and Earth System Sciences*, **11**, 1633–1644.
- Pettinga, Luke, Jobe, Zane, Shumaker, Lauren, & Howes, Nick. 2018. Morphometric scaling relationships in submarine channel-lobe systems. *Geology*, **46**(9), 819–822.
- Picard, M Dane, & High, Lee R. Jr. 1973. *Sedimentary structures of ephemeral stream*. Amsterdam: Elsevier Scientific Publishing Company.
- Pike, R.J., Evans, I.S., & Hengl, T. 2009. Geomorphometry: A Brief Guide. *Pages 1–9 of: Developments in Soil Science*, vol. 33. Elsevier B.V.
- Plink-Björklund, Piret. 2015. Morphodynamics of rivers strongly affected by monsoon precipitation: Review of depositional style and forcing factors. *Sedimentary Geology*, **323**, 110–147.

- Plink-Björklund, Piret. 2017. Latitudinal controls on river Systems: Implications of precipitation variability. *SEPM Special Publication*, **108**, 2–21.
- Powell, D Mark. 2009. Dryland Rivers: Processes and Forms. *Chap. 12, pages 333–373 of: Parson, A.J., & Abrahams, A.D. (eds), Geomorphology of Desert Environments*, 2nd edn.
- Radebaugh, Jani, Ventra, Dario, Lorenz, Ralph D, Farr, Tom, Kirk, Randy, Hayes, Alex, Malaska, Michael J., Birch, Sam, Liu, Zac Yung-chun, Lunine, Jonathan, Barnes, Jason, Gall, Alice Le, Lopes, Rosaly, Stofan, Ellen, Wall, Steve, & Paillou, Philippe. 2018. Alluvial and fluvial fans on Saturn’s moon Titan reveal processes, materials and regional geology. *Geological Society of London Special Publications*, **440**.
- Reid, I., & Frostick, L.E. 1997. Channel form, flows and sediments in deserts. *Pages 205–229 of: Thomas, D.S.G. (ed), Process, Form and Change in Drylands*, 2nd edn.
- Rittersbacher, Andreas, Howell, John A., & Buckley, Simon J. 2014. Analysis of Fluvial Architecture in the Blackhawk Formation, Wasatch Plateau, Utah, U.S.A., Using Large 3D Photorealistic Models. *Journal of Sedimentary Research*, **84**, 72–87.
- Robinson, John W., & McCabe, Peter J. 1997. Sandstone-Body and Shale-Body Dimensions in a Braided Fluvial System: Salt Wash Sandstone Member (Morrison Formation), Garfield County, Utah. *AAPG Bulletin*, **8**(8), 1267–1291.
- Shukla, U. K., Singh, I. B., Sharma, M., & Sharma, S. 2001. A model of alluvial megafan sedimentation: Ganga Megafan. *Sedimentary Geology*, **144**, 243–262.
- Singh, Harbhajan, Parkash, B., & Gohain, K. 1993. Facies analysis of the Kosi megafan deposits. *Sedimentary Geology*, **85**(1-4), 87–113.
- Sinha, Rajiv, & Friend, Peter F. 1994. River systems and their sediment flux, Indo Gangetic plains, Northern Bihar, India. *Sedimentology*, **41**, 825–845.
- Sinha, Rajiv, Latrubesse, Edgardo M., & Nanson, Gerald C. 2012. Quaternary fluvial systems of tropics: Major issues and status of research. *Palaeogeography, Palaeoclimatology, Palaeoecology*, **356-357**, 1–15.
- Sinha, Rajiv, Ahmad, Jawed, Gaurav, Kumar, & Morin, Guillaume. 2014. Shallow subsurface stratigraphy and alluvial architecture of the Kosi and Gandak megafans in the Himalayan foreland basin, India. *Sedimentary Geology*, **301**, 133–149.
- Smith, Andrew, Sampson, Christopher, & Bates, Paul. 2015. Regional flood frequency analysis at the global scale. *Water Resources Research*, **51**, 539–553.

- Sneh, Amihai. 1983. Desert Stream Sequences in the Sinai Peninsula. *Journal of Sedimentary Petrology*, **53**(4), 1271–1279.
- ømme2009ømme2009ømme2009
- Sømme, Tor O., Helland-Hansen, William, Martinsen, Ole J., & Thurmond, John B. 2009. Relationships between morphological and sedimentological parameters in source-to-sink systems: a basis for predicting semi-quantitative characteristics in subsurface systems. *Basin Research*, **21**, 361–387.
- Stanistreet, I.G., & McCarthy, T. S. 1993. The Okavanago Fan and the classification of subaerial fan systems. *Sedimentary Geology*, **85**, 115–133.
- Stear, Willo M. 1985. Comparison of the bedform distribution and dynamics of modern and ancient sandy ephemeral flood deposits in the Southwestern Karoo Region, South Africa. *Sedimentary Geology*, **45**, 209–230.
- Syvitski, James P.M., & Milliman, John D. 2007. Geology, Geography, and Humans Battle for Dominance over the Delivery of Fluvial Sediment to the Coastal Ocean. *The Journal of Geology*, **115**(1), 1–19.
- Syvitski, James P.M., Peckham, Scott D, Hilberman, Rachael, & Mulder, Thierry. 2003. Predicting the terrestrial flux of sediment to the global ocean: a planetary perspective. *Sedimentary Geology*, **162**, 5–24.
- Syvitski, James P.M., Cohen, Sagy, Kettner, Albert J., & Brakenridge, G. Robert. 2014. How important and different are tropical rivers? - An overview. *Geomorphology*, **227**, 5–17.
- Tooth, Stephen. 2000. Process, form and change in dryland rivers: a review of recent research. *Earth Science Reviews*, **51**, 67–107.
- Tucker, Gregory E. 2004. Drainage basin sensitivity to tectonic and climatic forcing: implications of a stochastic model for the role of entrainment and erosion thresholds. *Earth Surface Processes and Landforms*, **29**, 185–205.
- Tunbridge, Ian P. 1981. Sandy high-energy flood sedimentation - Some criteria for recognition, with an example from the Devonian of S.W. England. *Sedimentary Geology*, **28**, 79–95.
- Uba, Cornelius Eji, Heubeck, Christoph, & Hulka, Carola. 2005. Facies analysis and basin architecture of the Neogene Subandean synorogenic wedge, southern Bolivia. *Sedimentary Geology*, **180**, 91–123.

- Van Dijk, W. M., Densmore, A. L., Singh, A., Gupta, S., Sinha, R., Mason, P. J., Joshi, S. K., Nayak, N., Kumar, M., Shekhar, S., Kumar, D., & Rai, S. P. 2016. Linking the morphology of fluvial fan systems to aquifer stratigraphy in the Sutlej-Yamuna plain of northwest India. *Journal of Geophysical Research: Earth Surface*, **121**, 201–222.
- Ventra, Dario, & Clarke, Lucy E. 2018. Geology and geomorphology of alluvial and fluvial fans: current progress and research perspectives. *The Geological Society of London*, **440**.
- Wang, Bin, & Ding, Qinghua. 2008. Global monsoon: Dominant mode of annual variation in the tropics. *Dynamics of Atmospheres and Oceans*, **44**(3-4), 165–183.
- Wang, Jianqiao, & Plink-Björklund, Piret. 2019. Stratigraphic complexity in fluvial fans: Lower Eocene Green River Formation, Uinta Basin, USA. *Basin Research*, **31**(May 2018), 892–919.
- Wang, Jianqiao, & Plink-Björklund, Piret. 2020. Variable-discharge-river macroforms in the Sunnyside Delta Interval of the Eocene Green River Formation, Uinta Basin, USA. *Sedimentology*, 1–37.
- Weissmann, G. S., Hartley, A. J., Nichols, G. J., Scuderi, L. A., Olson, M., Buehler, H., & Banteah, R. 2010. Fluvial form in modern continental sedimentary basins: Distributive fluvial systems. *Geology*, **38**(1), 39–42.
- Weissmann, G. S., Hartley, A. J., Scuderi, L. A., Nichols, G.J., Davidson, S.K., Owen, A., Atchley, S.C., Bhattacharyya, P., Chakraborty, T., Ghosh, P., Nordt, L.C., Michel, L., & Tabor, N.J. 2013. Prograding Distributive Fluvial Systems-Geomorphic Models and Ancient Examples. *SEPM Special Publication*, 131–147.
- Weissmann, G S, Hartley, A J, Scuderi, L A, Nichols, G J, Owen, A, Wright, S, Felicia, A L, Holland, F, & Anaya, F M L. 2015. Fluvial geomorphic elements in modern sedimentary basins and their potential preservation in the rock record: A review. *Geomorphology*, **250**, 187–219.
- Whipple, Kelin X. 2009. Landscape texture set to scale. *Nature*, **460**, 468–469.
- Williams, George E. 1971. Flood deposits of the sand-bed ephemeral streams of Central Australia. *Sedimentology*, **17**, 1–40.
- Wilson, Lee. 1973. Variations in mean annual sediment yield as a function of mean annual precipitation. *American Journal of Science*, **273**, 335–349.
- Zellman, Kristine L. 2019. *Investigating links between climate perturbations, river discharge variability and fluvial fans in the Paleogene San Juan Basin, New Mexico, USA*. Ph.D. thesis, Colorado School of Mines.